INFORMATION TO USERS

This manuscript has been reproduced from the microfilm master. UMI films the text directly from the original or copy submitted. Thus, some thesis and dissertation copies are in typewriter face, while others may be from any type of computer printer.

The quality of this reproduction is dependent upon the quality of the copy submitted. Broken or indistinct print, colored or poor quality illustrations and photographs, print bleedthrough, substandard margins, and improper alignment can adversely affect reproduction.

In the unlikely event that the author did not send UMI a complete manuscript and there are missing pages, these will be noted. Also, if unauthorized copyright material had to be removed, a note will indicate the deletion.

Oversize materials (e.g., maps, drawings, charts) are reproduced by sectioning the original, beginning at the upper left-hand corner and continuing from left to right in equal sections with small overlaps. Each original is also photographed in one exposure and is included in reduced form at the back of the book.

Photographs included in the original manuscript have been reproduced xerographically in this copy. Higher quality 6" x 9" black and white photographic prints are available for any photographs or illustrations appearing in this copy for an additional charge. Contact UMI directly to order.

U·M·I

University Microfilms International
A Bell & Howell Information Company
300 North Zeeb Road, Ann Arbor, MI 48106-1346 USA
313/761-4700 800/521-0600

Order Number 9431864

Mechanism of bioactivation and DNA cross-linking activity of new mitomycin analogs

He, Qiao-Yun, Ph.D.

City University of New York, 1994

U·M·I
300 N. Zeeb Rd.
Ann Arbor, MI 48106

MECHANISM OF BIOACTIVATION AND DNA CROSS-LINKING ACTIVITY OF NEW MITOMYCIN ANALOGS

by

Qiao-Yun He

A dissertation submitted to the Graduate Faculty in Chemistry in partial fulfillment of the requirements for the degree of Doctor of Philosophy, The City University of New York.

1994

This manuscript has been read and accepted for the Graduate Faculty in Chemistry in satisfaction of the dissertation requirement for the degree of Doctor of Philosophy

4/26/94
Date

Chair of Examining Committee

4/26/94
Date

Executive Officer

Supervisory Committee

The City University of New York

ABSTRACT

MECHANISM OF BIOACTIVATION AND DNA CROSS-LINKING ACTIVITY OF NEW MITOMYCIN ANALOGS

by

Qiao-Yun He

Advisor: Professor Maria Tomasz

Two new disulfide derivatives of mitomycin C (MC), namely, BMY-25067 and KW-2149, are known to be more active but less toxic (especially, less myelosuppressive) than MC. A related synthetic dimeric mitomycin disulfide M-18 also shows remarkable antitumor activities. In order to understand the basis of the superior anticancer properties of this group of MC disulfide derivatives, experiments were conducted to investigate their mode of action as compared to that of MC. MC's mode of action is intrinsically related to its ability to bind covalently to DNA. The covalent reactivity of MC with DNA requires enzymatic or chemical reduction. In the first portion of this work, the transformations of BMY-25067 subjected to enzymatic or chemical reduction or acid-catalyzed "activation" were elucidated. It is found that the chemical behavior of BMY-25067 upon these activations is shown to be similar to that of MC, but the distribution of the activation products is very different from that of the analogous products of MC. M-18 gave similar transformation products. The results from enzymatic reduction kinetic studies of BMY-25067, M-18 and MC indicated that the new disulfide analogs

of MC are subject to the same bioreductive activation process as MC. They were found to differ from MC, however, in a very interesting way: BMY-25067, KW-2149 and M-18 are subject to reductive activation by the thiol, glutathione. Another important new property of BMY-25067 is its ready rearrangement to the symmetrical dimeric mitomycin disulfide M-18 by thiol-exchange. Two mechanisms are proposed to explain these findings.

The influence of the 7-substituent on the DNA-cross-linking activity of mitomycin analogs was studied in detail. It is clear from the present results that reductive activation is the key to DNA-cross-linking: Mitomycin A (MA) cross-links DNA under $Na_2S_2O_4$, NADPH-cytochrome c reductase and thiol reductive conditions, whereas a mitosene analog, WV-15, and MC do so only under $Na_2S_2O_4$ reductive conditions. The corresponding E^o's (MA > MC = WV-15) correlate with the fact that MA is activated faster than MC and WV-15. These results are also correlated with cytotoxicity. The most significant finding is that all three disulfide analogs (BMY-25067, KW-2149 and M-18) cross-link DNA under activation by thiols, despite the fact that they have low-redox-potentials like MC. It is shown that a new activation mechanism is responsible for this property, namely reduction of the disulfide group by thiols. This unique property may be responsible for the higher bioactivity of these analogs compared to mitomycin C.

The non-covalent interactions of mitomycins with DNA have been examined. It is found that mitomycins do not bind to DNA non-covalently, but their "activated form" can do so. The electrostatic attraction between drug and DNA predominately affects the binding. The hydrogen bonds between 10-carbamate group of drugs and DNA may contribute moderately to the stability of the complex. The binding of the drug is non-specific with respect to DNA composition and sequence.

ACKNOWLEDGEMENTS

With great pleasure, I wish to express my sincere thanks to my supervisor Dr. Maria Tomasz, for her enthusiastic support, encouragement and patient advice throughout the entire duration of my studies. Her inspirational guidance enabled the successful completion of this thesis.

I wish to extend my thanks to all my laboratory colleagues: Roselyn Lipman, Dr. Dario Gargiulo, Dr. Shiv Kumar, Dr. Mrinalni Sharma, Dr. Roland Bizanek and all others for their cooperation and encouragement and being wonderful friends.

I wish to thank to my thesis committee members, Drs. Richard W. Franck, Valeria Balogh-Nair and Carol Moore for reviewing my research progress reports, thesis and for their valuable suggestions.

My dearest thanks are extended to my parents and all family members for their continuous moral support and encouragement over all these years.

Finally I wish to express my deep appreciation and thanks to my dear husband, Hang-Yong Wang, for his patience, continuous support and understanding.

TABLE OF CONTENTS

Chapter II. DNA-cross-linking by novel antitumor analogs of mitomycin C

Chapter III. Non-covalent binding of mitomycins to DNA

LIST OF TABLES, SCHEMES AND FIGURES

Chapter I. Reductive metabolism of disulfide analogs of mitomycin C

Chapter II. DNA-cross-linking by novel antitumor analogs of mitomycin C

Chapter III. Non-covalent binding of mitomycins to DNA

Chapter I. Reductive metabolism of disulfide analogs of mitomycin C

INTRODUCTION

Mitomycin C (MC; **1**)[1] (Figure 1) is a clinically used antitumor agent. It is one of the most potent antitumor antibiotics, especially against solid tumors, *e.g.*, stomach and lung cancers (1). However, it also has strong side effects such as myelosuppression (2). Numerous approaches have been taken to reduce its toxicities. Recently great attention has been given to the modification of the 7-N-substituent in **1**, focusing on changing the physico-chemical characteristics of **1** and placing other functional groups at the 7-position (3-6). Two pharmaceutical research groups, at Bristol-Myers Squibb in Syracuse, NY and Kyowa Hakko Kogyo Company in Japan, have independently developed such derivatives of MC, BMY-25067 (**2a**) and KW-2149 (**2b**) respectively (Figure 1). Both contain a characteristic disulfide group in their 7-N substituent. These two novel anticancer drugs are more active but less toxic (especially, less myelosuppressive) than MC in animal tumor systems (7-11). BMY-25067 is reported to be active against MC-resistant human colon cancer cells (8). KW-2149 is found to be more active against xenografted human lung carcinoma Lu-65 and Lu-99, bladder carcinoma T24 and epidermoid carcinoma A431 than MC (12). It has been reported currently that M-18 (**2c**) (Figure 1), a new synthetic dimeric mitomycin derivative, shows

remarkable antitumor activities against rodent tumors (13). This dimer also contains a disulfide group by which the two mitosane moieties are linked together. In view of these interesting properties of this group of MC disulfide derivatives we undertook an investigation with respect to their mode of action as compared to the that of MC. It was hoped that such studies will lead to an understanding of the superior anticancer properties of the disulfide derivatives of MC. The results would be informative for designing more effective antitumor analogs of these drugs.

The mode of action of MC itself has been extensively studied ever since the seminal discovery by Szybalski and Iyer in 1963 that MC induces cross-linking of the complementary strands of DNA (14) and that this effect is dependent on reductive activation of the drugs (15). The monofunctional and bifunctional alkylation of DNA is thought to represent the ultimate cause of the cytotoxic and antitumor activity of MC. The DNA-alkylation is known to require bioreductive activation of the drug in the cell and the chemistry of the whole process can be mimicked in the test tube, utilizing chemical or biochemical reducing systems, for example NADPH-cytochrome c reductase or other flavoreductases (16, 17). Numerous model studies have been carried out that have unraveled considerable details of the mechanism of the reductive activation and subsequent interaction of MC with nucleophiles (18-24). The reductive activation of mitomycin C and the fate of the reaction intermediates were unknown until very recently. An "auto-catalytic pathway" has been put forward by Peterson and Fisher (21). An outline of the activation of mitomycin C under bioreductive conditions is given in Scheme I. Reduction of the quinone (MC) to the hydroquinone (MC_{red}) makes the carbinolamine more labile, allowing the loss of methanol with the formation of the electrophilic imine. Although this imine may be trapped by exceptional

nucleophiles, more commonly intramolecular tautomerization to the indole proceeds rapidly. This new intermediate however is also not stable, and aziridine ring opening ensues, leading to a quinone methide. Evidence for this quinone methide stems from its ambivalent character, where both electrophilic and nucleophilic characters are expressed in the reactions leading to the ultimate products. Three major products are obtained. At neutral pH in vitro the quinone methide's primary fate (pathway a, Scheme I) is a reaction as an electrophile toward water as a nucleophile, leading to the formation of the diastereomeric trans- and cis-1-hydroxy-2,7-diaminomitosenes[2] (M1 and M2). Under slightly more acidic conditions, mitomycin reductive activation gives M3 in addition to M1 and M2. M3 is produced from a nucleophilic reaction (pathway b) with a solvent-derived proton. The reduction of MC and the formation of M1 and M2 is autocatalytic. The activation process is propagated by electron transfer from reduced mitosenes to mitomycin C quinone (pathway a, Scheme I) as demanded by the relative redox potentials of mitosanes and mitosenes (the latter are 100 mV more negative) (25). Thus, non-stoichiometric reduction of mitomycin results in stoichiometric activation in a chain reaction. This finding explains why only the C1 position is activated under the usual model bioreductive alkylation conditions. However, with the use of stronger reducing agent (such as $Na_2S_2O_4$) C1 and C10- disubstituted products are isolated and characterized, providing the evidence for the postulated nucleophilic reactivity at C10 (26).

These model studies of the reduction of MC under physiological conditions suggested that similar reductive metabolism of MC occurred in the cell and therefore M1, M2 and M3 should be detected as major metabolites. This has been found to be the case (27, 28). These compounds have been found to have no antitumor activity.

The products and mechanism of the reactions of MC with DNA have been recently elucidated by the group of Tomasz and Nakanishi, in collaboration (26, 29-33). Reduction by flavoreductases or certain chemical reducing agents activates MC to a mono- and bifunctional alkylator of DNA, resulting in monoadducts and bisadducts of deoxyguanosine (Scheme II). Activated MC reacts with N^2 position of guanines in the minor groove of DNA. In cell-free systems, the reduction conditions determine whether MC is activated monofunctionally at C1 or bifunctionally at C1 and C10. In the former circumstance the DNA-bound monoadduct **a** is the final product, while in bifunctional activation, the initially formed **a** is further converted to the 10-decarbamoylated adduct **b**, or cross-link adducts **c** and **d** (Scheme II). In cultured tumor cells, all four adducts are formed side by side, indicating that in the intact cell both types of activation occur. It is also found that acids (pH < or = 4) activate MC. The metabolites of MC and the MC-DNA adducts have been identified under the acid activation in test tubes (34, 35).

It is apparent from the above review that the mechanism of the bio-reductive activation of MC, and the subsequent conversion of the active form to biologically inactive metabolites and to lethal DNA cross-links and DNA monoadducts is relatively well-understood on the molecular level. The main objectives of the present study were (i) a direct comparison of these processes with those displayed by the new, disulfide type MC analogs, and (ii) the potential discovery of new reactivities of these analogs, which may be relevant to their enhanced cytotoxic and antitumor properties as compared to MC.

As the first stage of this project, the transformations of BMY-25067 subjected to enzymatic or chemical reduction under physiological conditions or acid-catalyzed "activation" were elucidated and compared to such processes

observed previously with MC. In addition, we found that M-18 gave analogous transformation products, although these were more complex than those from BMY-25067, due to the dimeric structure of M-18. Enzymatic reduction kinetics of BMY-25067, M-18 and MC were compared, using two reductases, xanthine oxidase and NADPH-cytochrome c reductase, both of which had been implicated in intracellular reductive activation of MC (36). The results of these studies indicated that the new disulfide analogs of MC are subject to the same bioreductive activation process as MC. They were found to differ from MC, however, in a very interesting way: BMY-25067, KW-2149 and M-18 are subject to reductive activation by the thiol, glutathione. Although this was hypothesized earlier both by the Bristol-Meyers (37) and Kyowa Hakko Kogyo (9) chemists, the present work now provides experimental evidence for this assumption. Another significant new property of BMY-25067 is its ready rearrangement to the symmetrical dimeric mitomycin disulfide, M-18 by thiol-exchange (38). We reexamined and expanded the original findings on this interesting phenomenon.

MATERIALS

BMY-25067 and mitomycin C were generously supplied by Bristol-Myers Squibb Co., Wallingford, CT. KW-2149 was supplied by Dr. M. Kasai (Pharmaceutical Research Laboratories, Kyowa Hakko Kogyo Co., Ltd., Tokyo, Japan). NADPH-cytochrome c reductase was a gift from Dr. Wayne Backes (Louisiana State Medical School, New Orleans, LA). Xanthine oxidase, NADH, NADPH, and GSH were obtained from Sigma Chemical Co., St. Louis, MO. *Escherichia coli* alkaline phosphatase (type III-R) was purchased

from Worthington Biochemicals, Freehold, NJ. DTT and other reagents were obtained from Aldrich Chemical Co.

Preparation of M-18; **2a** (Figure 1): M-18 was synthesized from mitomycin A (MA)[1] (Figure 1) and cystamine as previously described (4, 38). MA (500 mg, 1.4 mmol) was treated with cystamine dihydrochloride (158 mg, 0.7 mmol) and triethylamine (0.6 ml, 4.3 mmol) in 40 ml of CH_3OH under an atmosphere of N_2 for 1.5 h. The solution was concentrated. Water was added to the solution, and the product was extracted with CH_2Cl_2. Purification of the product by column chromatography on silica gel using 20% CH_3OH in $CHCl_3$ as an eluant afforded M-18 (380 mg, 76% Yield) as a fine blue solid. The purity and identify of the desired dimer M-18 were confirmed by several analytical spectroscopies such as ^{1}HNMR, ^{13}C NMR and ES-MS (Figure 2-4).

Preparation of MA (Figure 1): MA was synthesized by a published procedure, by hydrolysis of MC to an unstable intermediate, 7-hydroxyl mitomycin, followed by methylation with 3-methyl-1-p-tolytriazene (39, 40). 1.5 g MC was used as a starting material and dissolved with 100 ml of 0.1 N NaOH (in 50% CH_3OH/H_2O) and stirred at room temperature for 24 hours. The pH of the solution was adjusted to 4.5 with 0.1 N HCl and the product was extracted with 4 x 300 ml EtOAc. The ethylacetate layer was dried over Na_2SO_4 and then the solvent was removed under reduced pressure to give an amorphous solid. Silica gel TLC (9:1 $CHCl_3/CH_3OH$ or 3:1 i-PrOH/1% NH_4OH) showed only one spot. The obtained 7-OH mitomycin was redissolved in 100 ml of CH_2Cl_2, and 850 mg of 3-methyl-1-p-tolyltriazene were added under stirring. The solution was stirred at room temperature for 24 hours. TLC indicated that 7-OH mitomycin was completely converted to MA. This was purified using a neutral alumina column (1.5 x 20 cm) by eluting first with 500 ml of $CHCl_3$ and then 5% $CH_3OH/CHCl_3$. Fractions

containing MA were concentrated to dryness under reduced pressure. The residue was redissolved with CH_2Cl_2 and precipitated with hexane as a dried powder (630 mg, 42% total yield).

SPECTROSCOPIC TECHNIQUES

^1H and ^{13}C-NMR spectra were recorded on a GE QE-300 (300 MHz) spectrometer in Me_2SO-d_6. Mass spectra were obtained by an electrospray analysis on a VG7070 double focusing mass spectrophotometer at Rockefeller University. UV spectra were measured on a Varian Cary 3 spectrophotometer. Gilford 250 instrument was used for absorbance determination.

METHODS

Quantitative analysis of drugs was usually carried out by UV spectrophotometry in solution. The following ε_{nm} values were used: $\varepsilon_{367} = 21.8 \times 10^3$ (in H_2O) for MC; $\varepsilon_{373} = 16.8 \times 10^3$ (in H_2O) for BMY-25067; $\varepsilon_{375} = 22.8 \times 10^3$ (in H_2O) for KW-2149; $\varepsilon_{370} = 33.6 \times 10^3$ (in CH_3OH) for M-18 and $\varepsilon_{320} = 8.91 \times 10^3$ (in CH_3OH) for MA.

Activation of BMY-25067 by catalytic hydrogenation: A solution containing 1 μmol of BMY-25067 and 1.2 mg PtO_2 in 2.5 ml of 20% ethanol in 0.015 M Tris-HCl, pH 7.05, was first deaerated with helium for 15 min, followed by bubbling H_2 gas for 10 min at 37 °C. A color change from green to purple was noticeable. After 5 min of helium bubbling the mixture was exposed to air. The reaction was monitored by HPLC. For the purification of reduction products, the reaction mixture was washed with chloroform several times to

extract the reduction products, then the content of the chloroform layer was purified by preparative TLC (Analtech preabsorbent silica gel, 500 microns, 20 x 20 cm, $CHCl_3$:CH_3OH 8:1 as an eluant).

Activation of BMY-25067 by enzymatic reductions: Unless otherwise stated, the enzyme reaction mixture contained 1 µmol of BMY-25067, 0.4 units of xanthine oxidase and 2 µmol NADH in 2 ml of 0.1 M phosphate, pH 7.8, or 3.63 units of NADPH-cytochrome c reductase and 1.33 µmol NADPH in 2 ml of 0.1 M phosphate, pH 7.4. All reaction mixtures contained 2% DMSO to dissolve BMY-25067. Anaerobic conditions were achieved by bubbling helium for 15 min. The reaction was initiated by the injection of enzymes (predeaeration). All reactions were carried out at 37 ^{o}C for 20 min. The same color change occurred as above. The mixture was exposed to air and analyzed by HPLC.

Activation of BMY-25067 by acid-catalyzed hydrolysis: 1 µmol of BMY-25067 was dissolved with 0.1 ml 95% EtOH, then 4 ml of 0.001 N HCl or 0.34 M phosphate, pH 3.0, was added. Hydrolysis was carried out at room temperature for 2 h with constant pH 3.0, and terminated by addition of 0.2 N NaOH to neutralize the pH. The reaction mixture was analyzed by HPLC. The hydrolysis products were purified with a Sephadex G-25 column (2.5 x 56 cm, eluted by 0.02 M NH_4HCO_3).

Acetylation of BMY-25067 metabolites: Acetylation of 8 µmol of BMY-25067 metabolites was carried out at room temperature for 2 h using 8 equivalents of acetic anhydride (distilled and dried, 6 ml) and 0.2 equivalents of DMAP in

0.4 ml dry pyridine under helium. The product of each reaction was isolated by TLC (see above).

Cytotoxicity assay of BMY-25067 metabolites: In vitro cytotoxicity of metabolite 3 of BMY-25067 was assayed in HCT 116 human colon carcinoma cells at Bristol-Meyers Squibb Company (Dr. Annamaria Casezza). IC_{50} was determined using XTT dye reduction after 72 hours of drug exposure (41).

Cleavage of the disulfide bond in BMY-25067 and KW-2149 by thiols and the formation of the dimer M-18 from BMY-25067: 20 µl of 2.5 mM drug stock solution in ethanol were diluted with 55-77.5 µl 0.015 M Tris-HCl, pH 7.5. 2.5-25 µl of 10 mM DTT or GSH[1] solution in the same buffer (the pH of DTT or GSH solutions was adjusted to 7.5 with NaOH before use) were added to the drug solution to a final drug concentration of 0.5 mM in constant total volume of 100 µl solution. The molar ratio of drug to DTT (or GSH) was 1:0.5, 1:1, 1:2 and 1:5, respectively, in these mixtures. The mixture was incubated at room temperature for 1 h under aerobic conditions. The sample was analyzed by HPLC. M-18 peak was identified by comparison with synthetic standard M-18. The drug disappearance (%) and the drug conversion (%) to M-18 were calculated as the following:

$$\%\ \text{Drug disappearance} = \frac{(\text{mol of drug at the start} - \text{mol of drug after 1 h}) \times 100}{\text{mol of drug at the start}}$$

$$\%\ \text{Yield of M-18} = \frac{2 \times \text{mol of M-18 formed} \times 100}{\text{mol of drug at the start}}$$

Mol of BMY-25067, KW-2149 and M-18 was obtained from their peak area of analyzed samples and the peak area of standard samples of BMY-25067, KW-2149 and M-18 injected in known quantity. For example,

$$\text{mol of BMY-25067 in an analyzed sample} = \frac{\text{peak area of BMY-25067 in the analyzed sample} \times \text{mol of standard BMY-25067 injected}}{\text{peak area of BMY-25067 from the standard sample}}$$

Conversion of the disulfide analogs BMY-25067, KW-2149 and M-18 to mitosenes by GSH, in comparison with MC and MA as controls: Drug solutions in 2.85 ml of 0.015 M Tris-HCl pH 7.5 containing 0.5% DMSO in the absorbance range 0.1-1.0 at 320 nm for MA and at 370 nm for all others were prepared. 0.15 ml of 100 mM GSH in 0.015 mM Tris-HCl, pH 7.5, were added into the drug solution to give a final concentration of 5 mM GSH. The UV spectrum of the reaction mixture was taken at 5, 10, 20, 40, 60, 90, 120 min and overnight and compared with that before adding GSH.

Activation of M-18 by catalytic hydrogenation, enzymatic reduction and acid-catalyzed hydrolysis were same as that of BMY-25067, unless otherwise stated.

HPLC analysis: A reverse-phase column (Beckman Ultrasphere ODS; 4.6 mm x 25 cm) was used with a flow rate of 1.0 ml/min. Gradient: (i) for BMY-25067 and its metabolites, 30%–60% CH_3CN in 0.03 M phosphate (pH 6.3), in 50 min, (ii) for dimer M-18, its metabolites and its formation from BMY-25067, 18%–48% CH_3CN in 0.03 M NH_4Ac (pH 7.0), in 50 min, unless otherwise stated. For peak area quantitation a Beckman Model 427 M integrator was

used and attached to a Model 265A absorbance detector (set at 254 nm), both as parts of a Model 338 HPLC system.

Comparison of the enzymatic reduction rate of BMY-25067 and M-18 with that of MC: (i) Reduction by xanthine oxidase/NADH: The reaction mixture contained 0.5 μmol/ml of NADH, 0.1 unit/ml (or 0.0784 mg protein /ml) of xanthine oxidase and 2% DMSO in 2 ml of 0.015 M Tris-HCl buffer, pH 7.8. (ii) Reduction by NADPH-cytochrome c reductase: The reaction mixture contained 1 μmol/ml of NADPH, 1.2 unit/ml of cytochrome c reductase and 2% DMSO in 2 ml of 0.015 M Tris-HCl buffer, pH 7.5. The concentration of drugs was varied from 50 to 700 nmol/ml. Reduction was carried out at 37 ^{o}C under anaerobic conditions. 100 μl aliquots of the reaction solution were taken with a syringe at 1, 3, 5, 7, 10, 15 and 20 min and diluted immediately to 300 μl with CH_3OH. These samples were analyzed by HPLC. The HPLC mobile phase was 12%–36% CH_3CN in 0.03 M NH_4Ac (pH 7.0) in 30 min for MC, 36%–60% CH_3CN in 0.03 M NH_4Ac (pH 7.0) in 30 min for BMY-25067 and 24%–60% CH_3CN in 0.03 M NH_4Ac (pH 7.0) in 30 min for M-18. The UV detector was set at 367 nm for MC, 373 nm for BMY-25067 and 370 nm for M-18. A known concentration standard of MC, BMY-25067 or M-18 was injected into HPLC, and the value of peak area/mol of the standard was determined. This number was used for calculation of the drug concentration of reaction samples. The reduction rate was determined by testing the disappearance of drugs for the initial 10 minutes which responded linearly to time.

RESULTS

I. Isolation and structure identification of BMY-25067 metabolites.

(i) Isolation of BMY-25067 metabolites resulting from drug activation by chemical or enzymatic reduction and acid-catalyzed hydrolysis in cell-free systems.

The reduction of BMY-25067 by H_2/PtO_2 in 20% EtOH in 0.015 M Tris-HCl, pH 7.05, buffer (10 min, 37 °C) yielded a major product **3**, as shown in figure 5b. Reduction by xanthine oxidase/NADH in 0.1 M phosphate buffer, pH 7.8, also produced **3** as a major product. In addition, 10-decarbamoyl-**3** (**D3**) and product **4** were also detected by HPLC (Figure 5c). Reduction by NADPH-cytochrome c reductase in 0.1 M phosphate buffer, pH 7.4, yielded again **3** and additional products **4**, **6** and **D3** (Figure 5d).

The acid-catalyzed hydrolysis of BMY-25067 in 0.001 N HCl at room temperature for 2 h resulted in the formation of two isomers, **4** and **5**, which were isolated by HPLC, as shown in figure 7a. In the acid-catalyzed hydrolysis of BMY-25067 in 0.34 M phosphate buffer, pH 3, two mitosene-phosphate alkylation products **6** and **7** were formed in addition to products **4** and **5** (Figure 7b).

(ii) Structural determination of BMY-25067 metabolites.

Preparation of samples: **3** was obtained from the reduction of 20 μmol BMY-25067 with H_2/PtO_2 in the presence of 24 mg PtO_2. The reaction mixture was

extracted with $CHCl_3$. The organic layer was dried with Na_2SO_4, filtered and evaporated. Purification was obtained by TLC, using $CHCl_3$: CH_3OH 8:1 as eluant. A major product (3) was separated (R_f of BMY-25067 is 0.77 and **3** is 0.41) with 35% yield. **4** and **5** were prepared from the acidic hydrolysis of BMY-25067 by preparative HPLC using a reverse-phase column (Beckman Ultrasphere-ODS 10 mm x 25 cm). The eluant was 36% to 60% CH_3CN in 0.03 M ammonium acetate (pH 7.0) over 50 min. The flow rate was 2 ml/min. In order to improve the resolution of the NMR spectra, all metabolites of BMY-25067 were acetylated. After **3** was acetylated, the product was purified by preparative TLC. The R_f of **3** and its acetylated derivative were 0.12 and 0.5 respectively in a solvent system $CHCl_3$: CH_3OH = 10:1. A large scale preparation of **4** and **5** was obtained after acidic hydrolysis of BMY-25067 and purification by a Sephadex G-25 column (2.5 x 56 cm, 0.02 M NH_4HCO_3 eluant). **4** and **5** were coeluted at 874 ml and BMY-25067 was eluted at 603 ml. This mixture of **4** and **5** was used for acetylation. Their acetylated derivatives were separated by TLC (R_f 0.56 and 0.5 respectively). All samples for NMR were further purified by a Sep-Pak C_{18} reverse-phase column (Waters) as the following: samples were dissolved in 1.5 ml of 30% CH_3CN/H_2O. A Sep-Pak column was washed with 5 ml each of 10% CH_3CN/H_2O and 30% CH_3CN/H_2O. The sample was loaded, then washed with 30% CH_3CN/H_2O, and was eluted with 100% CH_3CN.

The structures of metabolites **3**, **4** and **5** were assigned using several spectroscopic techniques, such as UV, MS, ^{1}H-NMR and 2D-NMR (COSY), as follows:

Ultraviolet Spectroscopy: The UV spectra of **3**, **4**, and **5** in water are shown in figure 8, as compared with BMY-25067. The UV spectra of the two classes, 7-amino mitosenes exemplified by M1, M2 and M3 (Scheme I) and 7-amino

mitosanes exemplified by MC are highly distinguishable[2]. The absorption spectrum of MC is characterized by the maxima at 220 nm and 367 nm in water. The UV absorption spectra of 7-diamino mitosenes (with or without substitution at C1) show two maxima, at 248 nm and 310 nm (18). The UV spectra of BMY-25067 metabolites **3**, **4** and **5** all revealed a characteristic 7-aminomitosene spectrum with λ_{max} at 250 nm and another one around 316-320 nm, indicating the presence of mitosene moiety in each metabolites.

NMR Spectroscopy: The ^{1}H-NMR spectra of **3**, acetylated **3**, acetylated **4** and acetylated **5** (Figures 10, 12, 14 and 15) were analyzed in comparison to the known NMR spectra of 1-dihydro-2,7-diaminomitosene (M3), 1α-hydroxy-2β,7-diaminomitosene (M1), 1β-hydroxy-2β,7-diaminomitosene (M2) and their acetylated derivatives (18). The ^{1}H NMR spectrum of BMY-25067 was also recorded (Figure 9). A list of ^{1}H-NMR chemical shifts (δ, ppm) in Me_2SO-d_6 is as follows.

3: 8.08 (d, 2, $C_{14}H$, J = 8.67 Hz), 7.74 (d, 2, $C_{13}H$, J = 8.70 Hz), 6.50 (br s, 2, $C_{10a}NH_2$), 6.31 (t, 1, C_7NH, 5.8 Hz), 4.99 (s, 2, $C_{10}H_2$), 4.23 (m, 1, C_3H_a), 4.12 (d, 1, C_2H, J = 5.29 Hz), 3.89 (dd, 1, C_3H_b), 3.74 (t, 2, $C_{11}H_2$, J = 5.4 Hz), 3.17 (m, 1, C_1H_a), 3.09 (t, 2, $C_{12}H_2$, J = 6.08 Hz), 2.67 (dd, 1, C_1H_b, J = 16.0, 4.6 Hz), 1.80 (s, 3, $C_{6a}H_3$).

Acetylated 3: 8.42 (d, 1, C_2NH, J = 6.51 Hz), 8.09 (d, 2, $C_{14}H$, J = 8.68 Hz), 7.76 (d, 2, $C_{13}H$, J = 8.71 Hz), 6.53 (br s, 2, $C_{10a}NH_2$), 6.39 (t, 1, C_7NH, J = 5.9 Hz), 5.01 (s, 2, $C_{10}H_2$), 4.79 (br s, 1, C_2H), 4.31 (dd, 1, C_3H_a, J = 12.9,7.13 Hz), 3.89 (dd, 1, C_3H_b, J = 12.9, 4.7 Hz), 3.74 (t, 2, $C_{11}H_2$, J = 5.4 Hz), 3.17 (m, 1, C_1H_a), 3.09 (t, 2, $C_{12}H_2$, J = 6.09 Hz), 2.67 (dd, 1, C_1H_b, J = 16.0, 4.6 Hz), 1.82 (s, 6, $NCOCH_3$, $C_{6a}H_3$).

Acetylated 4: 8.55 (d, 1, C_2NH, J = 6.49 Hz), 8.10 (d, 2, $2C_{14}H$), 7.80 (d, 2, $2C_{13}H$), 6.61 (t, 1, C_7NH, J = 5.91 Hz), 6.4 (s, 2, $C_{10a}NH_2$), 5.91 (s, 1, C_1H), 5.0 (AB qt, 2,

$C_{10}H_2$, J_{AB} = 13.1 Hz), 4.66 (br s, 1, C_2H), 4.45 (m, 1, C_3H_a), 4.05 (d, 1, C_3H_b), 3.80 (t, 2, $C_{11}H_2$, J = 5.5 Hz), 3.15 (t, 2, $C_{12}H_2$, J = 6.08 Hz), 2.04 (s, 3, $OCOCH_3$), 1.85 (d, 3, $NCOCH_3$), 1.75 (s, 3, $C_{6a}H_3$).

Acetylated 5: 8.34 (d, 1, C_2NH), 8.05 (d, 2, $2C_{14}H$), 7.76 (d, 2, $2C_{13}H$), 6.5 (t, 1, C_7NH), 6.4 (s, 2, $C_{10a}NH_2$), 6.02 (d, 1, C_1H), 5.0 (s, 3, C_2H, $C_{10}H_2$), 4.46 (m, 1, C_3H_a), 3.88 (m, 1, C_3H_b), 3.84 (d, 2, $C_{11}H_2$), , 3.17 (t, 2, $C_{12}H_2$), 2.04 (s, 3, $OCOCH_3$), 1.85 (d, 3, $NCOCH_3$), 1.75 (s, 3, $C_{6a}H_3$).

Notable features in NMR of BMY-25067 metabolites were (a) the two doublet peaks around 8 ppm assigned to the aromatic protons; (b) the signals of 11-CH_2 and 12-CH_2 protons at 3.80 ppm and 3.15 ppm, respectively; (c) The signals of 10-CH_2 at 5.0 ppm and 10a-NH_2 (broad singlet) at 6.5 ppm. These observation indicated that metabolites **3**, **4** and **5** also contained the disulfide bond and 10-carbamate of BMY-25067. Other protons of BMY-25067 metabolites showed very similar chemical shifts of their corresponding MC metabolite analogs (M1, M2 and M3). The C10 protons of **3**, acetylated **3** and acetylated **5** formed a sharp singlet rather than an AB quartet like acetylated **4**. This indicated that the asymmetry of C1, responsible for the AB quartet type splitting, was not present in **3**, acetylated **3** and acetylated **5**. C1 protons of acetylated **4** and acetylated **5** were shifted downfield, as compared with that of acetylated **3**: from 2.67 ppm and 3.17 ppm (1-CH_2 of acetylated **3**) to 5.91 ppm of acetylated **4** and 6.02 ppm of acetylated **5**. This observation is consistent with the structural change from 1-CH_2 of acetylated **3** to 1-C($OCOCH_3$)H of acetylated **4** or acetylated **5**. The chemical shifts of 1-C($OCOCH_3$)H, 5.91 ppm (singlet) of acetylated **4** and 6.02 ppm (doublet) of acetylated **5**, also indicated the α or β-stereochemistry of substituents at C1 (18). The NMR spectra of the acetylated derivatives showed one acetyl group at acetylated **3** and two at acetylated **4** or **5** between near 2 ppm and a low field doublet (8.5 ppm)

observed for the 2-NH proton in 2-NH-acetyl mitosenes. Further, the protons of 7-NH (6.39 ppm), 10a-NH_2 (6.53 ppm) and 2-NH (8.42 ppm) are all D_2O exchangeable. These and all other features of the spectra were fully consistent with the structures assigned to the metabolites **3**, **4** and **5**.

2D NMR (COSY) of **3** and acetylated **3** were also obtained (Figure 11 and 13), and showed cross-peaks between the protons of 1-CHa and 1-CHb, 1-CHa and 2-CH, 2-CH and 3-CHa, 3-CHa and 3-CHb, 7-NH and 11-CH_2, 11-CH_2 and 12-CH_2, 14-CH and 15-CH at **3** or 1-CHa and 1-CHb, 2-NH and 2-CH, 3-CHa and 3-CHb, 7-NH and 11-CH_2, 11-CH_2 and 12-CH_2, 14-CH and 15-CH at acetylated **3**. These results strongly support the structure assignment.

Mass Spectroscopy: Mass spectra (electrospray) of **3** and the mixture of two isomers **4** and **5** (**4**:**5** = 1:1.1) were recorded (Figure 16 and 17). The two spectra showed the molecular ion peak $(M+H)^+$ at m/z 518.2 and 534.3. These results prove that the nitro group in BMY-25067 is not reduced by H_2/PtO_2.

The structures of mitosene-phosphates **6** and **7** were characterized after hydrolysis with alkaline phosphatase to the corresponding mitosenes that were proved to be identical to the mitosene **4** and **5** by HPLC analysis (Figure 6 and 7) (34). **6** and **7** were prepared by acidic hydrolysis of BMY-25067 at room temperature for 2 h in 0.34 M phosphate buffer, pH 3, following by purification with a Sephadex G-25 column (2.5 x 56 cm). Fractions, which contained **6** and **7** (at elution volume 541 ml), were collected and lyophilized. 6 OD_{315} units of this sample were hydrolyzed by adding 32 units alkaline phosphatase in 5 ml of 0.01 M Tris-HCl–0.002 M $MgCl_2$ buffer, pH 8.5, for 1.5 h at 37 ^oC. HPLC analysis has shown that the resulted products were **4** and **5** with a ratio of 1:4.3 (Figure 7c and d). Similarly, the mitosene-phosphate **6** from NADPH-cytochrome c reductase/NADPH reductive activation was identified as shown in figure 6c and d.

The structure **D3**, of the decarbamoyl derivative of **3** was proved by the conversion of **3** to **D3** with xanthine oxidase/NADH. 4 OD_{320} units of **3** were reduced under an anaerobic condition by 0.4 units of xanthine oxidase and 2 μmol of NADH in 4 ml of 0.015 M Tris-HCl, pH 7.8, at 37 ^{o}C for 1 h. The reductive mixture was analyzed by HPLC which showed 58% conversion of **3** into **D3** (Figure 6a and b). It has been known (18) that M3 (1-dihydro-2,7-diaminomitosene, Scheme I) is easily decomposed to 10-decarbamoyl M3 (DM3), but M1 and M2 (1-hydroxy, 2,7-diamino mitosene, Scheme I) are relative stable. Futhermore, the disulfide bond and nitro group in **3** should be not reduced by this reductive condition. Therefore, the structure of **D3** is assumed to be 10-decarbamoyl **3** (Scheme I).

(iii) Determination of extinction coefficients (ε) of BMY-25067 and its metabolites.

The extinction coefficients of BMY-25067 at 225 nm and 373 nm and its metabolites at 320 nm was determined, based on the Lambert-Beer Law, $A = \varepsilon CL$, where C is molar concentration, L is pathlength in cm.

(a) The extinction coefficient (ε) of BMY-25067: Weighed 1.06 mg of BMY-25067, dissolved it with 2 ml of CH_3OH then diluted to 100 ml H_2O to a final concentration 1.93×10^{-5} M. The absorbance was measured at 225 nm and 373 nm with 1 cm path length cuvette. The experiment was performed in duplicate. The calculated extinction coefficient was 22.5×10^3 l · mol^{-1} · cm^{-1} at 225 nm and 16.8×10^3 l · mol^{-1} · cm^{-1} at 373 nm (Table I).

(b) The extinction coefficient (ε) of BMY-25067 metabolites: Metabolites **3**, **4** and **5** have only minor differences in their chemical structures (one hydroxyl group at C1 position for **4** and **5**). The extinction coefficient of **3**, **4** and **5** was

therefore considered to be the same. It was reported as above that BMY-25067 was completely converted to **4** and **5** by 0.001 N HCl. Therefore, the extinction coefficient of BMY-25067 metabolites was obtained by determining the absorbance of the solution in H_2O at room temperature before and after hydrolysis of BMY-25067. A solution of BMY-25067 was prepared in 3 ml H_2O, the absorbance was determined at 373 nm, then the pH of this solution was adjusted to 3 with 0.01 N HCl. After three hours incubation at room temperature, pH was neutralized with 0.01 N NaOH. The solution's volume and absorbance at 320 nm were measured. The experiment was conducted in triplicate. The molar extinction coefficient was calculated from the following equation, resulting in 12.1×10^3 l · mol^{-1} · cm^{-1} (Table II):

$$\varepsilon = (A2/A1) \times (V2/V1) \times 16.8 \times 10^3 \text{ l} \cdot \text{mol}^{-1} \cdot \text{cm}^{-1}$$

A1: absorbance at 373 nm before hydrolysis

A2: absorbance at 320 nm after hydrolysis

V1: solution volume before hydrolysis

V2: solution volume after hydrolysis

16.8×10^3 is the extinction coefficient of BMY-25067 at 373 nm in H_2O

1 cm path length cuvette was used for the determination of absorbance.

(iv) Cytotoxicity of the metabolites of BMY-25067.

Since **3** was a major metabolite, separated from the bioreductive activation of BMY-25067, IC_{50} (μM) of BMY-25067 and **3** has been determined and compared with that of MC and its metabolite M3; **3** is the structural analog of M3. IC_{50} (μM) values obtained for these compounds are shown in Table III, by using a human colon tumor cell line HCT 116 and a mutant, HCT/Vm46 resistant to etoposide.

II. Formation of a dimer of MC (M-18) from BMY-25067 and KW-2149 in the presence of thiols.

The difference in chemical structure between BMY-25067, KW-2149 and MC is the substituent at C_7 position. A simple NH_2 group is attached to the 7-carbon in MC, while in BMY-25067 and KW-2149 a long sidechain, containing a disulfide bond, replaces an hydrogen of the 7-amino group of MC. This structural modification results in higher bioactivity of BMY-25067 and KW-2149 than MC. Does this disulfide bond play an important role in bioactivity of BMY-25067? To solve this question, BMY-25067 and KW-2149 were treated with thiols. A varying amounts of DTT or GSH were added to BMY-25067 solution in neutral Tris-HCl buffer. The molar ratio of drug to DTT (or GSH) was 1:0.5, 1:1, 1:2 and 1:5. It was noticed that the solution's color immediately changed to golden yellow from green, then gradually converted to orange. HPLC analysis showed that BMY-25067 disappeared and a dimer of MC (M-18) was formed from BMY-25067 by adding one or less than one equivalent thiols, either DTT or GSH. However, when adding excess thiols BMY-25067 disappeared faster but only a small amount of dimer was detected (Figure 18 and 19). This dimer was identical with a known compound M-18 (40) by coinjecting them into HPLC. When KW-2149 was treated with DTT or GSH as BMY-25067, it also disappeared quickly; however only a small amount of M-18 was observed by HPLC analysis (Figure 20 and 21). Based on HPLC analysis data, plots of (%) yield of M-18 or (%) drug disappearance versus the thiol/drug molar ratio were calculated (Figure 22 and 23).

III. Activational conversion of the disulfide analogs of MC to mitosenes by GSH. Comparison with that of MC and MA.

Above results have shown that at one or less than one equivalent of thiol to drug ratio the disulfide bond of BMY-25067 and KW-2149 was cleaved, resulting in a dimer of MC (M-18); however, all BMY-25067 or KW-2149 disappeared but no dimer was observed when 5-fold more thiols than drugs were added. To understand the chemical transformation mechanism of these disulfide analogs of MC after addition of the excess of thiols, a series of UV spectra of BMY-25067, KW-2149, M-18 were recorded before and after addition of the excess GSH (approximately 140-fold) at 5, 10, 20, 40, 60, 90, 120 min and overnight, as compared with that of MC and MA (Figure 24). The UV spectra of MC did not change after adding GSH; however, the UV spectra of BMY-25067, KW-2149, M-18 and MA gradually changed into absorption spectra which resembled that of mitosenes[2]. It was also notable that when GSH was added to BMY-25067, KW-2149, M-18, MA and MC solutions, all solution color was changed except that of MC, as shown in Table IV. The immediately observed golden yellow color and the dramatic shift of λ_{max} in the UV spectrum of BMY-25067 after addition of GSH, indicated that the disulfide bond of BMY-25067 has been suddenly cleaved to give 4-para-nitro-thiophenol (Figure 24e and f). All these observations demonstrated that BMY-25067, KW-2149, M-18 and MA were activated by GSH, to become mitosenes but MC was not. The percentage of conversion from mitosane to mitosene at a given time was calculated from the absorbance of the formed mitosenes as follow:

$$\text{Conversion (\%)} = \frac{A_{325} - A_{370} \times [A_{325(i)}/A_{370(i)}]}{A_{325(f)}} \times 100$$

Where $A_{325(i)}$ and $A_{370(i)}$ are the initial absorbance, i.e. absorbance at 0 time, at 325 nm (the λ_{max} of mitosenes) and at 370 nm (the λ_{max} of mitosanes); $A_{325(f)}$ is the final absorbance, i.e. absorbance after overnight, at 325 nm. In the case of BMY-25067 $A_{325(i)}$ and $A_{370(i)}$ were actually the A_{325} and A_{370} observed at 5 min rather than at 0 min, since the p-nitrophenyl-disulfide chromophore, which overlaps the 370 nm absorbance of the mitosane chromophore and thus complicates the analysis, is completely gone by this time, while conversion to the mitosene has hardly begun. This makes the 5-min A_{325} and A_{370} value a good approximation for the A_{325} and A_{370} at 0 min. For the case of MA the λmax of MA and its mitosene are 316 nm and 284 nm rather than 370 nm and 325 nm, respectively.

The result shown in figure 25 indicated that within 2 h almost 100% of disulfide analogs were converted to mitosenes, while only 50% of MA and none of MC was activated. It was clear that the 7-substituent of mitomycins effected their activation by thiols.

IV. Comparison of the enzymatic reduction rates of BMY-25067, M-18 and MC.

Two sets of flavoenzymes, xanthine oxidase/NADH and NADPH-cytochrome c reductase/NADPH were used as reducing agents. The plot of reduction rate versus the drug concentration showed a sigmoidal shape and no saturation for all three drugs under these conditions (Figure 26).

BMY-25067 and M-18 have higher reduction rate than MC by both xanthine oxidase/NADH and NADPH-cytochrome c reductase/NADPH. Using xanthine oxidase/NADH the reduction rate of BMY-25067 and M-18 is

2.6 and 2.2 fold higher than that of MC respectively, and with NADPH-cytochrome c reductase/NADPH the reduction rate of BMY-25067 and M-18 is approximately 2.5 fold higher than that of MC at 250 nmol/ml drug concentration. The difference in reduction rate is increased with increasing drug concentration. It is also shown that the enzymatic activation of these drugs does not follow the Michaelis-Menten model. Thus the Michaelis-Menten kinetic parameters (V_{max} and K_M) could not be obtained.

The mitomycin activation by enzymes is shown in comparison with that by thiols. MC, BMY-25067 and M-18 were all activated by both NADPH-cytochrome c reductase/NADPH and xanthine oxidase/NADH. The kinetic curves of the drug disappearance (%) versus the reaction time did not show much difference between the disulfide analogs and MC (figure 27a and b). However, the disulfide analogs of MC (such as BMY-25067 and M-18) were activated by GSH with 100% conversion to mitosenes in 2 hours, but MC was not activated at all (Figure 27c).

V. Isolation and structure identification of M-18 metabolites by means of activation by acidic hydrolysis and reduction.

It was reported that M-18 has higher bioactivity than MC (13). M-18 was also a metabolite of BMY-25067 and KW-2149 by treatment with thiols as described above. Therefore, we conducted a model study of the chemical and enzymatic reduction of M-18. The easier accessibility of acidic hydrolysis products was helpful to identify the reductively formed metabolites.

(i) Isolation of M-18 metabolites (See Figure 32).

Acidic activation of M-18 by 0.001 N HCl: 0.2 μmol M-18 stock solution in 4 μl DMSO was dissolved with 1 ml of 0.001 N HCl, and incubated at 37 °C. The color of solution gradually changed from green-blue to purple. Aliquots of 0.15 ml hydrolysis solution were taken at 10, 30, 60, 120 min and 4.5 h respectively. The pH was neutralized with 0.01 N NaOH, and then the mixture was diluted to 1 ml with CH_3OH. These samples were analyzed by HPLC. It was found that two products (**8** and **9**) were formed at 10 min, which were then further hydrolyzed to another three products (**10**, **11** and **12**). The hydrolysis was completed in two hours (Figure 28).

Acidic activation of M-18 by 0.05 N HCl: When 0.2 μmol of M-18 (in 4 μl DMSO) was hydrolyzed with 1 ml of 0.05 N HCl at room temperature, the color of the solution changed from green-blue to very purple in 2 min and was orange after 30 min. The hydrolysis was terminated at 1 h by adjusting pH to neutral. It was noticed that the orange color was changed to purple by this pH adjustment. The reaction mixture was injected into HPLC. Two compounds (**13** and **14**) were eluted by using a mobile phase 3%–21% CH_3CN in 0.03 M NH_4Ac in 30 min and no M-18 can be detected in the solution (Figure 30).

Activation of M-18 by hydrogenation and enzymatic reductions: M-18 was also reduced by H_2/PtO_2, xanthine oxidase/NADH and NADPH-cytochrome c reductase/NADPH. Hydrogenation of M-18 resulted in two major products (**15** and **16**), while the enzymatic reduction of M-18 led to several other compounds in addition to **15** and **16** (Figure 31). The UV spectra of **15** and **16** showed that **15** had the UV absorbance character of both mitosane and mitosene and **16** had the pure mitosene character (Figure 33b). This

observation indicated that the two mitosanes of the dimer M-18 were not activated at same rate, but eventually both mitosanes could be reduced. The reductive metabolism studies of MC have shown that MC was reduced to three products (M1, M2 and M3, Scheme I). Therefore, the two mitosane moieties of M-18 should result in a complex combination of these three reductive products (Nine possible products could be formed from the reduction of M-18).

(ii) Structure determination of the M-18 metabolites

UV spectroscopy: It was found that the UV spectrum of **8** was identical to that of **9**, showing a mitosane-mitosene[2] combination and the UV spectrum of **10** was identical to that of **11** and **12**, showing a mitosene-mitosene combination (Figure 33a). Very similarly, **15** showed a UV spectrum of a mitosane-mitosene and **16** showed that of a mitosene-mitosene (Figure 33b). The UV spectra of **13** and **14** were identical showing pure mitosenes. The λ_{max} of **13** and **14** was dependent on pH, and it shifted from 309 nm to 292 nm, when the pH of the solution was changed from neutral to pH 3 (Figure 34). This shift gave the evidence that the products **13** and **14** were 7-OH mitosenes.

The structures of **10, 11** and **12** have been identified by the treatment of a 1:1 mixture of **4** and **5** (1,2-trans and cis mitosene isomers, two BMY-25067 metabolites) with DTT. **4** and **5** would be theoretically converted to **10, 11** and **12** by DTT. The reaction was conducted as the following: 0.5 μmol of **4** and **5** mixture was dissolved with 2 ml of CH_3OH. 4.3 μl of triethylamine (3 μmol) and 12.5 μl of 40 mM DTT (0.5 μmol) were added into the solution, and the mixture was incubated for 2 h at room temperature. 10 μl of the above

solution were analyzed by HPLC, using a C18 analytical column (4.6 mm x 25 cm) and a mobile phase 18%_48% CH_3CN in 0.03 M NH_4Ac, pH 7.0, in 50 min. Three compounds were produced from this treatment and they were shown to be identical to **10, 11** and **12** by coinjecting them to HPLC (Figure 29).

The structures of **13** and **14** were identified by coinjecting them with two known compounds [(7-OH-1,2-trans-mitosene (7-OH-M1) and 7-OH-1,2-cis-mitosene (7-OH-M2)]. As shown in figure 30, **13** and **14** were identical to 7-OH-M1 and 7-OH-M2 respectively.

Mass spectroscopy: A sample containing isomers **8** and **9** was prepared by purification with a Sephadex G-25 column (2.5 x 56 cm, eluted with 0.02 M NH_4HCO_3) after hydrolysis of M-18. The procedure was following: 3 μmol M-18 was hydrolyzed with 15 ml of 0.001 N HCl for 1 h at room temperature. After reaction was terminated by adjusting the solution pH to 5.5, the mixture was loaded on a Sephadex G-25 column directly and fractionated. Fractions (elution volume 826 ml) were collected and then lyophilized. A sample containing **10, 11** and **12** was also prepared: After hydrolysis of M-18 in 0.001 N HCl for 2 h at 37 ^{0}C, the reaction mixture was loaded on a Sephadex G-25 column. These three compounds which coeluted at 873 ml were collected. HPLC showed that they were pure. The mass spectra (electrospray analysis) of the sample that contained **8** and **9** (1:1.6) or that contained **10, 11** and **12** (1:2.5:1.6) all showed their molecular ion peak $(M+H)^+$ at m/z 759.4 and 773.2, respectively (Figure 35 and 36).

1,2-trans or -cis configuration of **8, 9, 10, 11** and **12** have been determined based on the knowledge that elution time of 1,2-trans mitosenes from MC and BMY-25067 is always shorter than that of their corresponding 1,2-cis isomers by using a C18 HPLC column (Beckman) (42).

DISCUSSION

Reductive and non-reductive transformations of BMY-25067 and M-18: Comparison with MC.

Enzymatic reductions. To find out whether the long 7-sidechains of BMY-25067 and the dimer M-18 affect the enzymatic activation or not, the enzymatic reduction rates of BMY-25067 and M-18 have been determined. These were compared with that of MC. It is very significant that the long 7-sidechain does not inhibit the activation. On the contrary, BMY-25067 and M-18 were both reduced faster than MC (approx. 4-fold). The results also indicated that the enzymatic activation of these drugs does not follow the Michaelis-Menten Model. This has been noted previously by Pan and Gonzales for MC and BMY-25067 (43). It is probable that the enzymatic activation of BMY-25067 and M-18 is autocatalytic as proven in the case of MC activation (Peterson and Fisher) (21). The activation process was propagated in that case by electron transfer from reduced mitosene to unreduced mitomycin quinone as demanded by the relative redox potentials of mitosanes and mitosenes (the latter is 100 mV more negative) (25). The reduction rate of BMY-25067 and M-18 is more dependent on the drug concentration than that of MC. Therefore, this autocatalytic pathway may play a more important role in the activation of BMY-25067 and M-18 than in that of MC.

Products of reductive and non-reductive transformation of BMY-25067 and M-18. The rigorously characterized structures of the products of the reduction of BMY-25067 under enzymatic or model chemical conditions and comparison with MC reduction products indicate that BMY-25067 undergoes the same type of reductive metabolism and bioactivation as MC. The

mechanism of this process is shown in Scheme III, in analogy to the well-established mechanism in the case of MC, shown in Scheme I. The reduction of the quinone to hydroquinone renders the carbinolamine more labile, allowing the loss of methanol. The intermediate formed, not being stable ensues opening of the aziridine, leading to a quinone methide. Evidence for the quinone methide stems from its ambient character, where both electrophilic and nucleophilic characters are expressed in the reactions leading to the ultimate products. The initial electrophilic attack at C1 by solvent derived protons results in product **3**. The nucleophilic attack at C1 by water or the phosphate group in the aqueous medium leads to 1,2-trans- and 1,2-cis- products (**4, 5** or **6, 7**). **3** may be further reduced and attacked by water, producing **D3**. A difference from MC should be noted, however: the distribution of the activation products, is very different from that of the analogous products from MC, as shown in Table V. Upon chemical reduction by H_2/PtO_2 and enzymatic reduction by xanthine oxidase/NADH or NADPH-cytochrome c reductase/NADPH, 1-dihydromitosene (**3**) is the predominant product from BMY-25067, but it is a relatively minor product from reduction of mitomycin C. The 1,2-trans/1,2-cis ratio of the 1-hydroxy mitosenes (compounds **4/5**) or the 1-phosphate mitosenes (compounds **6/7**) is much higher than that of the MC series.

Why is **3**, the product of protonation at C1, predominant in the overall product mixture in contrast to the low yield of the analogous M3 in the corresponding MC reduction mixture (Table V)? The 7-substituent of BMY-25067 is a stronger electron donor than 7-amino group of MC. As a result, the electrophilic attack by a proton at C1 of BMY-25067 quinone methide is more favored than the nucleophilic attack, 1-dihydro-mitosene **3** is the predominant metabolite. As another difference in distribution, in the case of

MC the ratio of 1,2-trans / 1,2-cis products is approximately 1:1; however, only 1,2-trans products (**4** and **6**) are formed under bioreductive activation of BMY-25067. This observation is consistent with the hypothesis that the stronger electron donor at 7-position of BMY-25067 accelerates the electrophilic attack, while the nucleophilic attack slows down. Therefore, the thermodynamical control products (1,2-trans products **4** and **6**) were formed.

The results showed that **3** is the predominant bioreductive metabolite of BMY-25067. It was of interest to see whether this metabolite had biological activity itself. In a limited study we determined the cytotoxicity of **3** and its analog M3, the corresponding metabolite of MC, in a human colon tumor cell line HCT 116 and a mutant HCT/VM46 resistant to etoposide (Table III). The cytotoxicity of **3** is 11.3-fold higher than that of its analog M3 in HCT 116 cells and 8.6-fold higher in HCT/VM46. Although **3** and M3 are both less cytotoxic than their parent BMY-25067 and MC respectively, **3** is only 23.4-fold less than BMY-25067 in HCT 116 and 12.5-fold less in HCT/VM46, while M3 is 194.3-fold less cytotoxic than MC in HCT116 and 89.0-fold less in HCT/VM46. In other words, the relative loss of cytotoxicity upon elimination of the mitosane-aziridine function is significantly lower in the case of BMY-25067 than in the case of MC. It appears that the 7-sidechain of BMY-25067 has its own contribution to the cytotoxicity, which is retained upon conversion to **3**.

The acid catalyzed hydrolysis of mitomycin C has been studied extensively (34, 35 and 44). Based on the products of hydrolysis of BMY-25067, determined in the present work, we propose the analogous mechanism, shown in scheme IV. It involves two separate steps. The first step, which has been shown to be rate-limiting, is the acid catalyzed conversion of the mitosane framework to the aziridinomitosene by elimination of water or methanol at C9a. In the second step, the aziridinomitosene is protonated and

ring-opened to afford a mixture of 1,2-cis/trans isomers **4** and **5** or **6** and **7**, where the trapping nucleophilic species have been water or the phosphate group in the medium respectively. The 1,2-cis products are predominant: the ratio of **5** to **4** is 1.2:1 and that of **7** to **6** is 4.3:1. This is qualitatively analogous to the ratio in the acid-catalyzed reactions of MC (3:1 and 19:1, respectively) (34). The simple rationale given in the latter case was that the protonated aziridine opens to the benzylic carbonium ion and that the protonated amine function is solvated by water molecules or phosphate groups which are properly situated to attack the carbonium ion to give the cis products (44). The lower cis/trans ratio of the hydrolysis and phosphorolysis products from BMY-25067 than those from MC may be explained as a result of their different of 7-position substituent. It is possible that the 7-substituent of BMY-25067 stabilizes more the intermediate benzylic carbonium ion due to its stronger electron donor property than that of the 7-amino group in MC. This stabilization results in a favorable competition of thermodynamically stable products (1,2-trans mitosene) with the kinetically favored products (1,2-cis mitosene) due to solvatation.

The reductive and non-reductive hydrolytic metabolism studies of M-18 have shown that the chemical behavior of M-18 is very similar to that of BMY-25067 and MC. Although the two mitosane moieties in the dimer M-18 are not hydrolyzed or reduced at a same rate, they are both converted to mitosenes eventually (Figure 28 and 31). The ratio of 1,2-cis to trans mitosene from hydrolysis of M-18 is 1.5 : 1, very close to that of BMY-25067 metabolites (cis : trans 1.1:1). This result further underlines the 7-sidechain effects on the distribution of mitomycin metabolites. It is possible that this dimer could cross-link to DNA by a monofunctional activation, resulting in higher bioactivity than MC.

Conversion of BMY-25067 and KW-2149 to the dimeric mitomycin M-18 by thiols. From the HPLC analysis of reaction mixtures it is apparent that BMY-25067 is converted to M-18 with a much higher yield than KW-2149 under the same conditions, employing either DTT or GSH as the thiol. This is explicitly summarized in Figure 22. An additional characteristic is that the yield of the dimer M-18 reaches a sharp maximum with increasing concentration of thiol, corresponding to approximately 0.5-1.0 mol thiol per mole drug for the maximum yield (Figure 22). No BMY-25067 and M-18 can be detected by HPLC when 5 equivalent thiols are added to the BMY-25067 reaction solution. However, TLC analysis shows that several purple color products are formed. It is very possible the products are firmly bound to HPLC column and could not be washed out by these eluants. The increasing rate of drug disappearance with increasing thiol concentration (Figure 23) confirms that reactions other than dimer formation become prevalent when the thiol is in excess. These results can be explained by the proposed mechanism of formation of the dimer M-18, shown in Scheme V: Reduction of the disulfide group of BMY-25067 by GSH leads to intermediate **X**. The sulfhydryl anion of **X** then attacks the disulfide group of another BMY-25067 molecule, displacing the p-nitrothiophenol anion. This mechanism requires a stoichiometry of only 0.5 mol GSH per mol BMY-25067 (Scheme V). This is in striking correspondence with the experimental finding that 0.5 molar stoichiometry of DTT or GSH leads to more than 50% yield of M-18 (Figure 22) and more than 50% disappearance of BMY-25067 (Figure 23). The decline of dimer yield at higher stoichiometric ratios of thiol may simply be explained by further thiol exchange reactions with excess exogenous thiol, although an additional different type of reaction is also likely to contribute, as will be discussed below. The slower rate of overall reduction of KW-2149 and the much lower yields

of dimer M-18 from it as compared with BMY-25067 may be a result of the presence of a strong electron withdrawing group (4-nitrobenzene group) in BMY-25067. This group makes the disulfide bond of BMY-25067 to be reduced easier by thiols than that of KW-2149. Thus more BMY-25067 is reduced than KW-2149. However, Kyowa Hakko's research group has reported that KW-2149 reacts very rapidly with -SH groups in biological fluids and M-18, 7-N-[2-(methylthio)-ethyl]mitomycin C (M-16; **10**, Figure 1 of Chapter II) and an albumin conjugate are detected in the plasma (44). A conjugate, in which BMY-25067 is covalently bound to proteins through -S-S- bonds, has also been detected when BMY-25067 is added to human plasma, as reported from Gaver and Deeb (Bristol-Myers Squibb Co. Syracuse, NY). These results all show that the disulfide bond in both BMY-25067 and KW-2149 can be easily reduced by a thiol or a protein which contains SH groups.

Significance: The dimer M-18 has been previously synthesized (4, 38) and an extensive SAR study of such symmetrical mitomycin disulfide dimer analogs indicated significant antitumor activities (13). Senter et al. (38) reported briefly that dimer M-18 is also formed directly from the non-symmetrical disulfide MC analog BMY-25067 by reduction of DTT. We reexamined and extended this finding by including GSH as another thiol and KW-2149 as another substrate in a similar study. Our results differ slightly from the previous ones by showing that not 1.0 but 0.5 equivalent of thiol is required for the optimal yield of M-18 both theoretically and experimentally. Since GSH is an ubiquitous thiol in mammalian cells it is reasonable to expect that the transformation of BMY-25067 and KW-2149 to M-18 also occurs intracellularly. The Kyowa Hakko Kogyo research group (45) reported, while this work was in progress, that M-18 could be detected in plasma of rats upon intravenous KW-2149 administration, indicating that this is indeed the case.

It is not known at this time as to what extent this transformation takes place and in what proportion M-18 contributes to the observed antitumor activity of BMY-25067 or KW-2149.

Reductive activation of the disulfide-containing mitomycin analogs BMY-25067, KW-2149 and M-18 by GSH. Both the researchers at Bristol-Myers (37) and Kyowa Hakko Kogyo (9) Companies have envisaged the possibility of the intramolecular reductive activation of mitomycin by an auxiliary at the 7-position. Consequently, 7-mercapto-ethylamino derivatives of MC were synthesized but the free ω-thiol in this substituent was too unstable and had to be masked by oxidation to a disulfide group. This design principle led to the syntheses of BMY-25067 (37), KW-2149 (9), and M-18 (9, 38). The underlying hypothesis for the intramolecular reductive activation of these compounds was that GSH reduced the disulfide group, to release a free thiol group in the 7-substituent which then reduced the quinone and, as a result, the mitomycin alkylating functions became activated (9, 37). However, no experimental evidence has been provided. First we used UV spectroscopy to assay the mitosane to mitosene conversion[2] as characteristic of the reductive activation process. Large excess (140-fold) of GSH was used, at the physiological concentration of 5 mM. Almost 100% of all disulfide analogs of MC are converted to mitosenes within 2 h. MC, however, is not changed at all. The behavior of MA is intermediate between that of these two classes: Only 50% MA is converted in 2 h. This in itself indicates that the conversion of the disulfide analogs takes place *via* an indirect mechanism for the following reasons: The reduction potential of MA is the highest of all of these mitomycins (-0.19 V). The 7-N-substituted ones are in the -0.40 to -0.45 V range (43). Therefore, simple direct reduction of the quinone by a thiol would be expected to be fastest with MA and slower with the latter, low-redox-

potential group, contrary to the experimental results. Direct evidence that the disulfide-type mitomycin C analogs are uniquely activated to DNA-alkylating agents by GSH alone was obtained in our subsequent work, described in the next chapter. Although this investigation is continuing, compelling evidence is emerging for the intramolecular activation mechanism. Mechanistic details are proposed in Scheme VI. The thiol anion of **X** is proposed to add to the quinone 8-carbonyl group *via* a 6-membered ring intermediate, followed by an internal redox reaction to yield the biradical **Y**. Since excess GSH is present, it reduces the semiquinone radical **Y** to the hydroquinone (46). Which then undergoes the usual mitomycin "activation cascade" (Scheme I), resulting in bifunctional alkylation end-products. The fate of the sidechain thiyl radical is likely to be dimerization or oxidation (under aerobic conditions) (47).

In summary of this chapter: The chemical behavior of BMY-25067 upon reduction under model chemical and bioreductive reactions is shown to be analogous to that of MC, but the distribution of the activation products is very different from analogous products of MC. The disulfide group of BMY-25067 is not reduced under the chemical (H2/PtO2) and enzymatic reducing conditions. However, it is cleaved by DTT or glutathione resulting in the formation of a disulfide dimer of MC. Furthermore, the disulfide analogs of mitomycin C including BMY-25067, KW-2149 and M-18 all are activated and converted to mitosenes by excess glutathione. This unique property seems very likely to be responsible for the higher bioactivity of the disulfide analogs of MC than that of MC.

Table I. Determination of the extinction coefficient (ε) of BMY-25067.

	Experiment 1	Experiment 2	Average value
Weight of BMY-25067 (mg)	0.63	1.06	
Concentration of BMY-25067 (M)	1.15×10^{-5}	1.93×10^{-5}	
Absorbance at 225 nm	0.254	0.441	
Absorbance at 373 nm	0.190	0.330	
ε at 225 nm ($l \cdot mol^{-1} \cdot cm^{-1}$)	22.1×10^3	22.9×10^3	22.5×10^3
ε at 373 nm ($l \cdot mol^{-1} \cdot cm^{-1}$)	16.5×10^3	17.1×10^3	16.8×10^3

Table II. Determination of the extinction coefficient (ε) of BMY-25067 metabolites.

	Experiment 1	Experiment 2	Experiment 3	Everage value
A1	0.504	0.536	0.410	
A2	0.271	0.303	0.246	
V1 (ml)	3.00	3.10	3.20	
V2 (ml)	3.95	4.00	4.00	
ε ($l \cdot mol^{-1} \cdot cm^{-1}$)	11.5×10^3	12.3×10^3	12.6×10^3	12.1×10^3

Table III. Cytotoxicity of BMY-25067 and its predominant metabolite 3 formed in vitro. Comparison with that of MC and its metabolite M3 (an analog of 3).

Compound	IC_{50} (μM)[a]	
	HCT 116	HCT/VM46[b]
MC	0.194	0.146
BMY-25067	0.141	0.121
M3	37.3	13
3	3.3	1.51

[a] Determined using the XTT dye reduction method after 72 h drug exposure.

[b] Human colon carcinoma cell lines; HCT/VM46 is resistant to etoposide.

Table IV. Color change of reaction solutions upon addition of GSH.

Drugs	Before adding GSH	After adding GSH		
		5 sec	30 min	2 hr
BMY-25067	Green	Golden Yellow	Yellow	Orange
Kw-2149	Green-Blue	Green-Blue	Yellow	Brown
M-18	Green-Blue	Green-Blue	Yellow	Brown
MA	Red	Red	Purple	Brown
MC	Blue	Blue	Blue	Blue

Table V. Relative distribution of reductive and acidic activation products of BMY-25067, comparison with mitomycin C.

Reaction conditions		Relative distribution				
		3	**4**	**5**	**6**	**7**
H_2 / PtO_2 in tris buffer		1 (0.30)	0 (1)	0 (0.83)	0 (0)	0 (0)
Cytochrome c reductase -NADPH in phosphate buffer		12 (0.65)	1 (1)	0 (0.95)	2.7 (1.5)	0 (1.2)
Hydrolysis	in HCl	0 (0)	1 (1)	1.1 (3)	0 (0)	0 (0)
	in phosphate buffer (pH 3.0)	0 0	1 (1)	1.2 (2)	0.72 (0.14)	3.1 (2.8)

The number in parenthesis indicates the corresponding distribution of the analogous product from MC.

Scheme I. Reductive activation mechanism of mitomycin C.

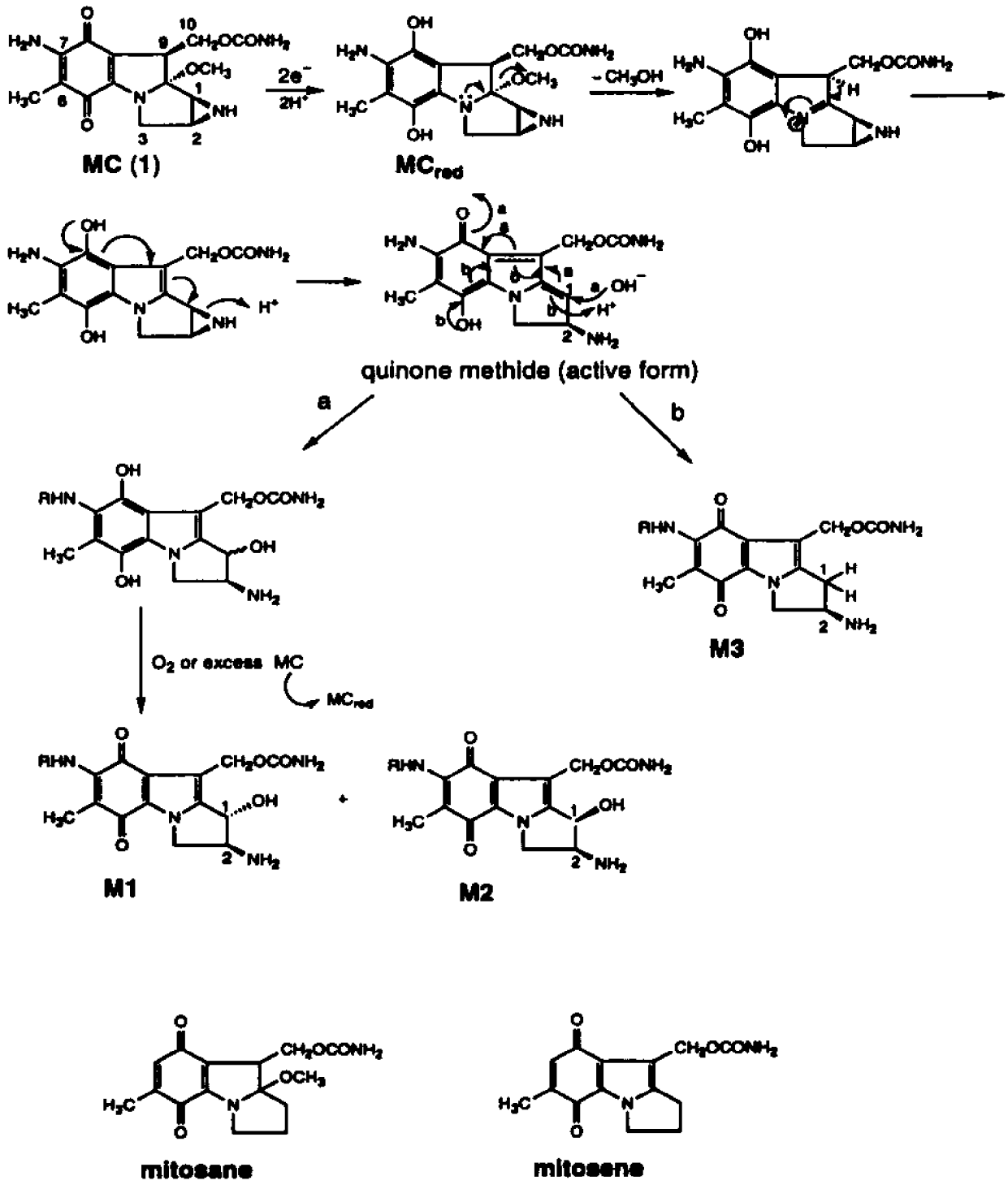

Scheme II. The structures of MC-DNA adducts.

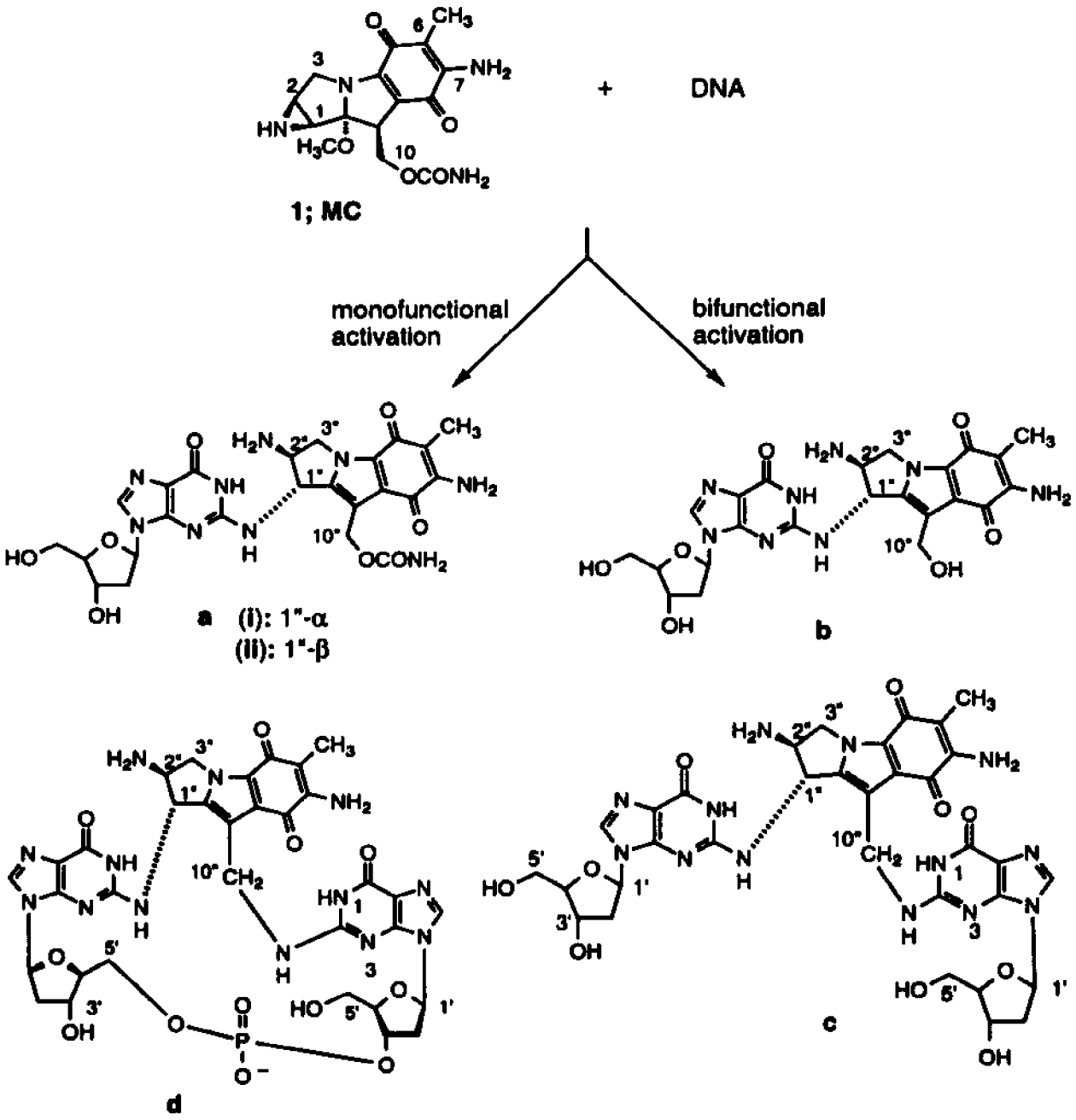

Scheme III. Reductive activation mechanism of BMY-25067.

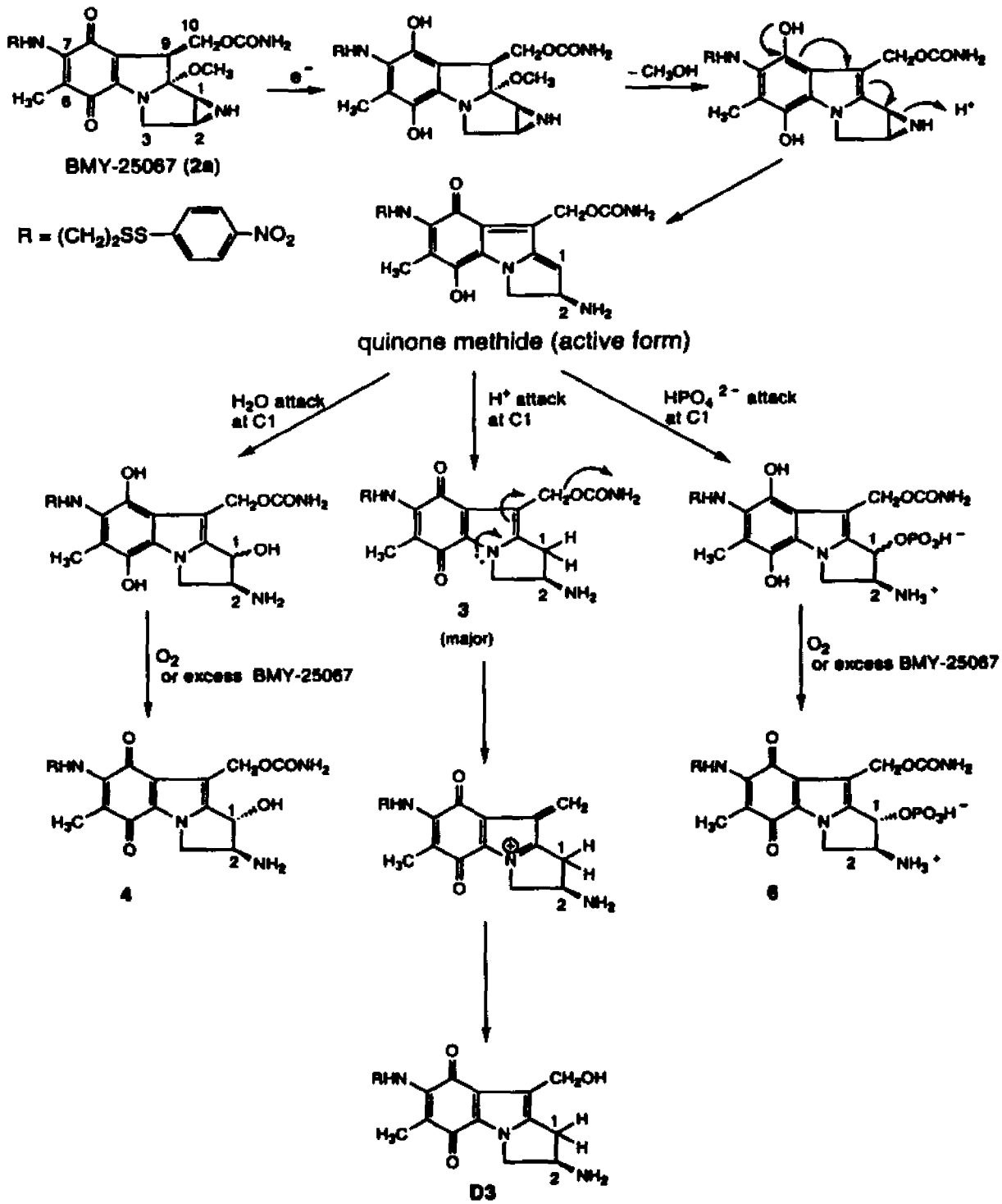

Scheme IV. Acid-catalytic hydrolysis mechanism of BMY-25067.

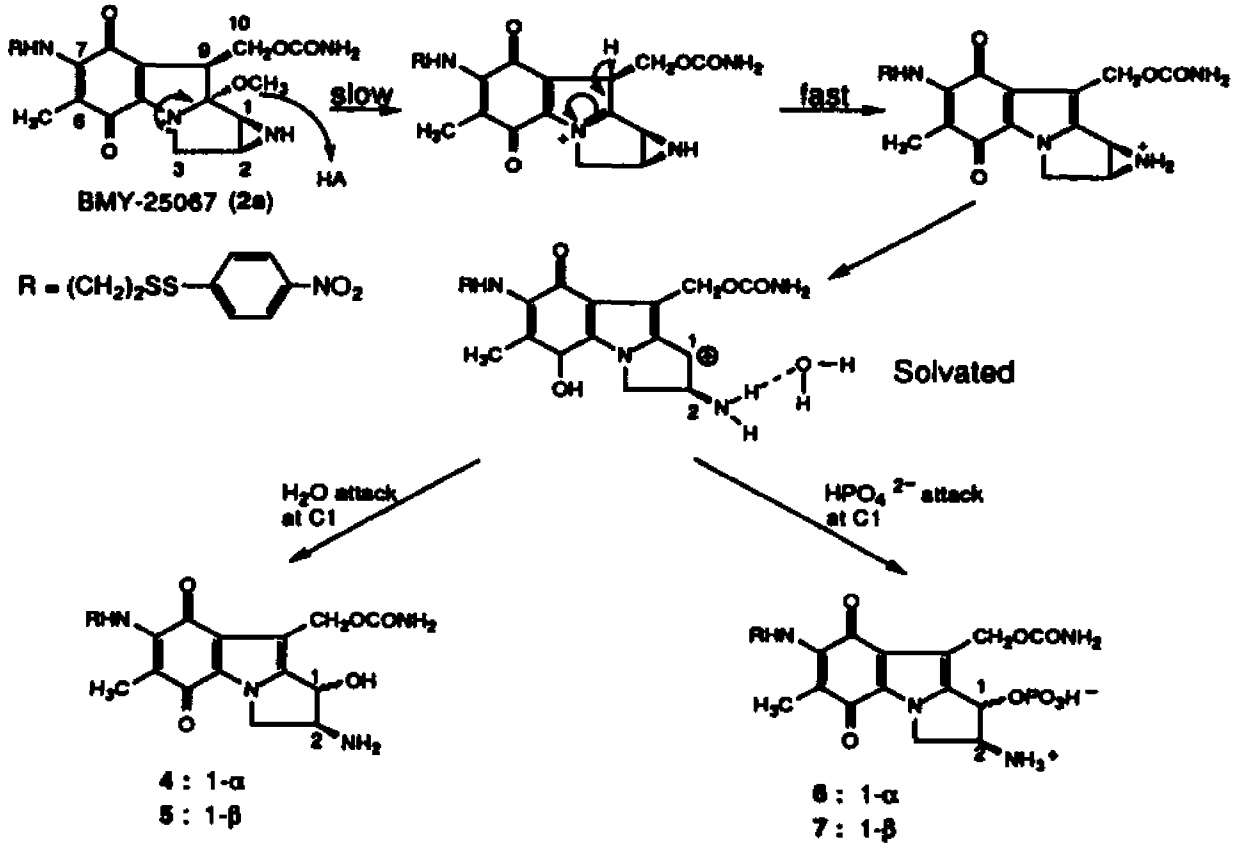

Scheme V. Reaction of BMY-25067 with GSH leading to the formation of disulfide dimer M-18.

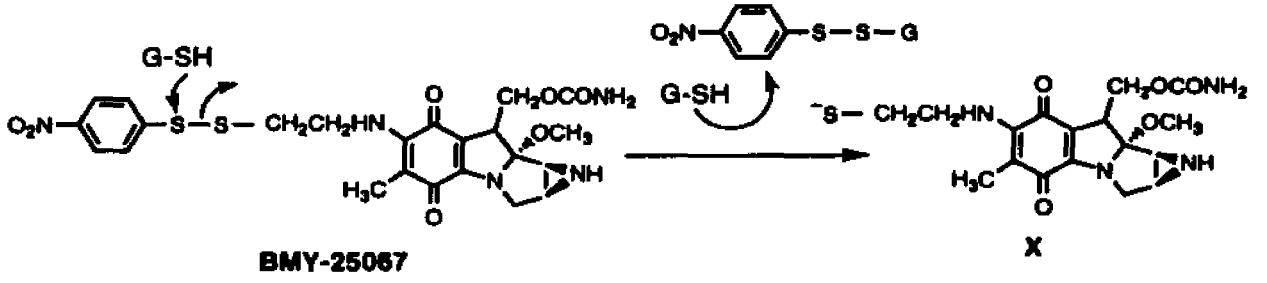

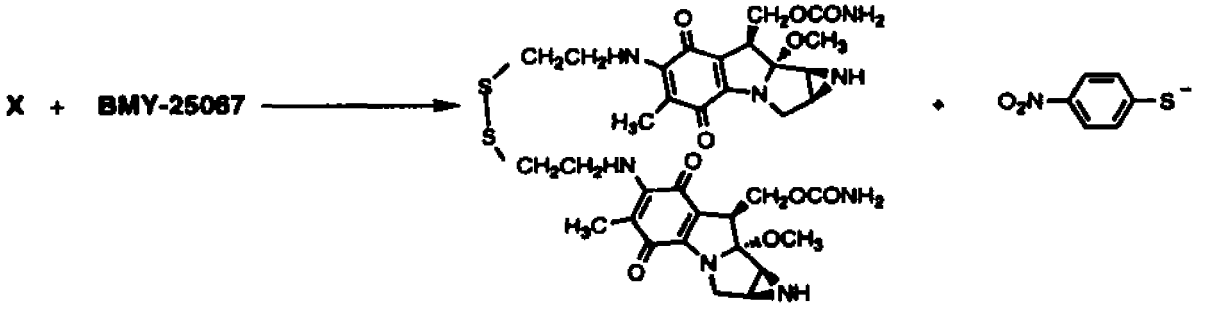

Scheme VI. Thiol activation mechanism of BMY-25067.

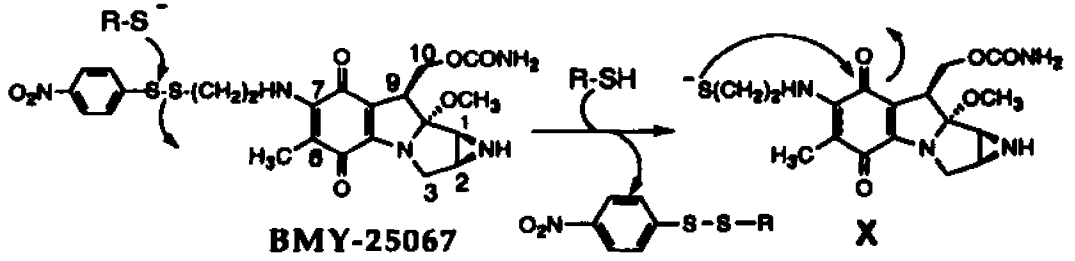

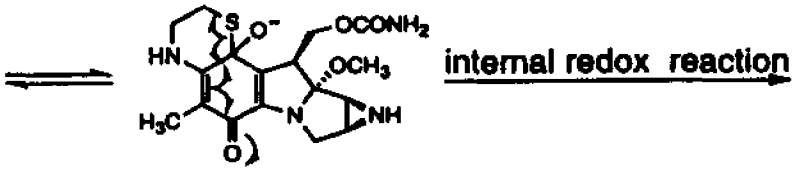

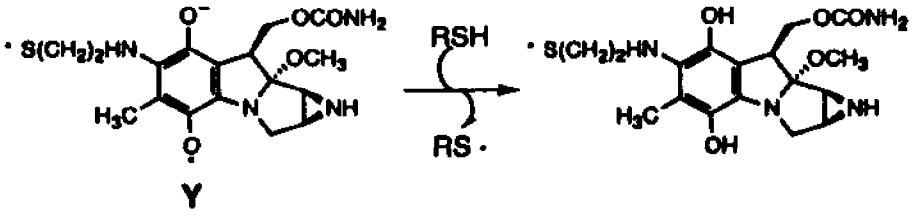

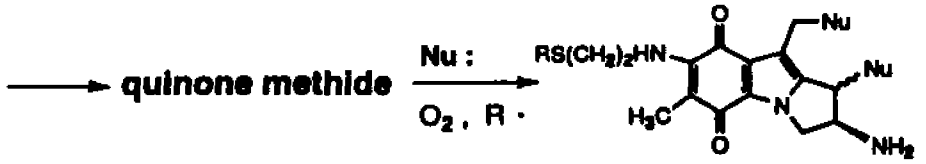

R = undefined; see text
Nu = nucleophile

Note: Two other possible mechanisms are shown as follows.

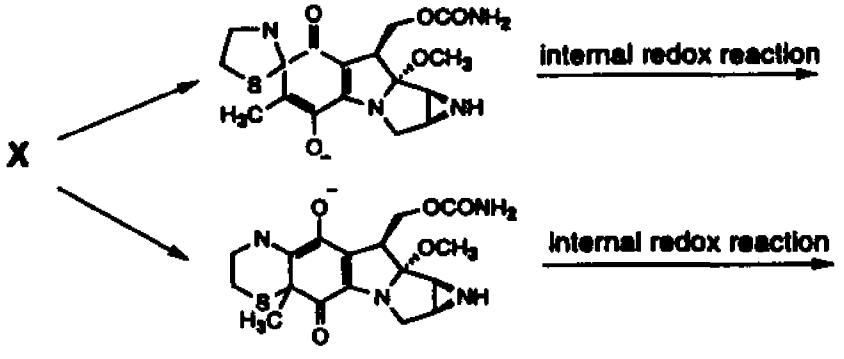

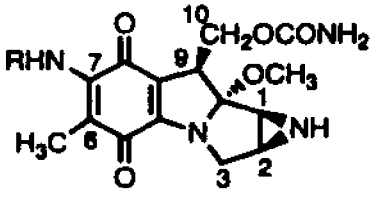

1 (Mitomycin C): R = H

2a (BMY-25067): R = $(CH_2)_2$-S-S- 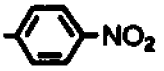

2b (KW-2149): R = $(CH_2)_2$-S-S-$(CH_2)_2$NH-γ-L-Glu

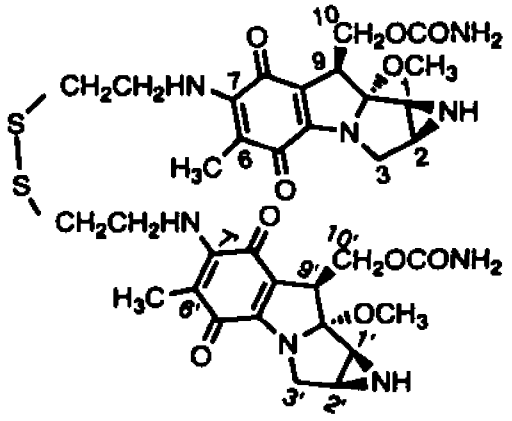

2c (M-18)

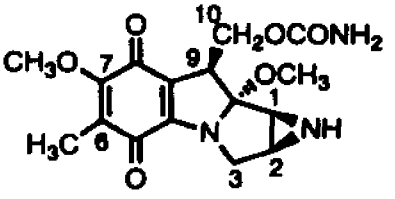

Mitomycin A

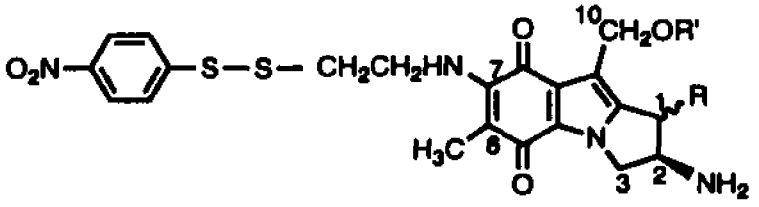

3: R = H, R' = $CONH_2$

4: R = OH, α; R' = $CONH_2$

5: R = OH, β; R = $CONH_2$

6: R = OPO_3^-, α; R' = $CONH_2$

7: R = OPO_3^-, β; R' = $CONH_2$

D3: R = H, R' = H

Figure 1. Structures of MC, its analogs, and metabolites of BMY-25067.

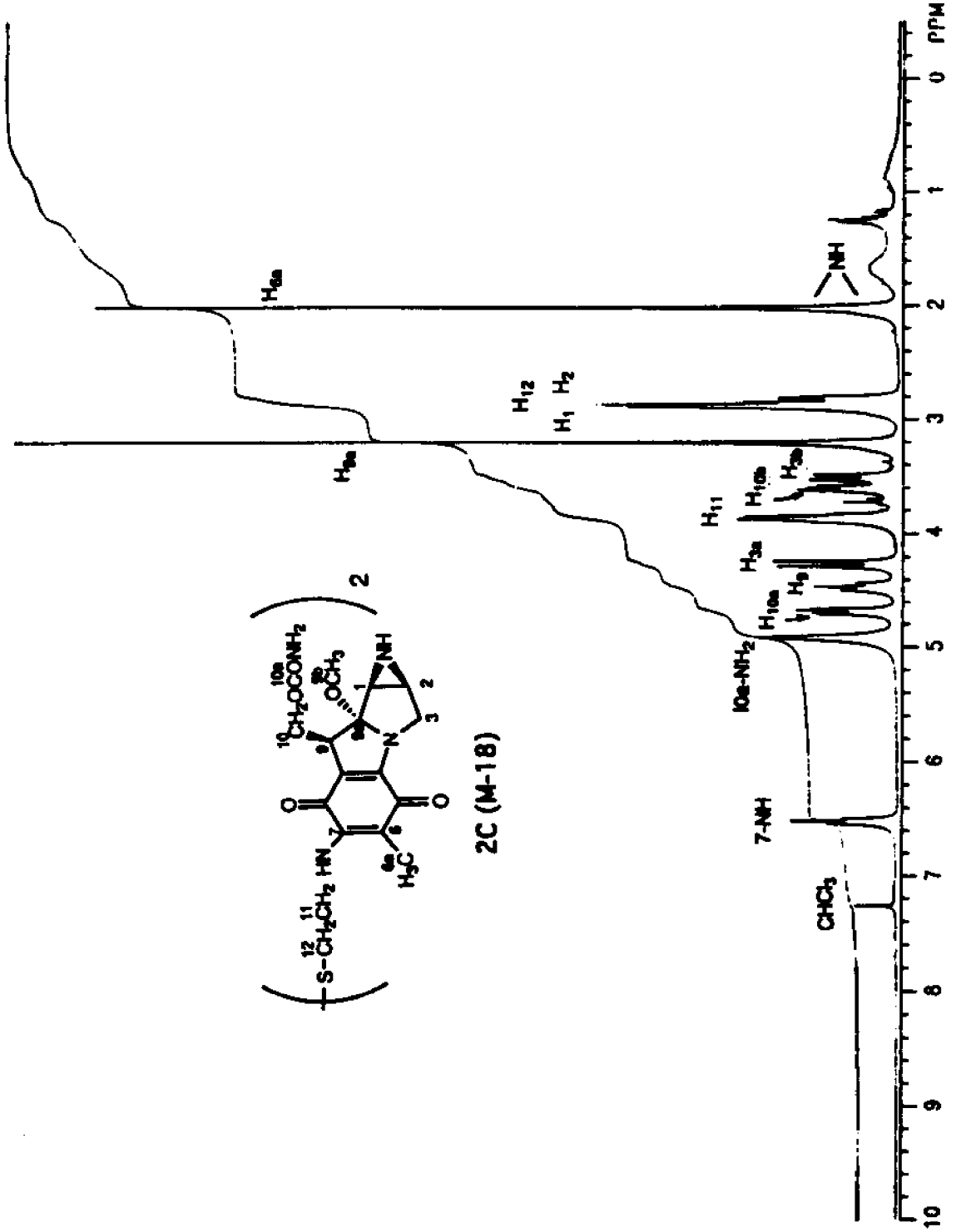

Figure 2. Proton NMR spectrum of M-18 in $CDCl_3$.

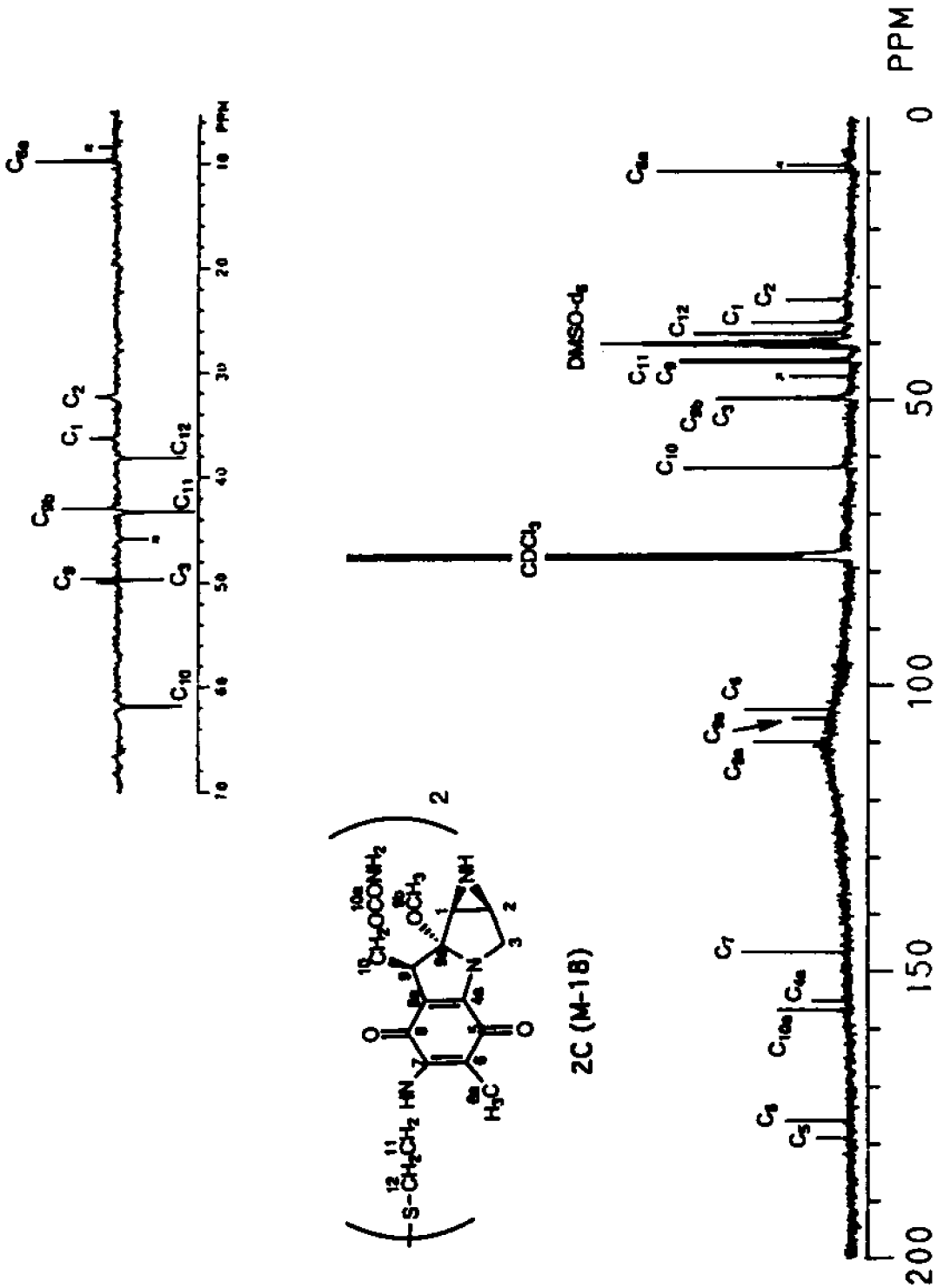

Figure 3. ^{13}C-NMR spectrum of M-18 in CDCl3 (containing three drops of DMSO-d6 in 0.5 ml of CDCl3).

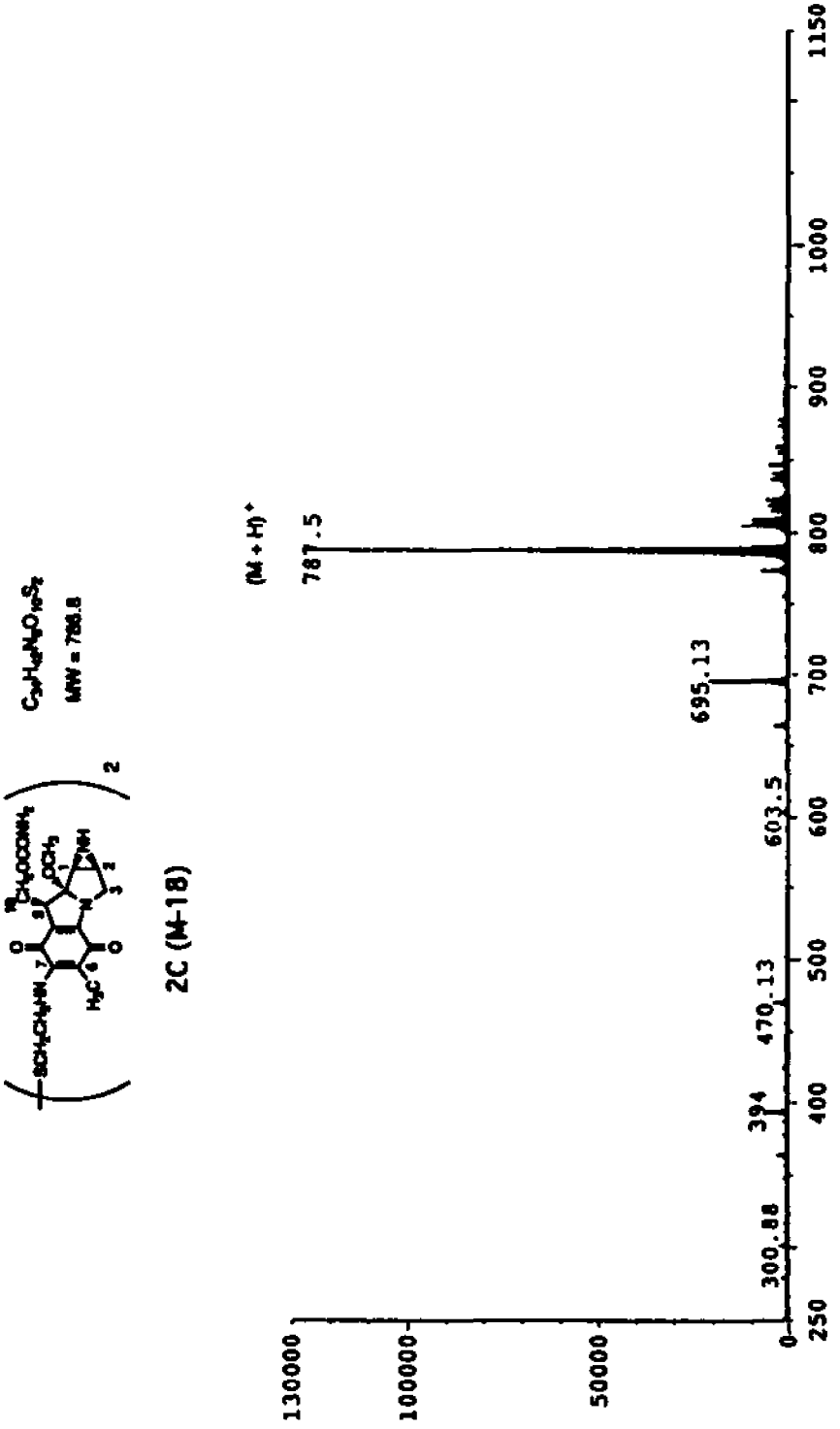

Figure 4. Mass spectrum of M-18 by an electrospray analysis.

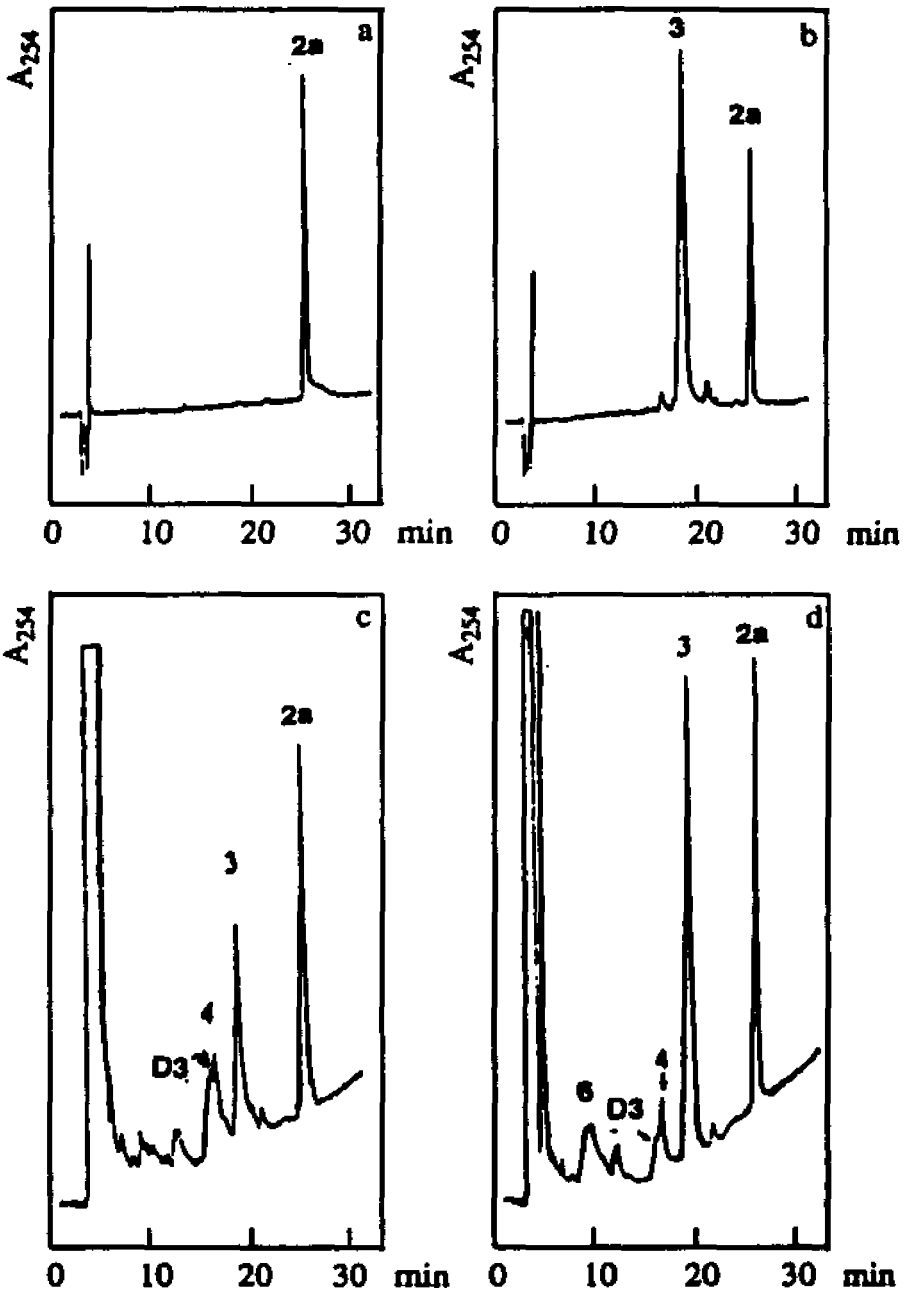

Figure 5. HPLC analysis of BMY-25067 metabolites formed in the chemically and enzymatically reductive activation of BMY-25067. (a) Standard BMY-25067 (2a). (b) Catalytic hydrogenation (H_2/PtO_2). (c) Xanthine oxidase/NADH activation. (d) NADPH-cytochrome c reductase/NADPH activation.

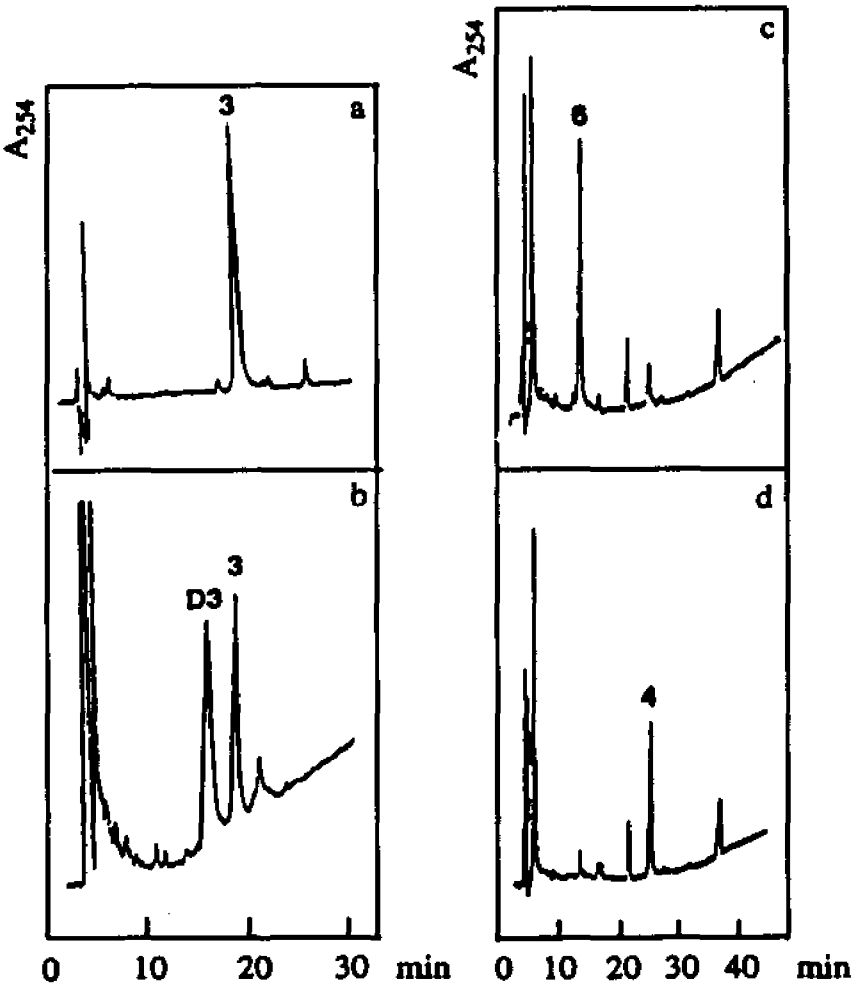

Figure 6. HPLC analysis of the formation of D3 from the reduction of 3 by xanthine/NADH activation and the conversion of 6 to 4 by alkaline phosphatase treatment. (a) and (b) before and after the reduction of 3 by xanthine/NADH activation; (c) and (d) Before and after the alkaline phosphatase treatment of 6, using a HPLC eluant: linear gradient of 24-48% acetonitrile in 0.03 M phosphate buffer, pH 6.3 in 40 min.

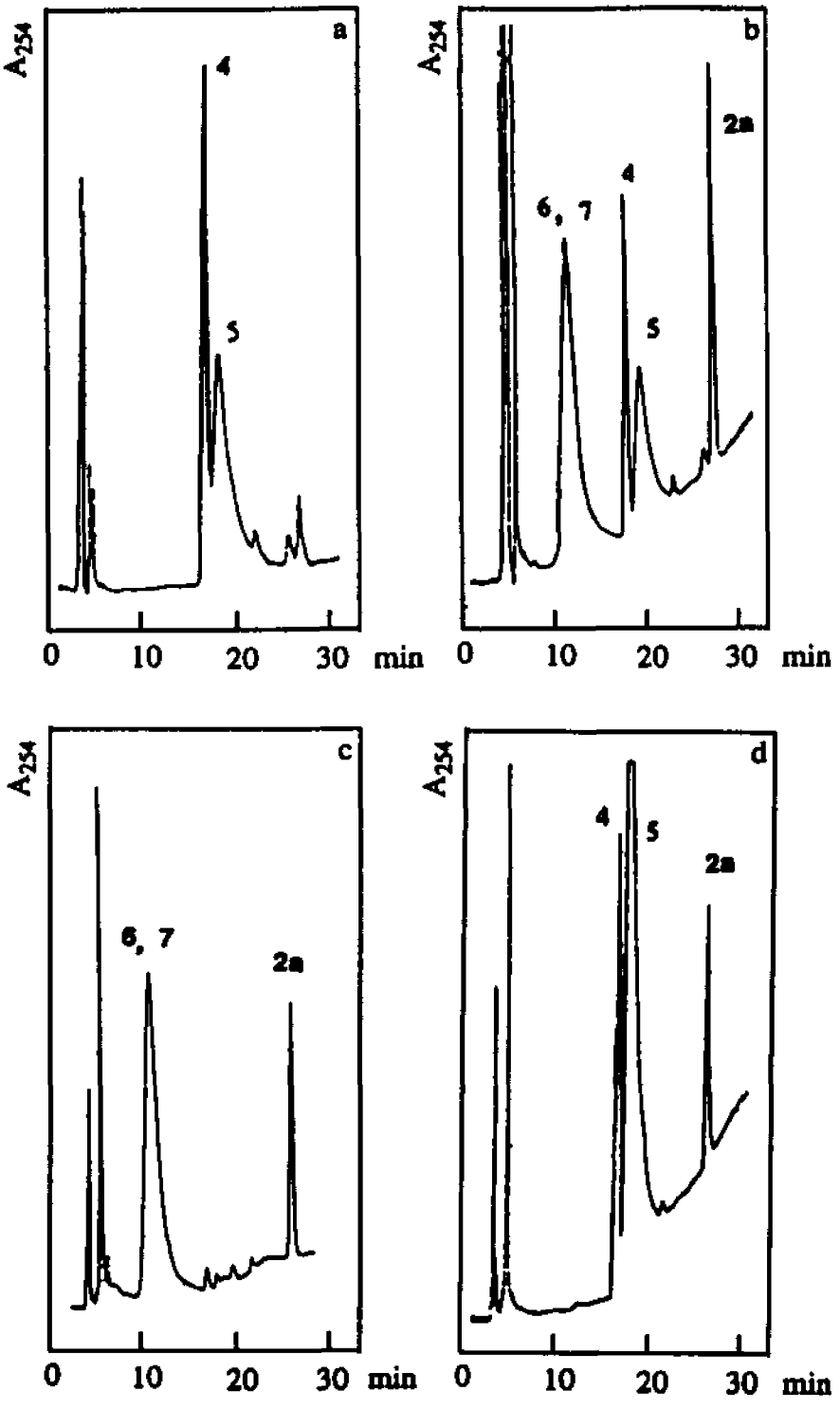

Figure 7. HPLC analysis of BMY-25067 metabolites formed in the acid-catalytic hydrolysis of BMY-25067 (2a). (a) in 0.001 N HCl. (b) in 0.34 M phosphate buffer pH 3.0. (c) and (d) Before and after the alkaline phosphatase treatment of 6 and 7.

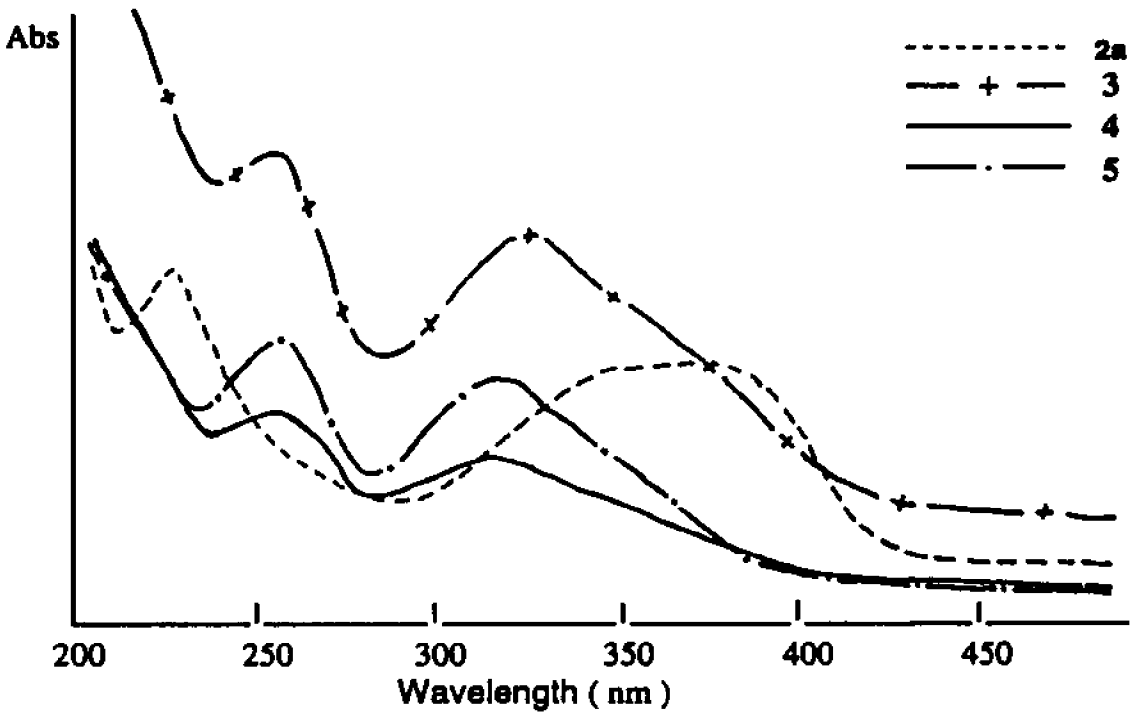

	2a	3	4 and 5
λmax (nm)	222, 370	250, 320	252, 316

Figure 8. Ultraviolet spectra of BMY-25067 and its metabolites in water.

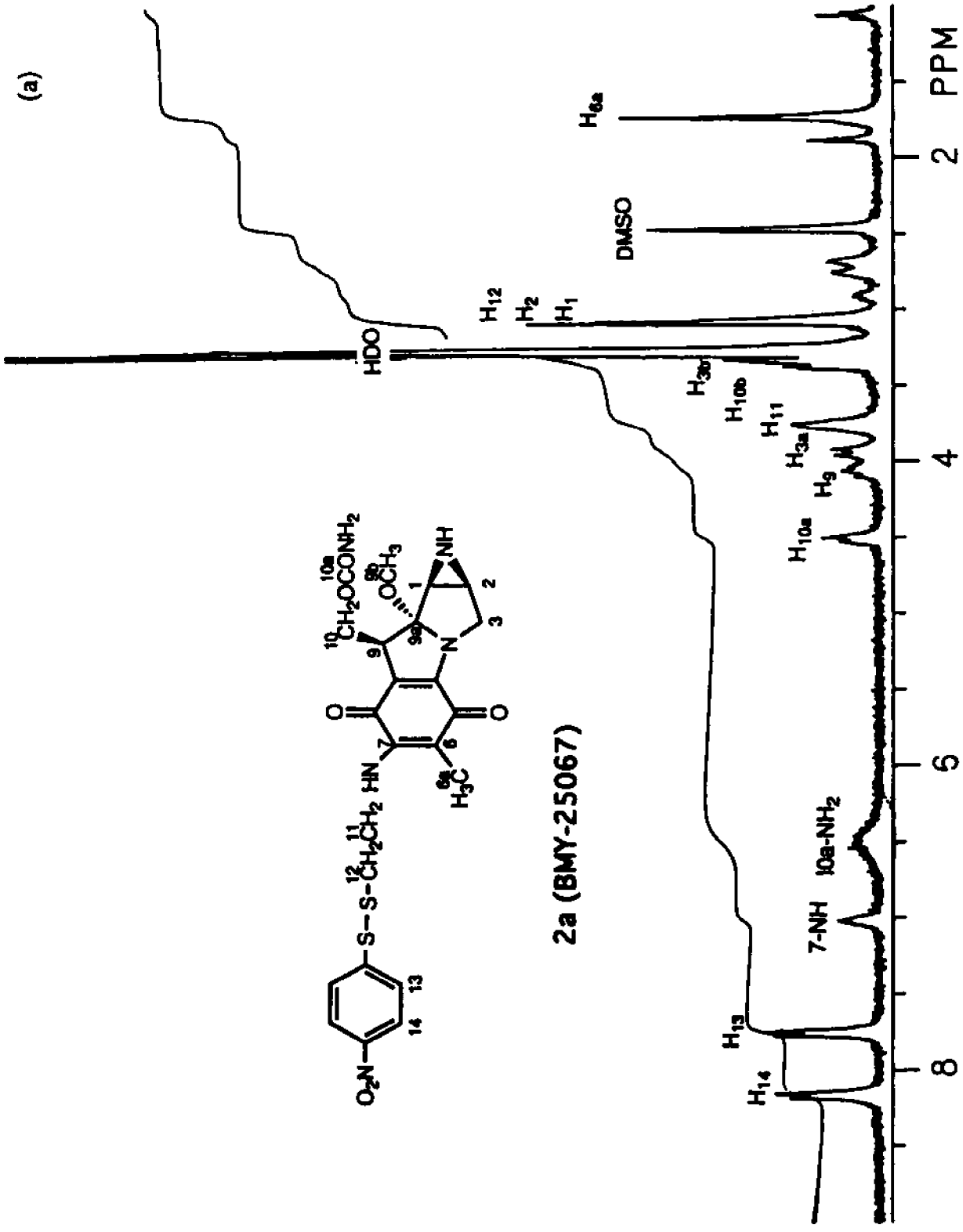

Figure 9. Proton NMR spectrum of BMY-25067. (a) in DMSO-d6. (b) in CDCl3.

(b)

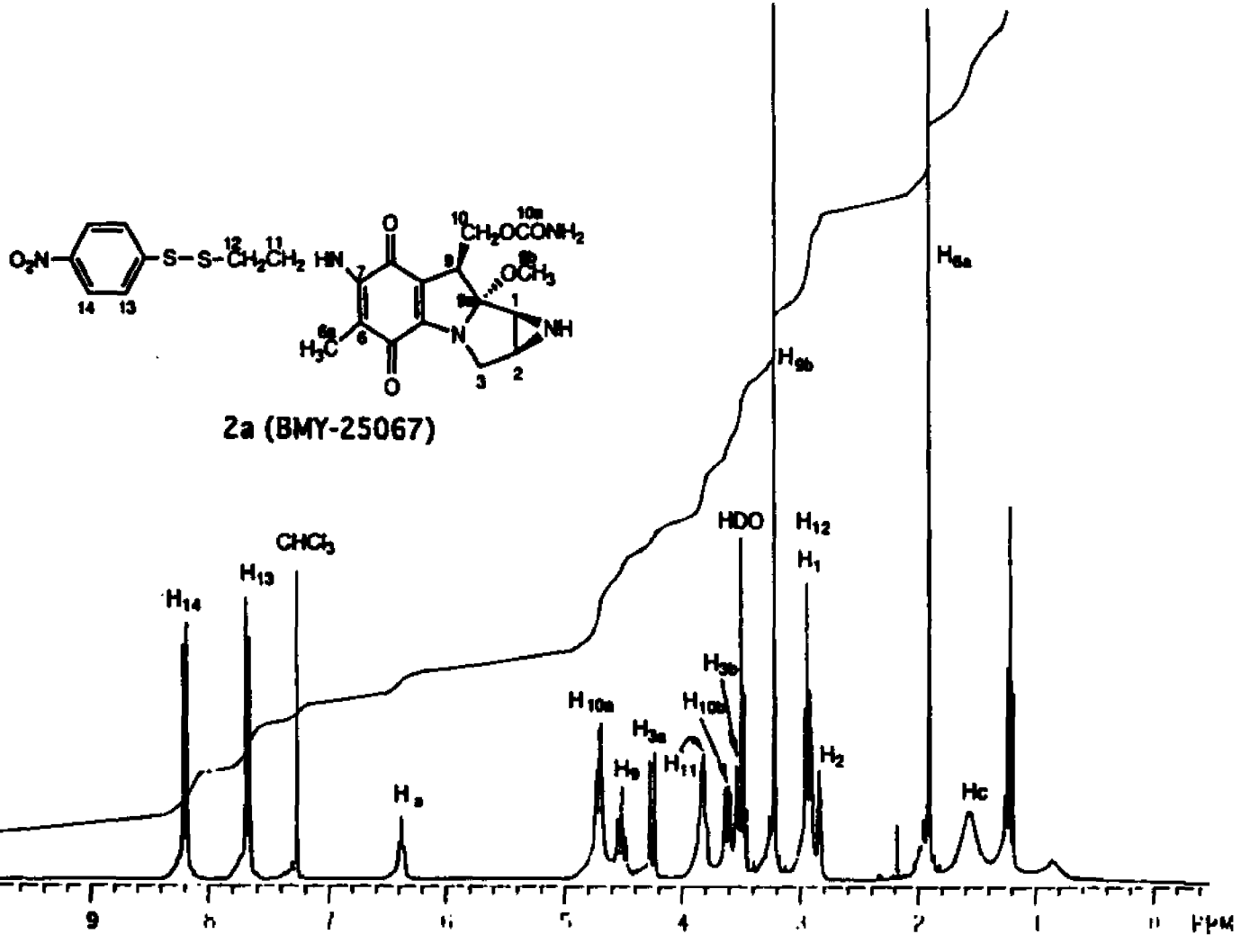
2a (BMY-25067)
CHCl3
HDO
H14
H13
H12
H1
H2
H9b
H6a
H10a
H3a
H9
H11
H3b
H10b
Ha
Hc
FPM

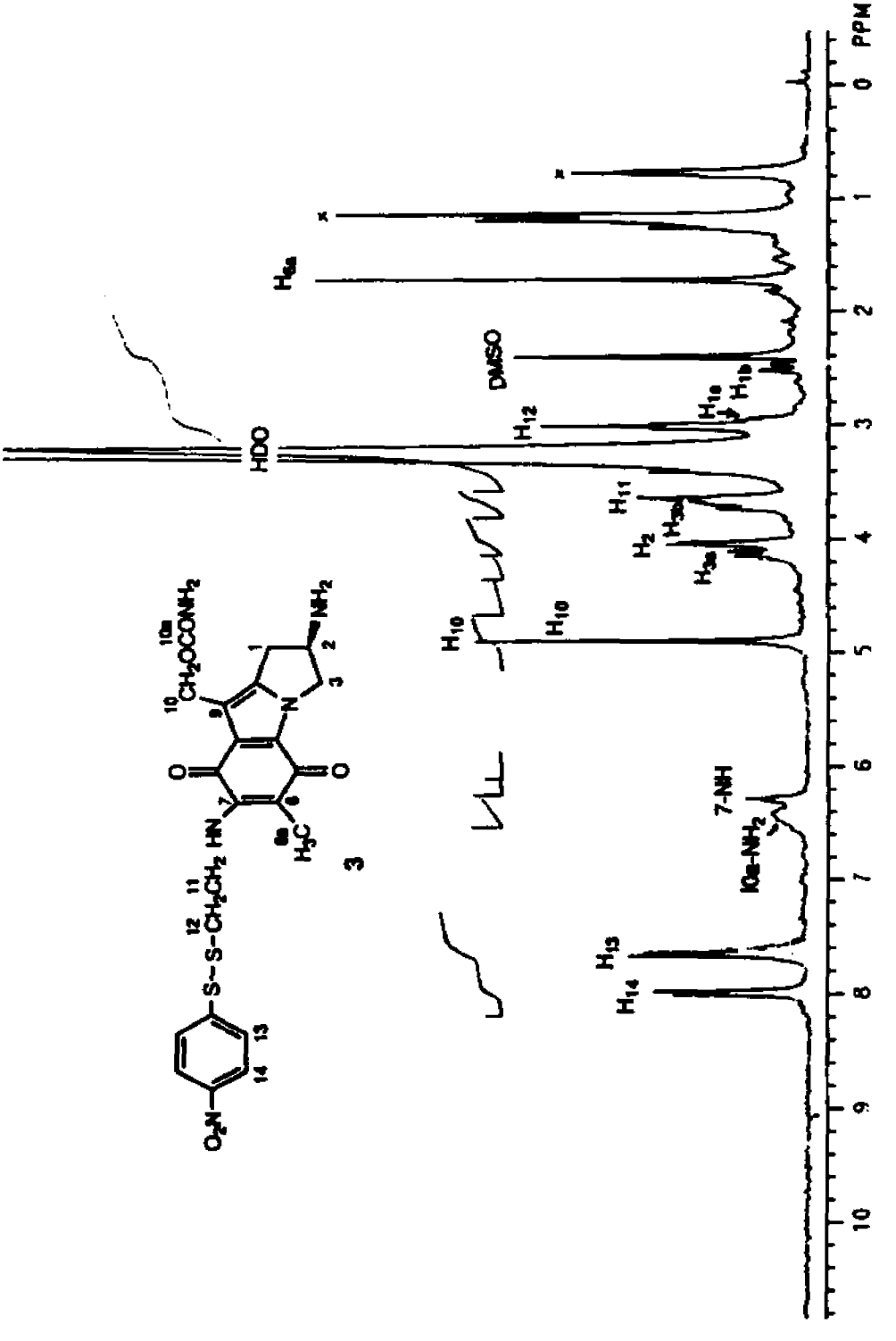

Figure 10. Proton NMR spectrum of 3 in DMSO-d6.

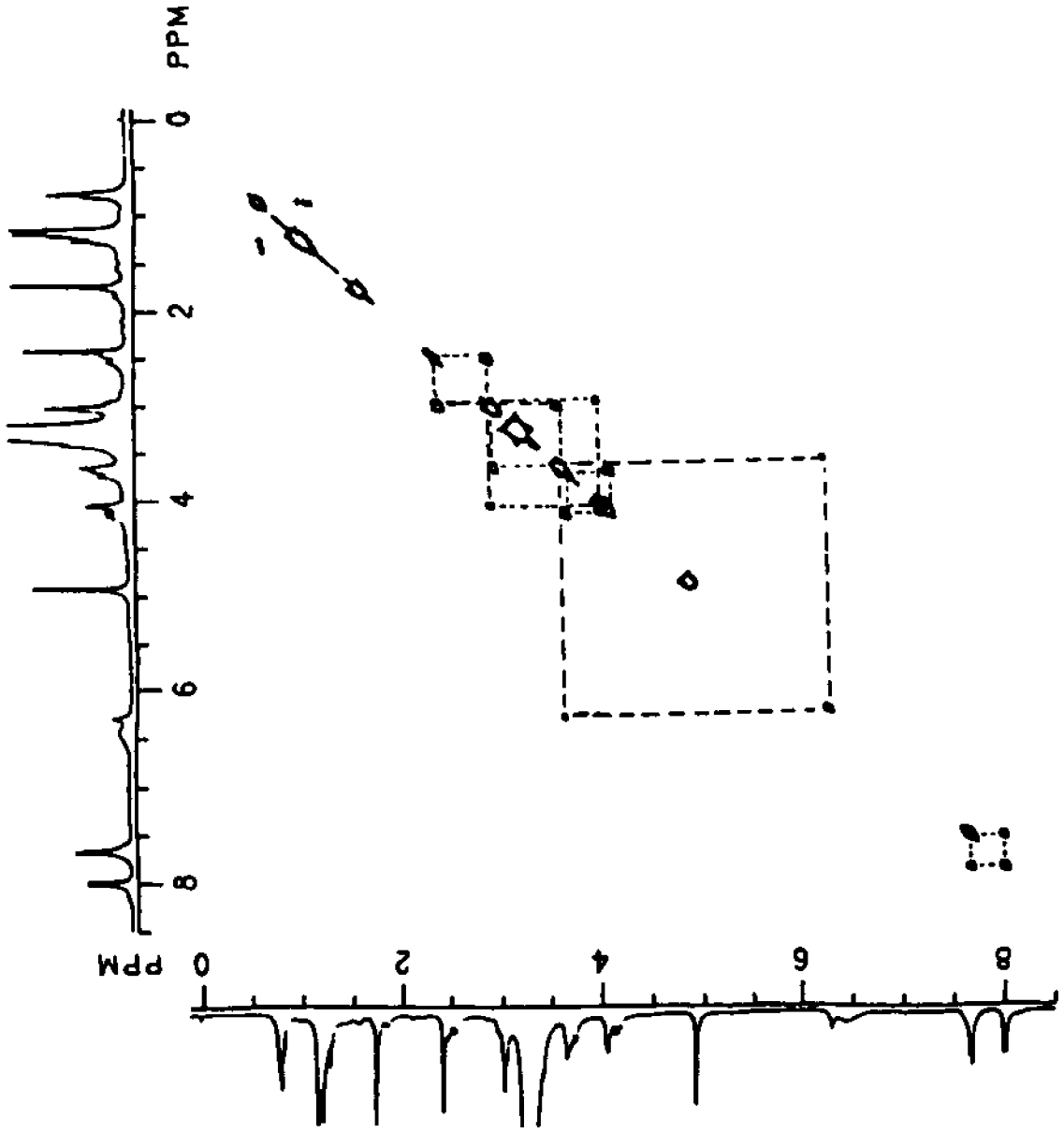

Figure 11. 2D NMR spectrum of 3 in DMSO-d6.

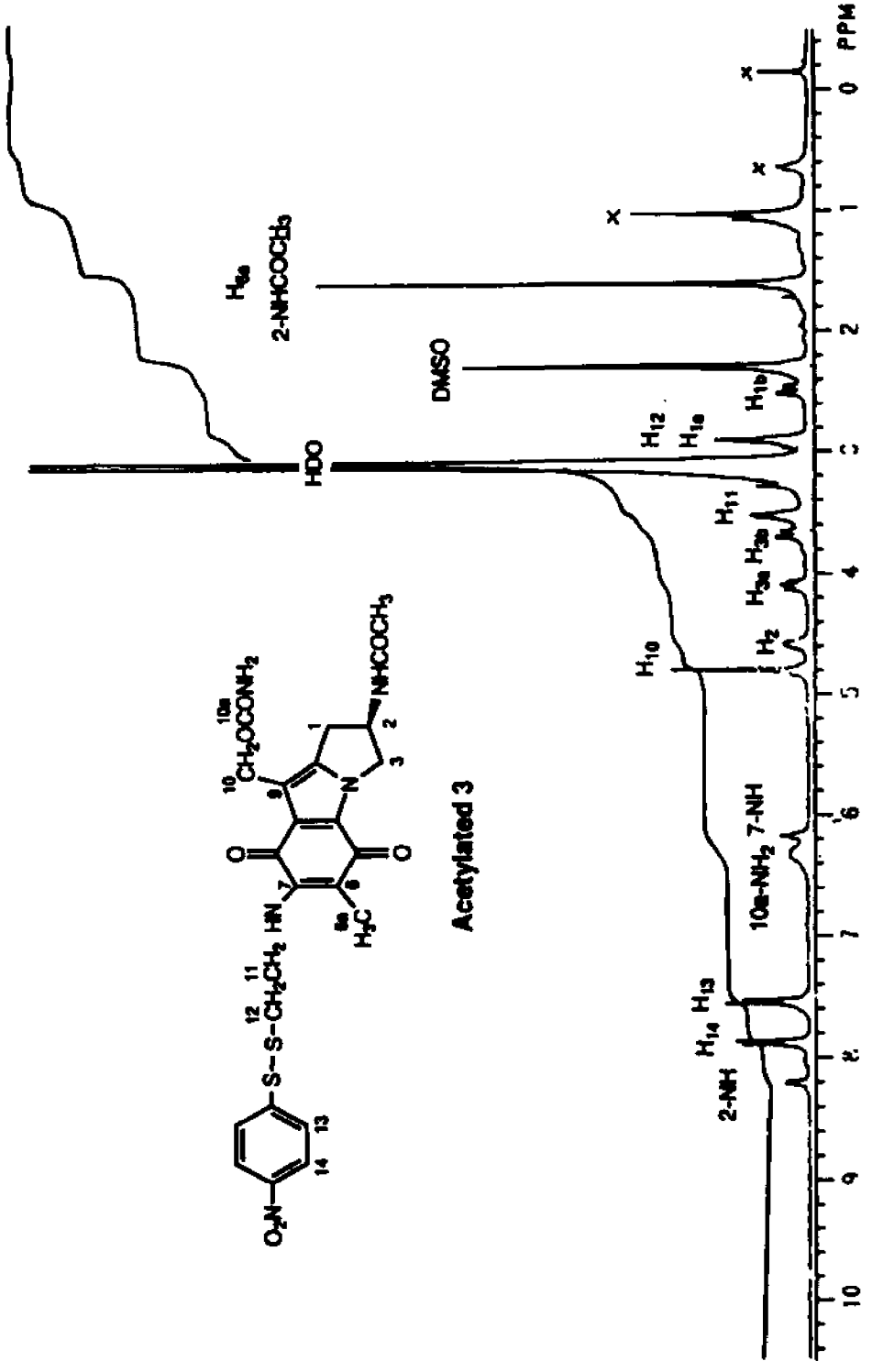

Figure 12. Proton NMR spectrum of **acetylated 3** in DMSO-d6.

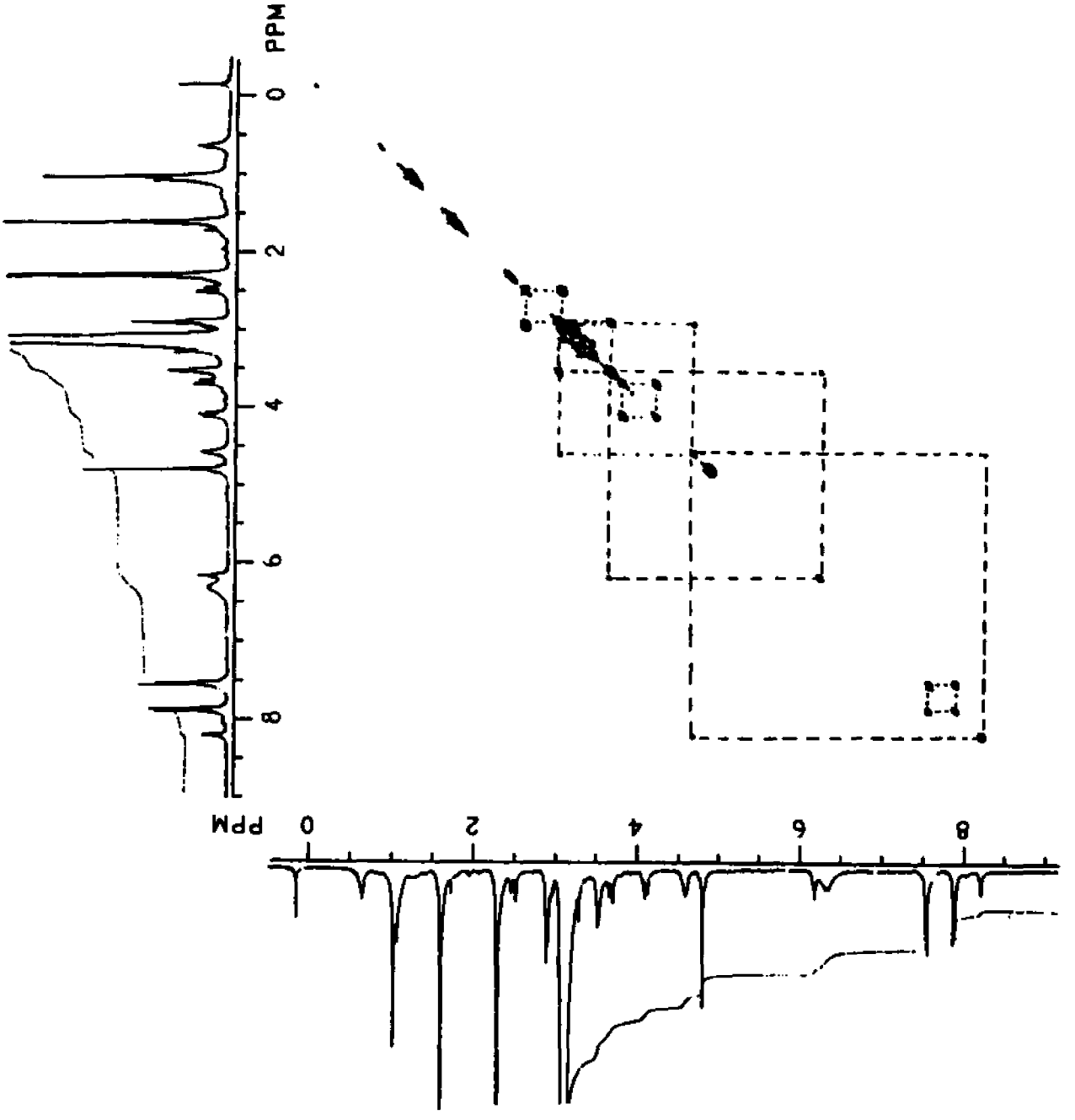

Figure 13. 2D NMR spectrum of acetylated 3 in DMSO-d6.

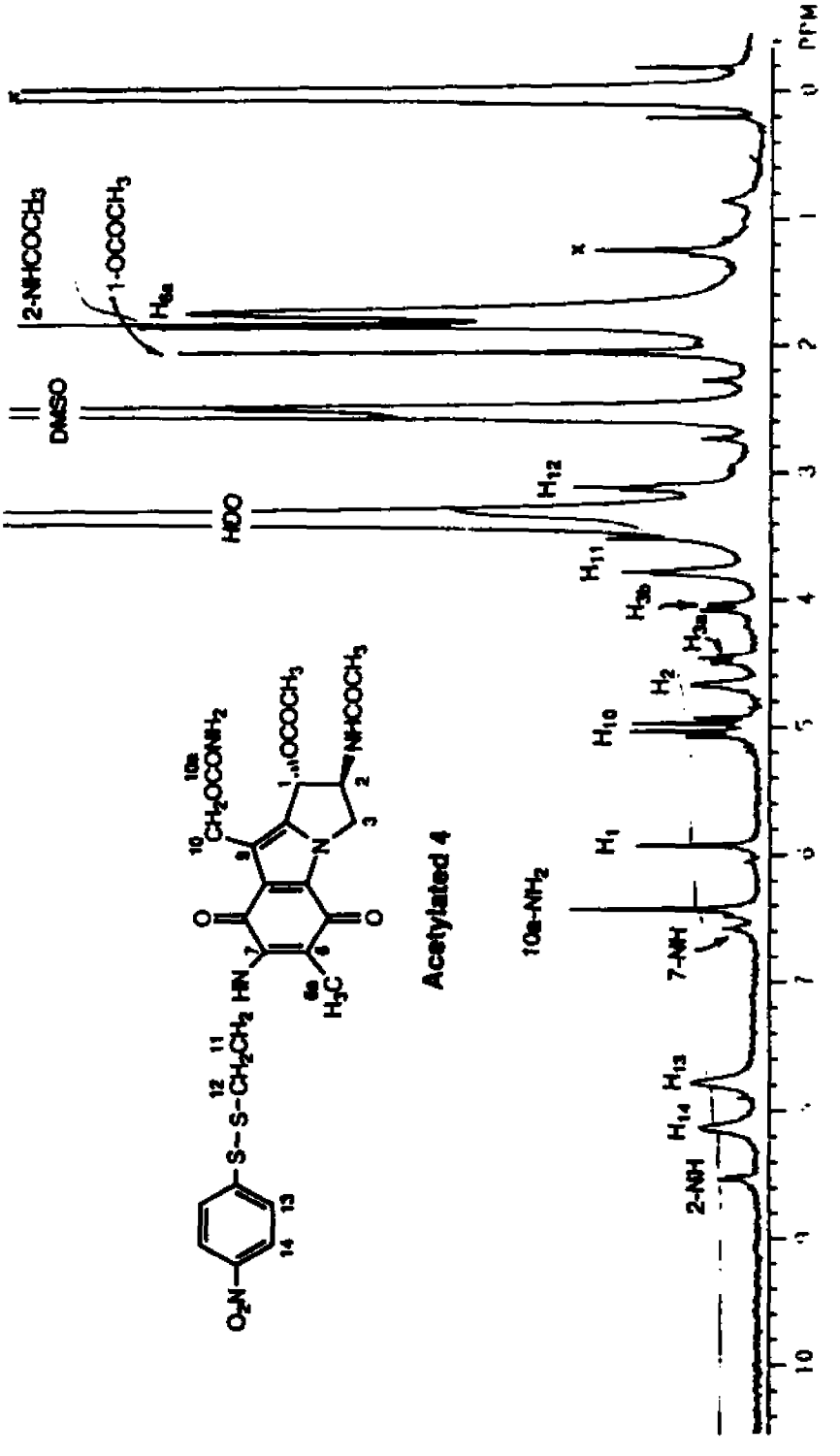

Figure 14. Proton NMR spectrum of **acetylated 4** in DMSO-d6.

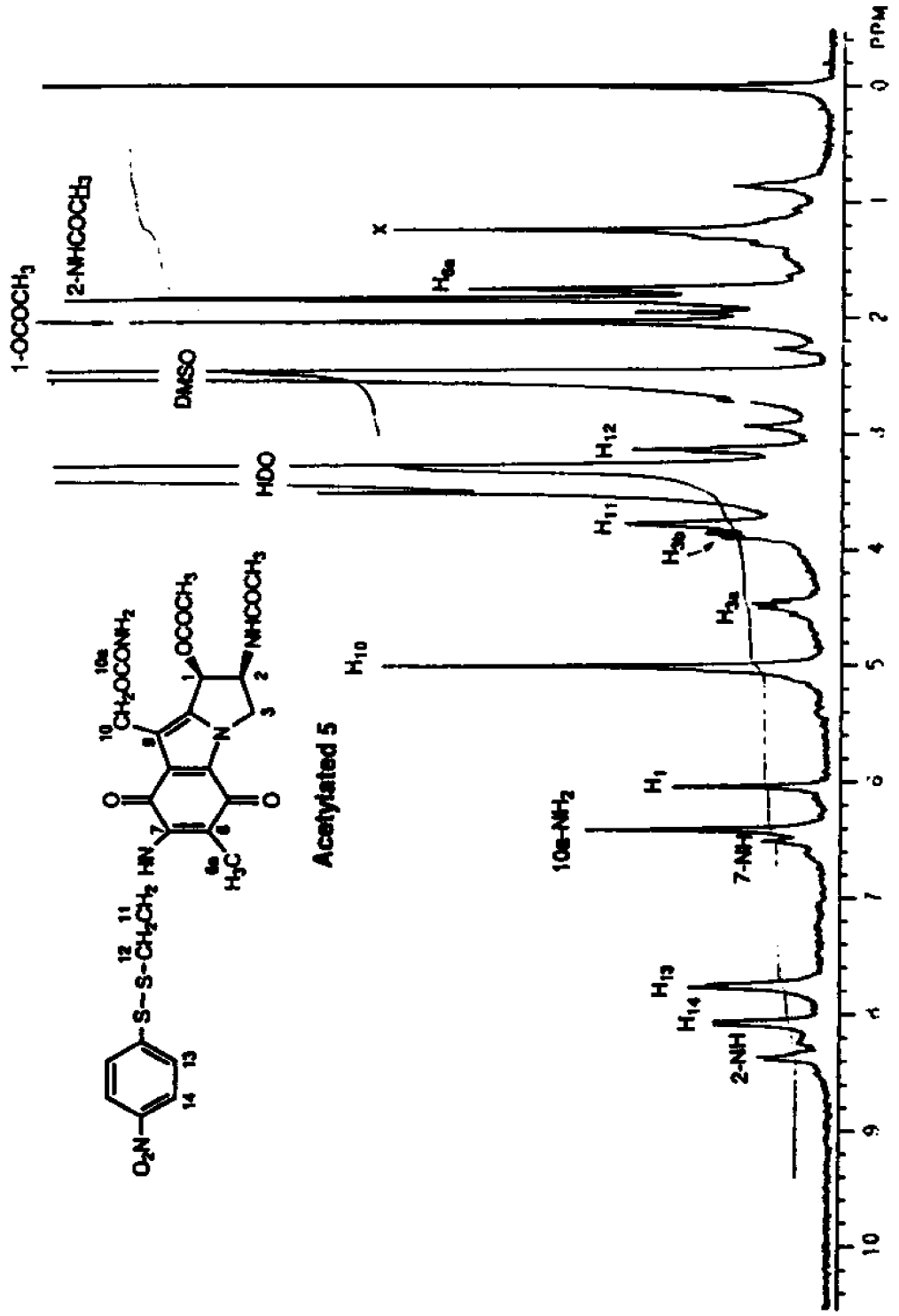

Figure 15. Proton NMR spectrum of acetylated 5 in DMSO-d6.

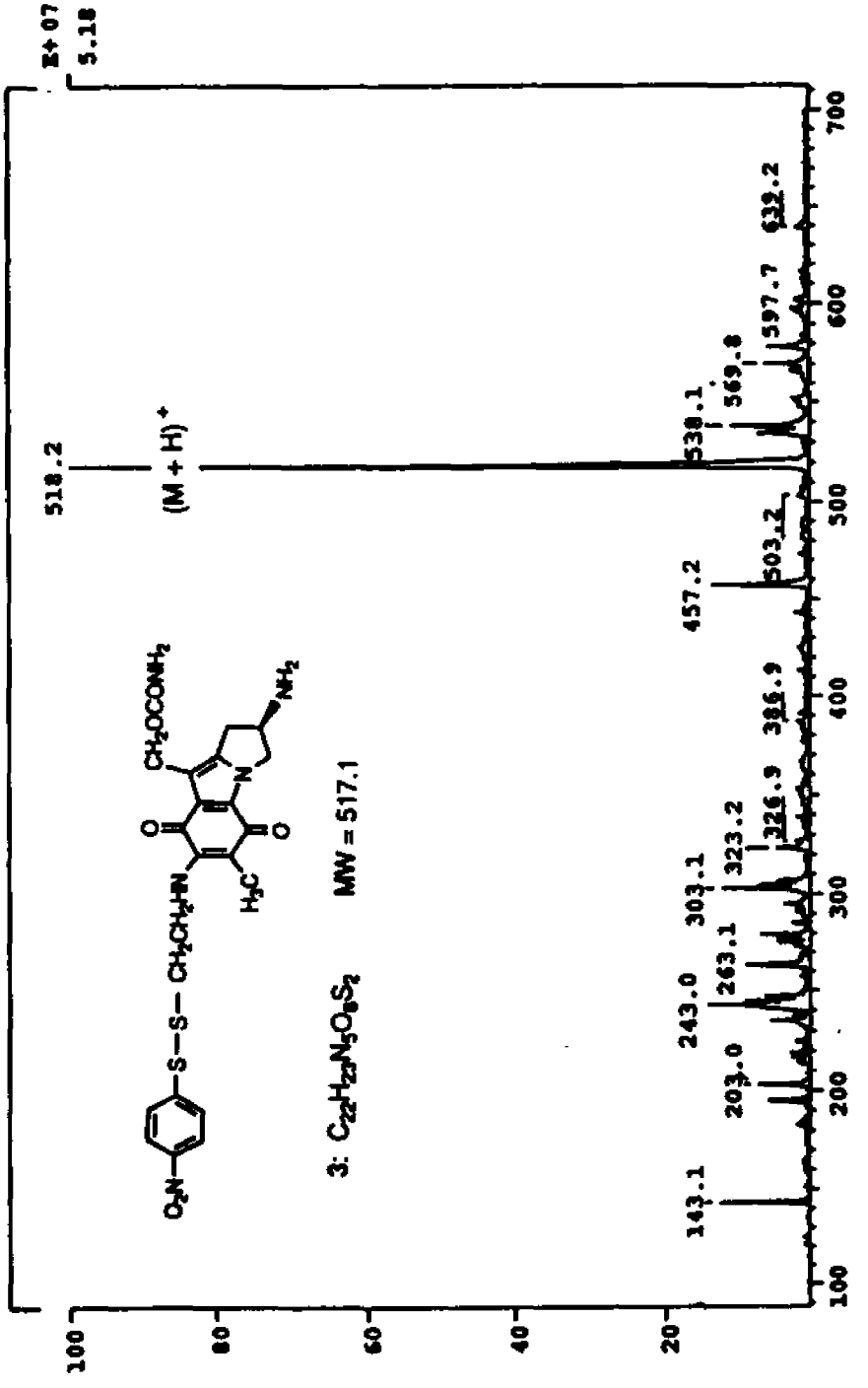

Figure 16. Mass spectrum of 3 in an electrospray analysis.

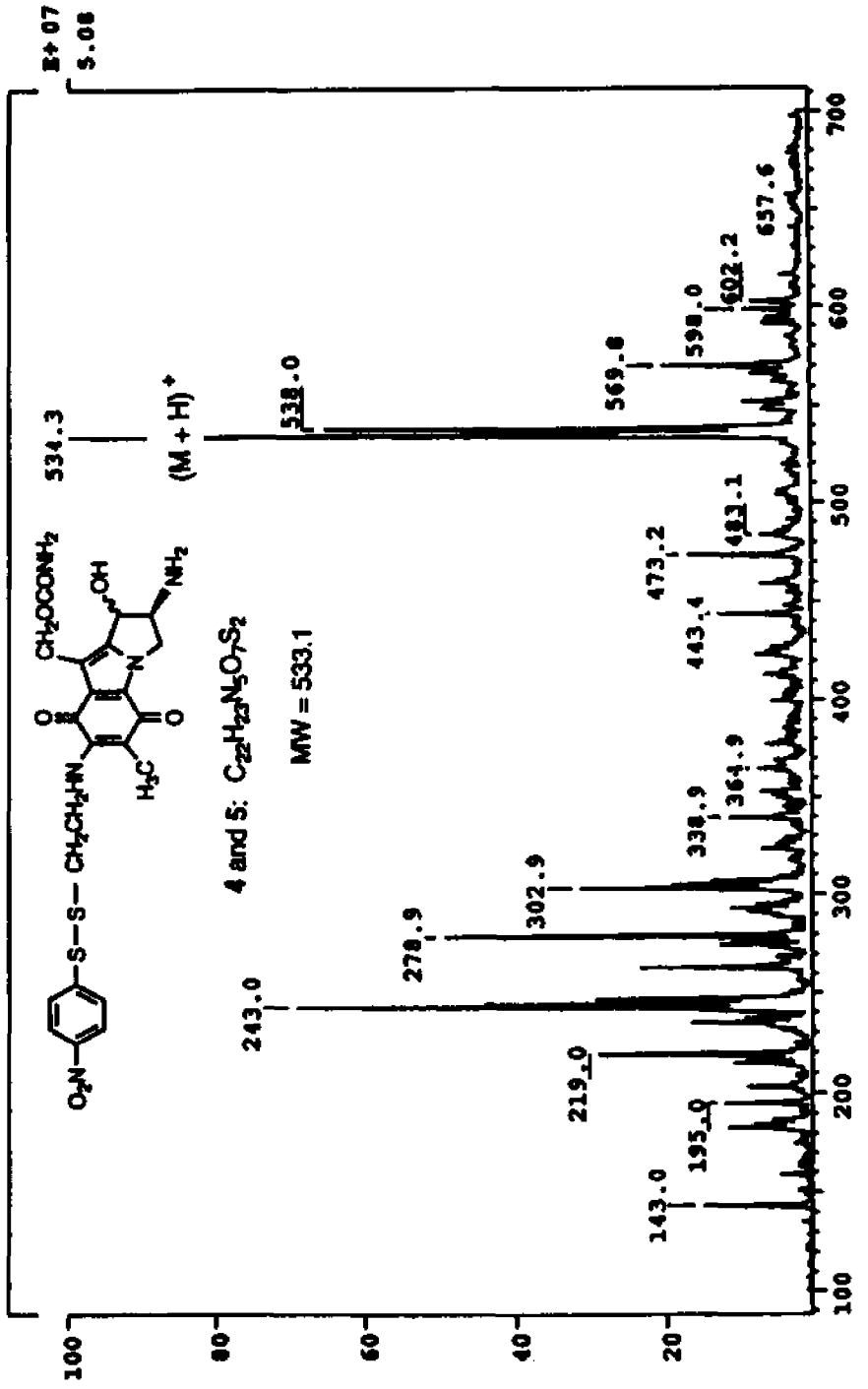

Figure 17. Mass spectrum of 4 and 5 mixture (4/5 1:1.2) in an electrospray analysis.

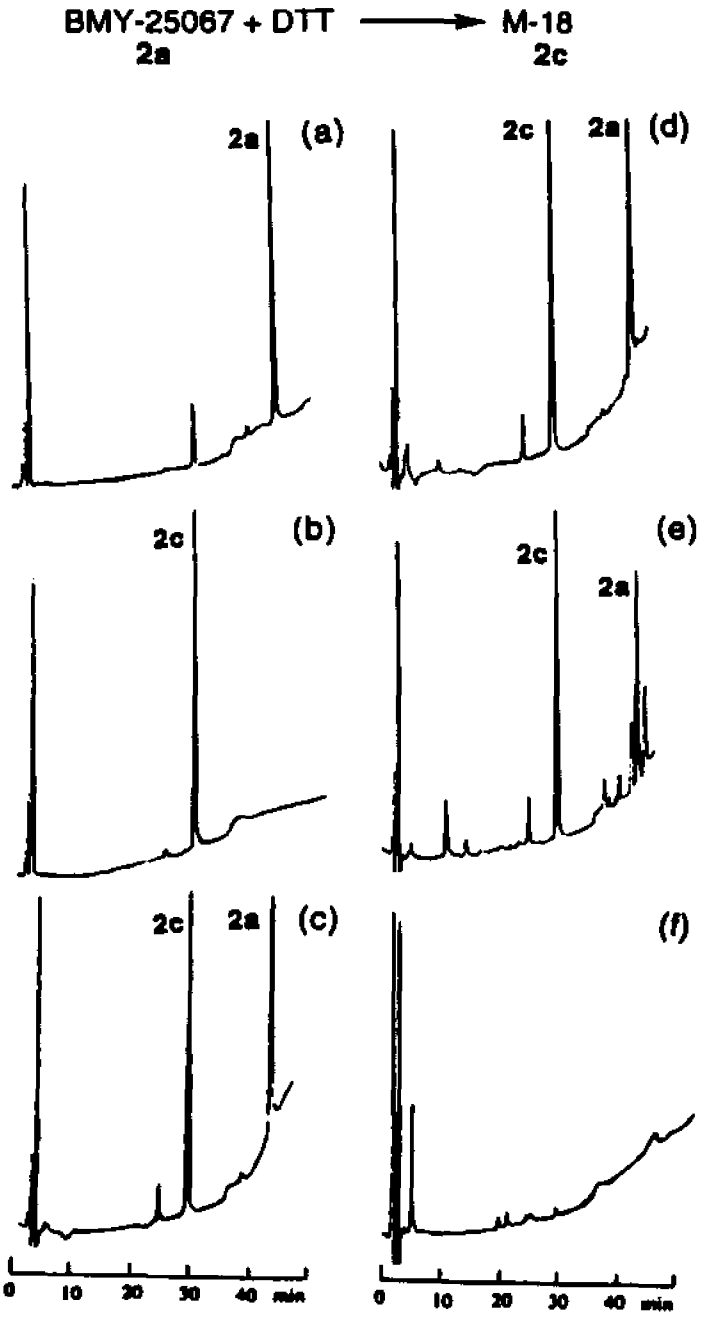

Figure 18. HPLC analysis of the reduction of BMY-25067 and the formation of the dimer of MC (M-18) from BMY-25067 by DTT activation in the various molar ratio of BMY-25067 : DTT. (a) Standard BMY-25067 (2a). (b) Standard M-18 (2c). (c) BMY-25067 : DTT 1:0.5. (d) BMY-25067 : DTT 1:1. (e) BMY-25067 : DTT 1:2. (f) BMY-25067 : DTT 1:5.

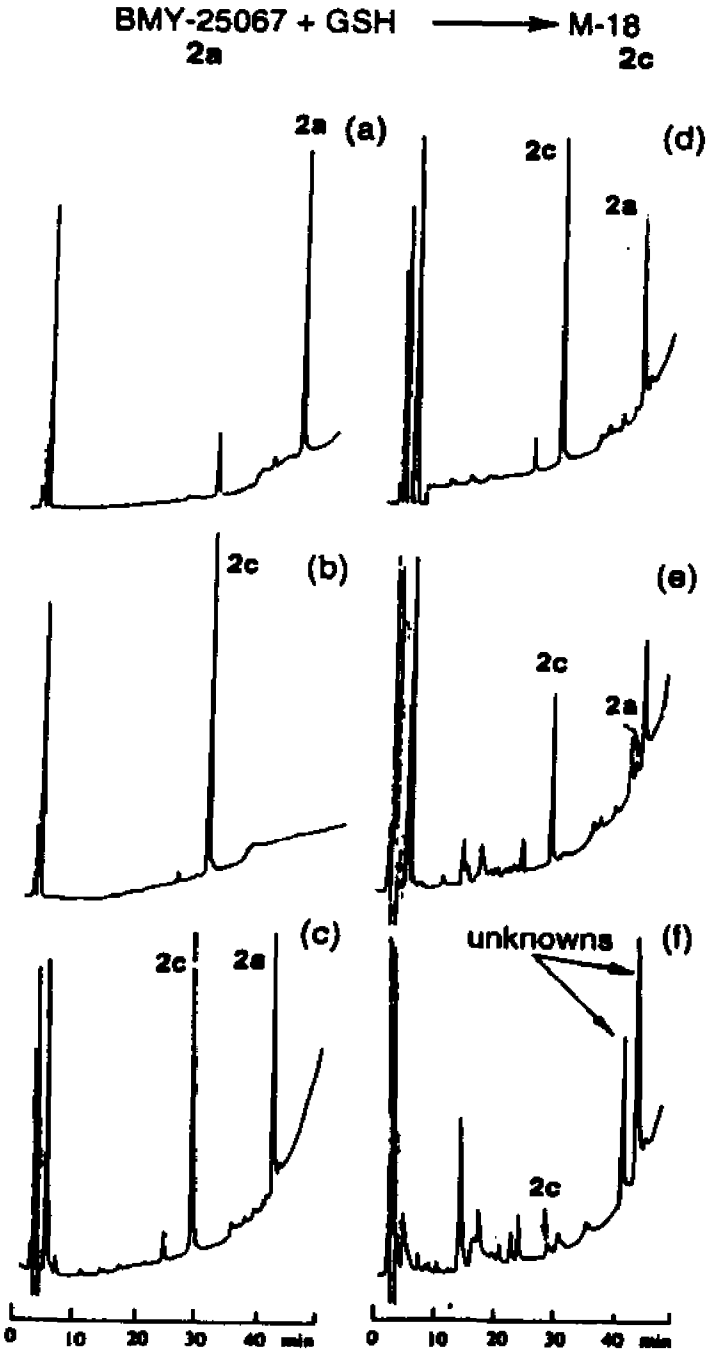

Figure 19. HPLC analysis of the reduction of BMY-25067 and the formation of the dimer of MC (M-18) from BMY-25067 by GSH activation in the various molar ratio of BMY-25067 : GSH. (a) Standard BMY-25067 (2a). (b) Standard M-18 (2c). (c) BMY-25067 : GSH 1:0.5. (d) BMY-25067 : GSH 1:1. (e) BMY-25067 : GSH 1:2. (f) BMY-25067 : GSH 1:5.

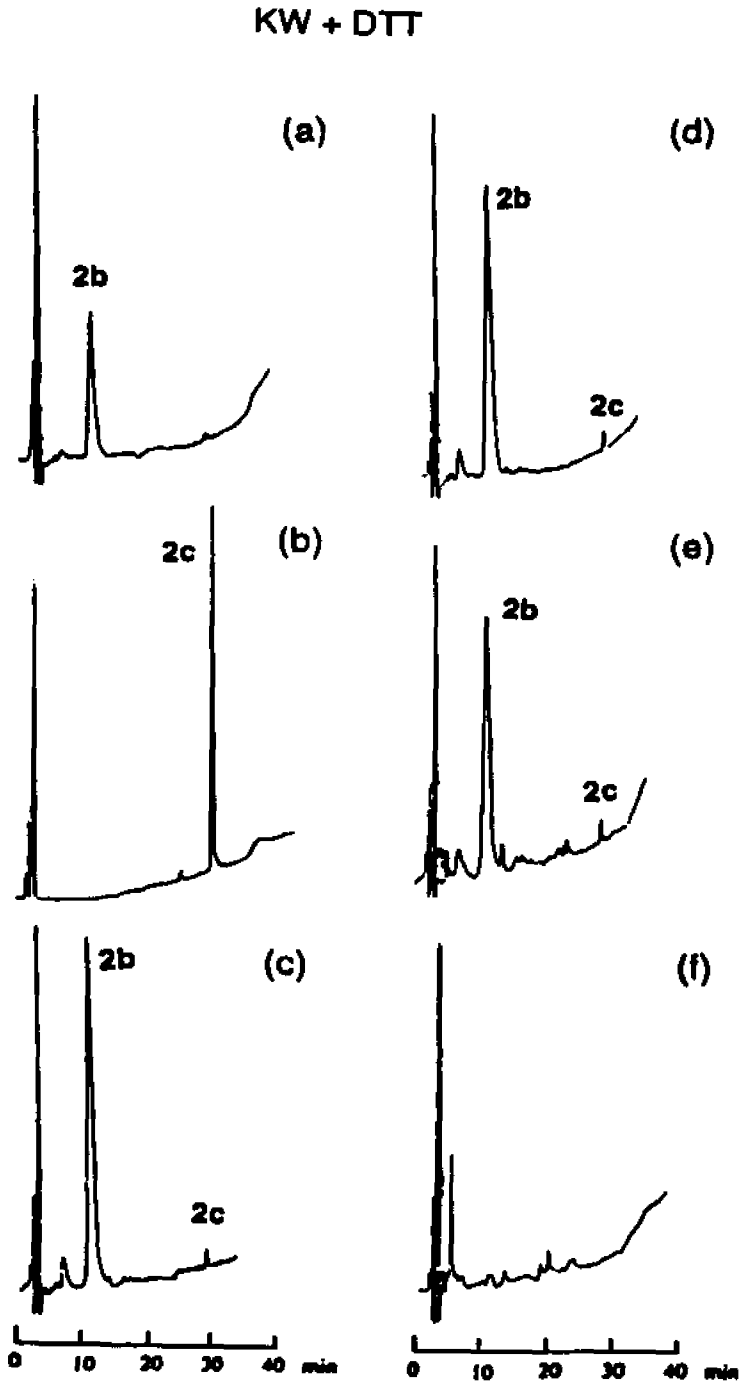

Figure 20. HPLC analysis of the reduction of KW-2149 and the formation of the dimer of MC (M-18) from KW-2149 by DTT activation in the various molar ratio of KW-2149 : DTT. (a) Standard KW-2149 (2b). (b) Standard M-18 (2c). (c) KW-2149 : DTT 1:0.5. (d) KW-2149 : DTT 1:1. (e) KW-2149 : DTT 1:2. (f) KW-2149 : DTT 1:5.

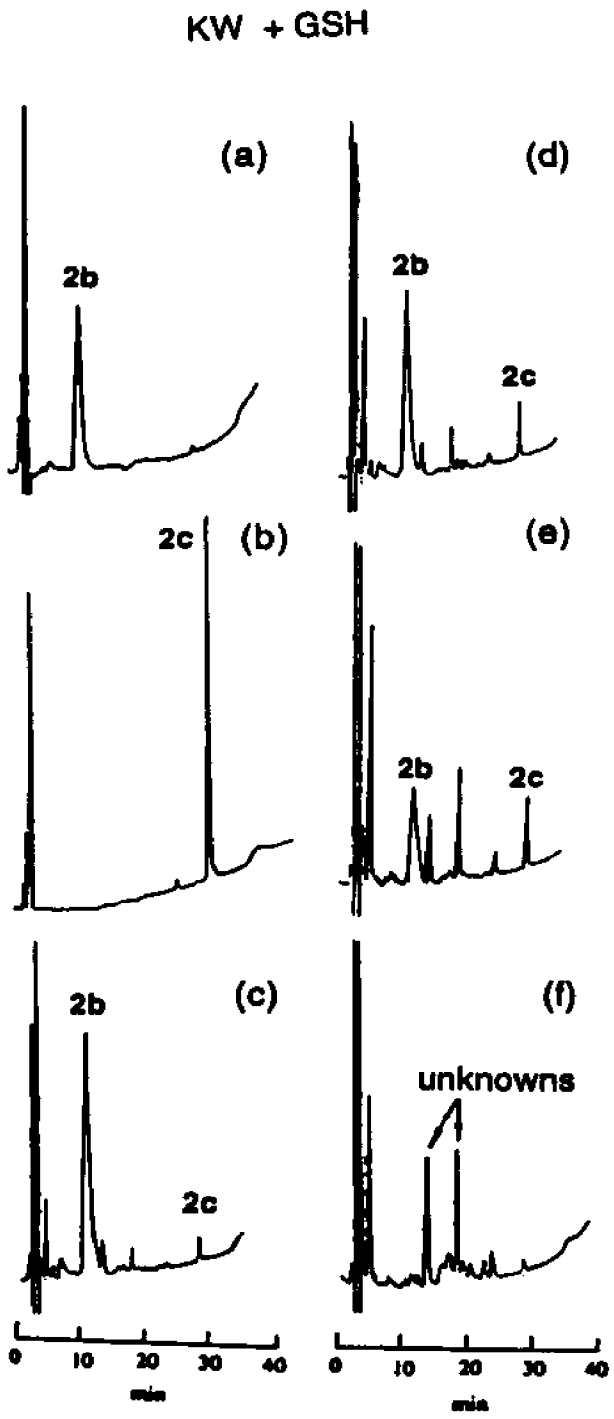

Figure 21. HPLC analysis of the reduction of KW-2149 and the formation of the dimer of MC (M-18) from KW-2149 by GSH activation in the various molar ratio of KW-2149 : GSH. (a) Standard KW-2149 (2b). (b) Standard M-18 (2c). (c) KW-2149 : GSH 1:0.5. (d) KW-2149 : GSH 1:1. (e) KW-2149 : GSH 1:2. (f) KW-2149 : GSH 1:5.

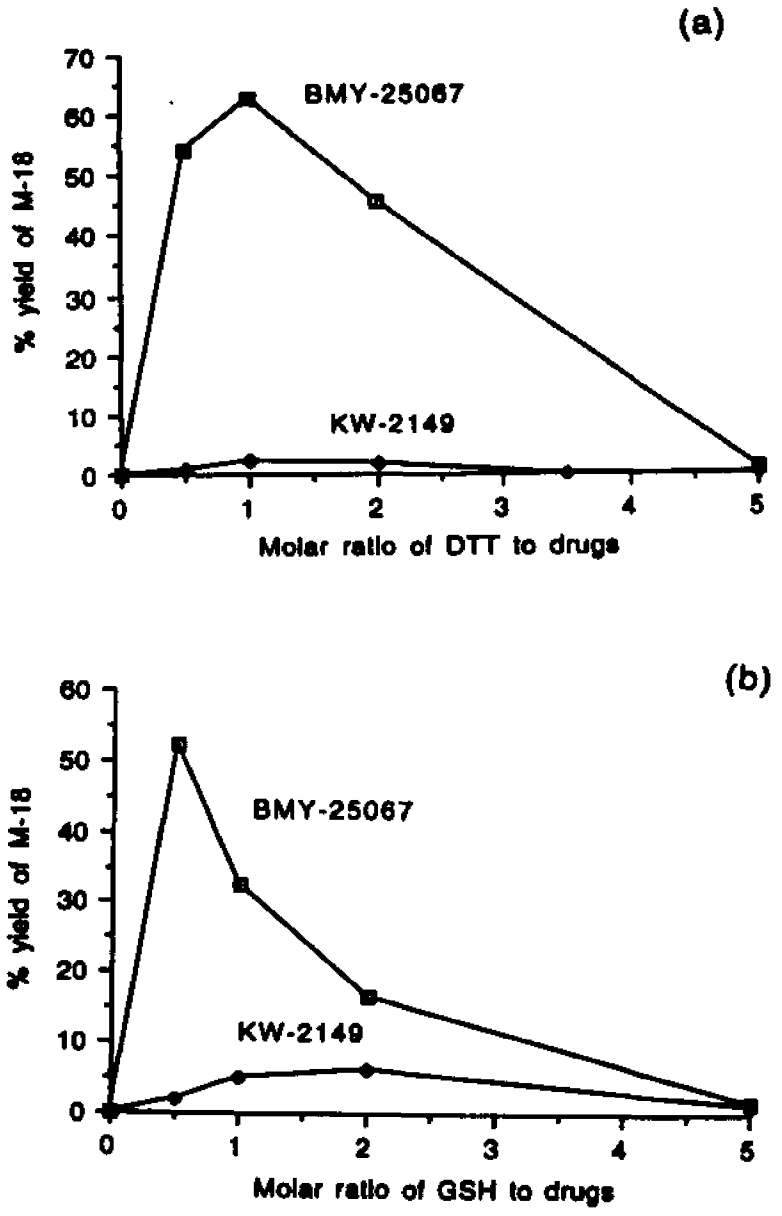

Figure 22. Plot of the conversion of BMY-25067 and KW-2149 to the dimer of MC (M-18) (% yield of M-18) in the presence of thiols as the function of the molar ratio of thiol to drug under otherwise standard conditions. (a) Thiol: DTT. (b) Thiol: GSH.

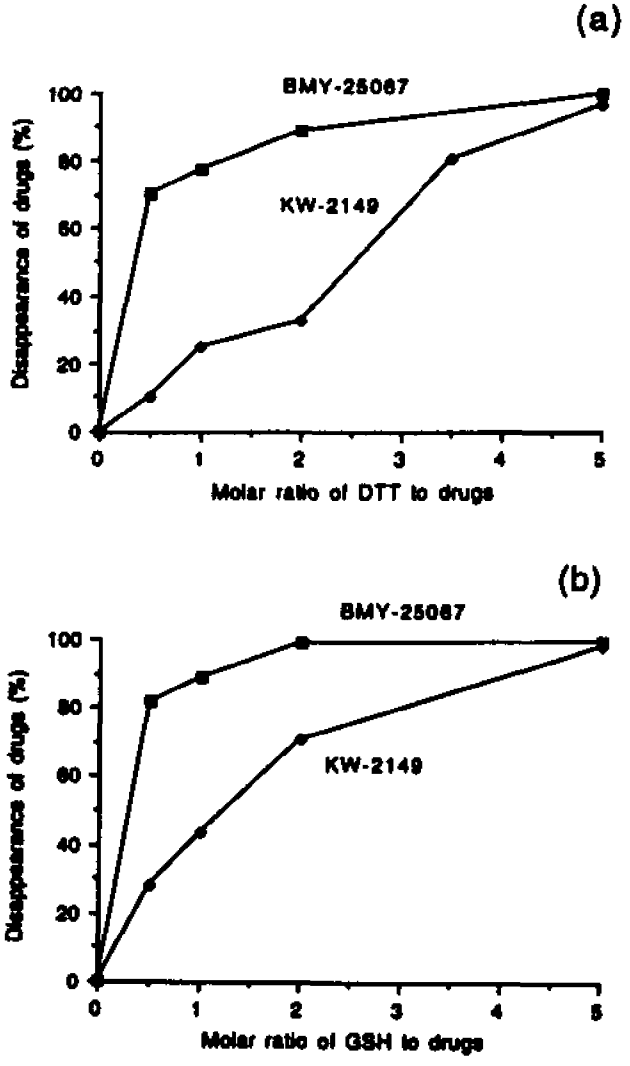

Figure 23. Plot of disappearance (%) of BMY-25067 and KW-2149 in the presence of thiols as function of the ratio of thiol to drug under otherwise standard conditions. (a) Thiol: DTT. (b) Thiol: GSH.

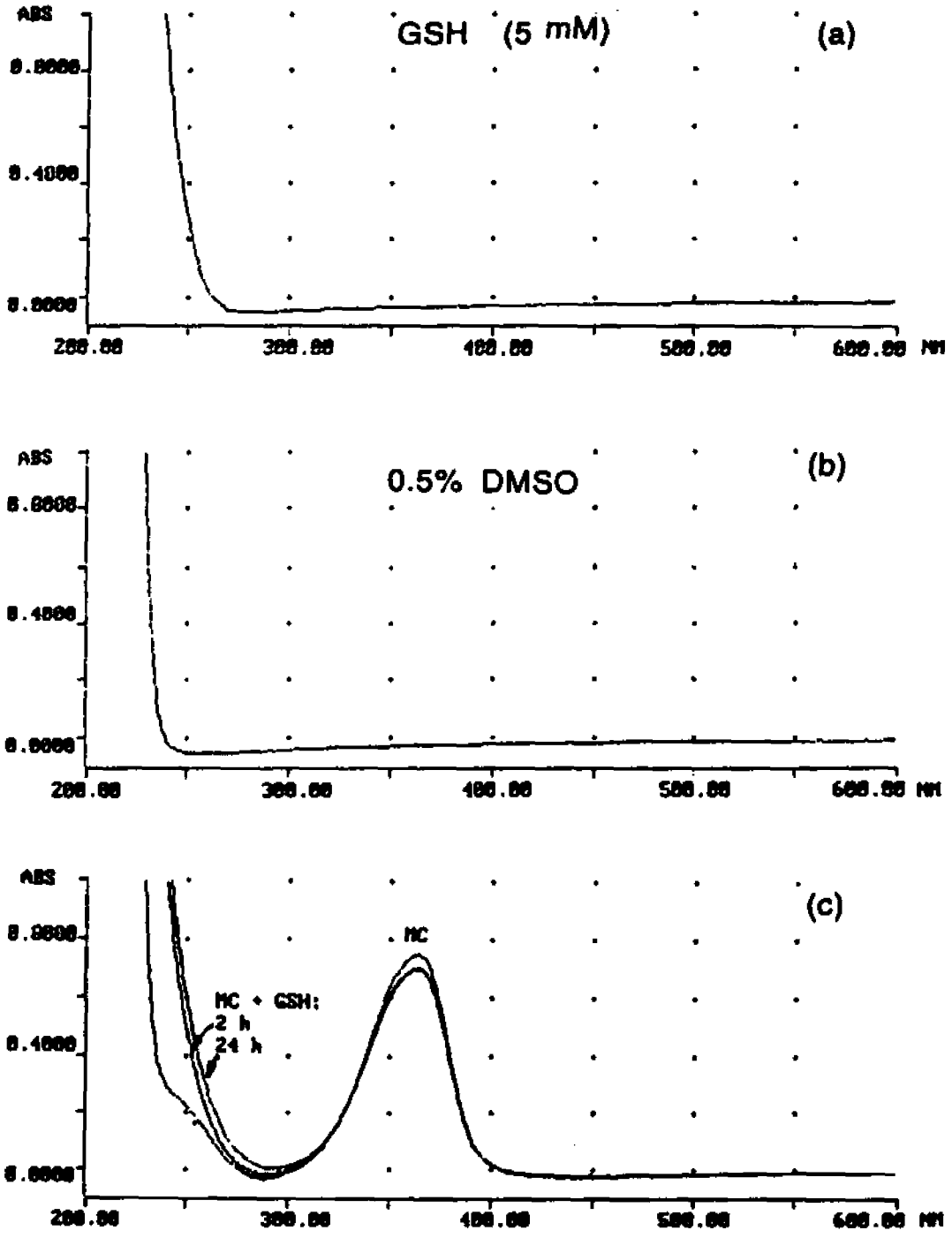
ABS
GSH (5 mM)
(a)
0.8000
0.4000
0.0000
200.00
300.00
400.00
500.00
600.00 NM
ABS
0.5% DMSO
(b)
0.8000
0.4000
0.0000
200.00
300.00
400.00
500.00
600.00 NM
ABS
(c)
MC
MC + GSH:
2 h
24 h
0.8000
0.4000
0.0000
200.00
300.00
400.00
500.00
600.00 NM

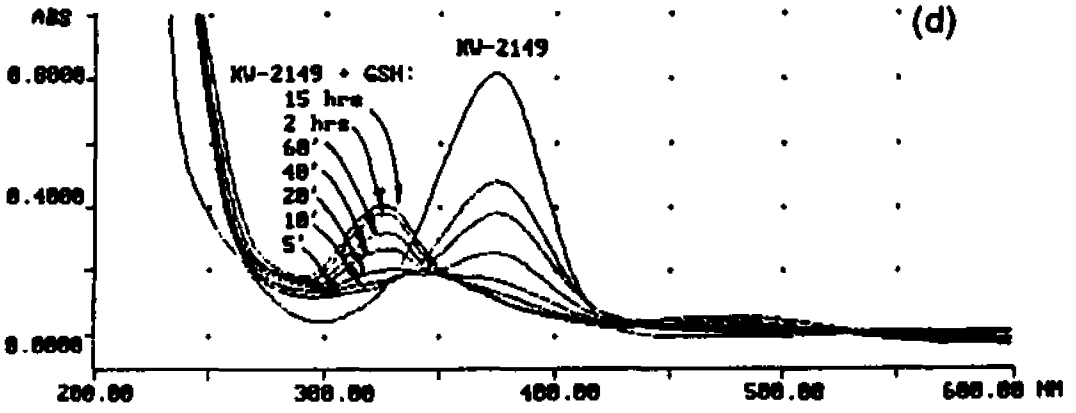
ABS
0.8000
0.4000
0.0000
(d)
KV-2149
KV-2149 + GSH:
15 hrs
2 hrs
60'
40'
20'
10'
5'
200.00
300.00
400.00
500.00
600.00 NM

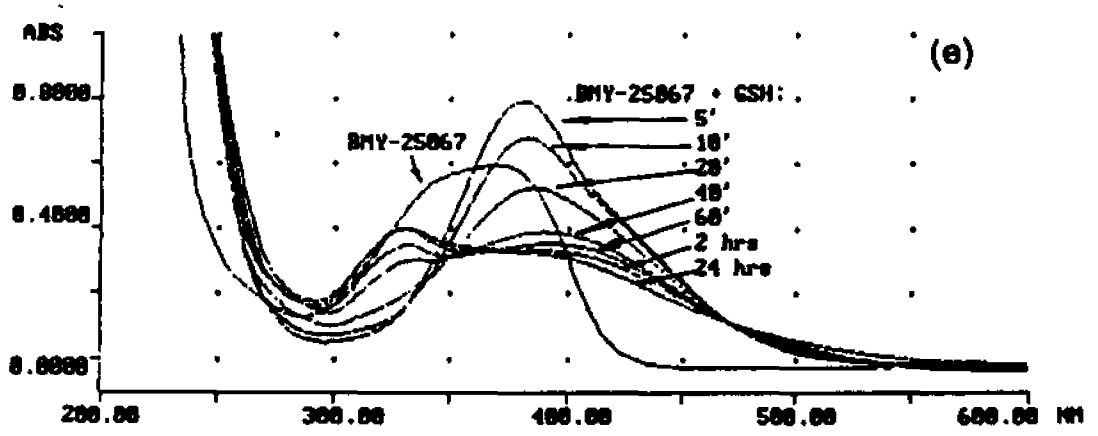
ABS
0.8000
0.4000
0.0000
(e)
BMY-25867 + GSH:
5'
10'
20'
40'
60'
2 hrs
24 hrs
BMY-25867
200.00
300.00
400.00
500.00
600.00 NM

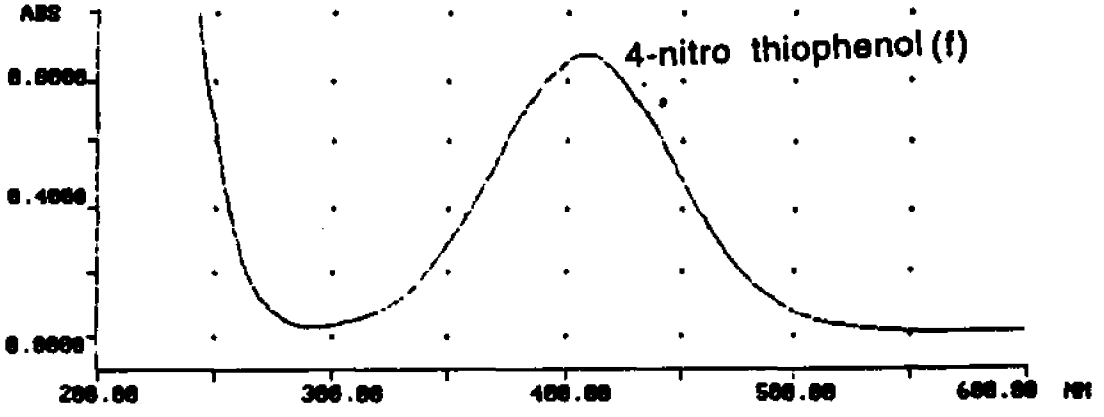
ABS
0.8000
0.4000
0.0000
4-nitro thiophenol (f)
200.00
300.00
400.00
500.00
600.00 NM

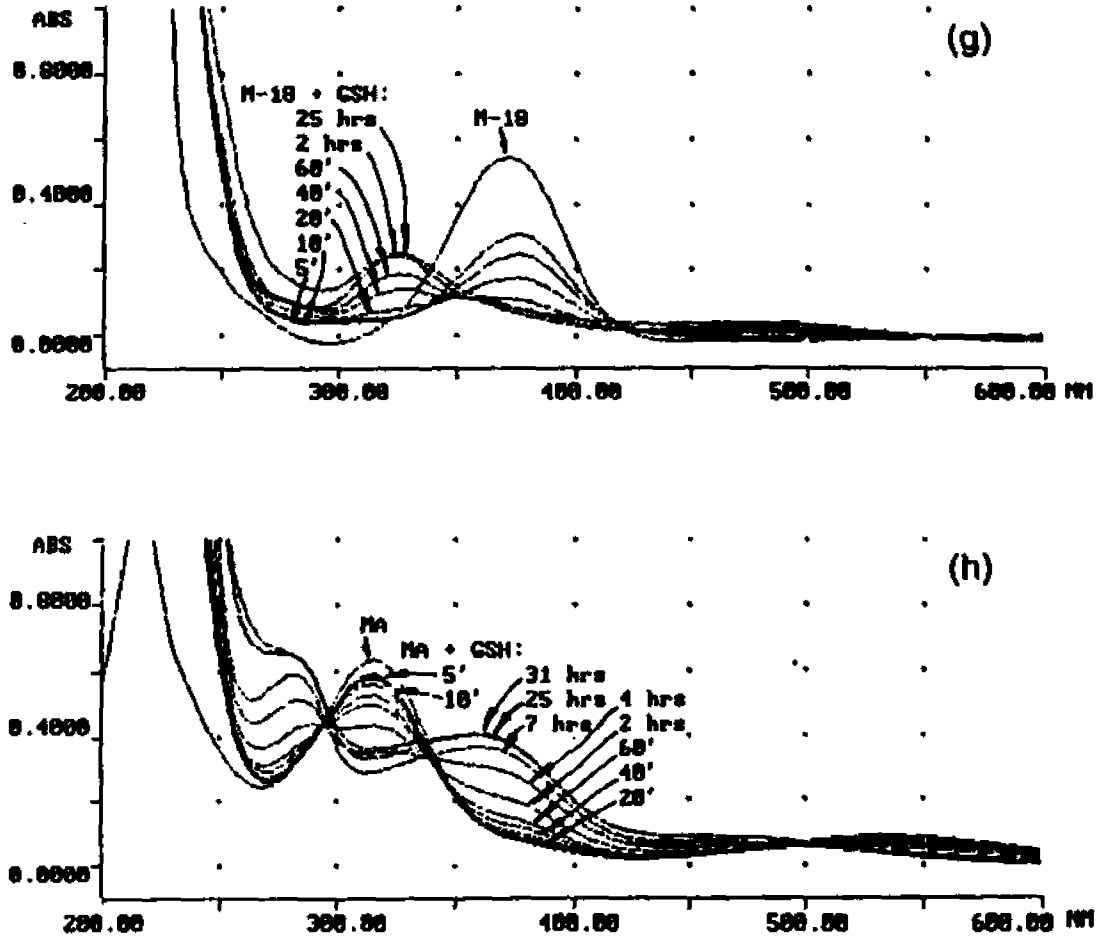

Figure 24. Kinetics of the reduction of the disulfide analogs of MC by the activation of GSH (5 mM) in 0.015 M tris, pH 7.5, assayed by UV. Comparison with that of MA and MC. (a) Control UV spectrum of GSH (5 mM) in 0.015 M tris, pH 7.5. (b) Control UV spectrum of 0.5% DMSO in 0.015 M tris, pH 7.5. (c) UV spectra of MC before adding GSH and after adding GSH at 120 min and overnight. (d) UV spectrum of KW-2149 before adding GSH and the UV spectra of the solution of KW-2149 after adding GSH at 5, 10, 20, 40, 60 and 120 min and also overnight. (e) UV spectrum of BMY-25067 before adding GSH and the UV spectra of the solution of BMY-25067 after adding GSH at 5, 10, 20, 40, 60 and 120 min and also overnight. (f) Control UV spectrum of 4-nitro thiophenol (0.035 mM). (g) UV spectrum of M-18 before adding GSH and the UV spectra of the solution of M-18 after adding GSH at 5, 10, 20, 40, 60 and 120 min and also overnight. (h) UV spectrum of MA before adding GSH and the UV spectra of the solution of MA after adding GSH at 5, 10, 20, 40, 60, 120 min, 7 h, 25 h and also 31 h.

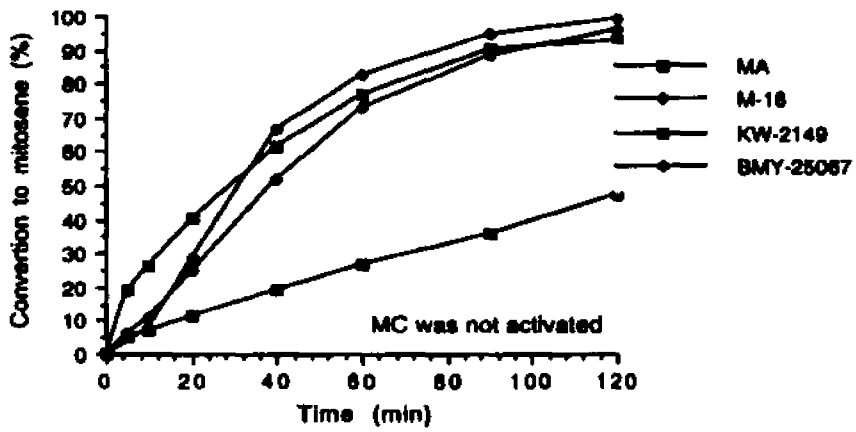

Figure 25. Plot of the conversion of mitosanes to the mitosenes (%) by the activation of GSH as the function of incubation time (minutes). Comparison of the conversion to mitosene from KW-2149, BMY-25067 and M-18 with that from MA and MC.

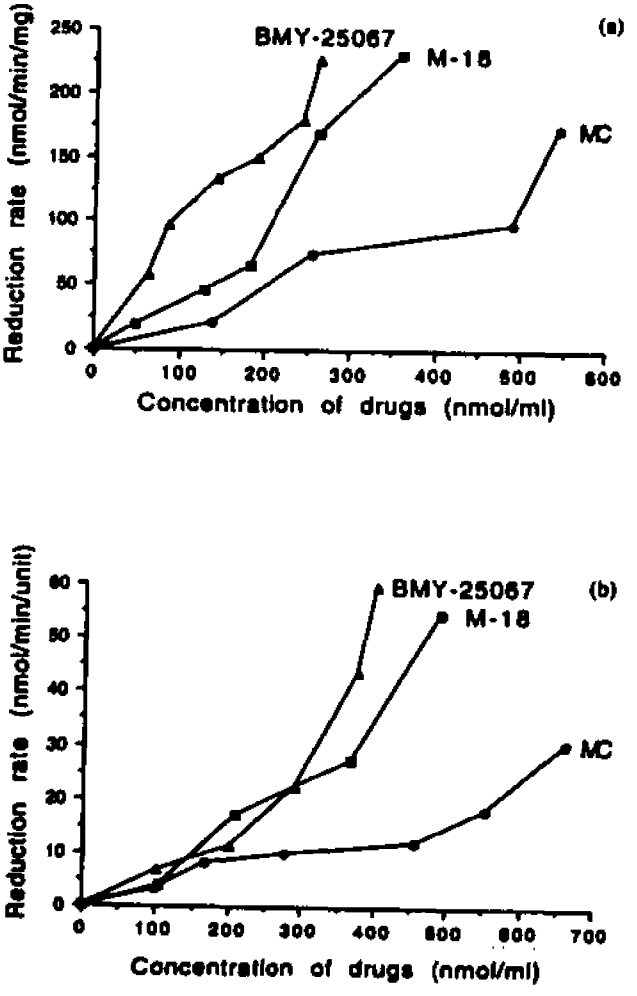

Figure 26. Comparison of the enzymatic reduction rate of BMY-25067 and M-18 with that of MC. (a) Activation by xanthine oxidase/NADH. (b) Activation by NADPH-cytochrome reductase/NADPH.

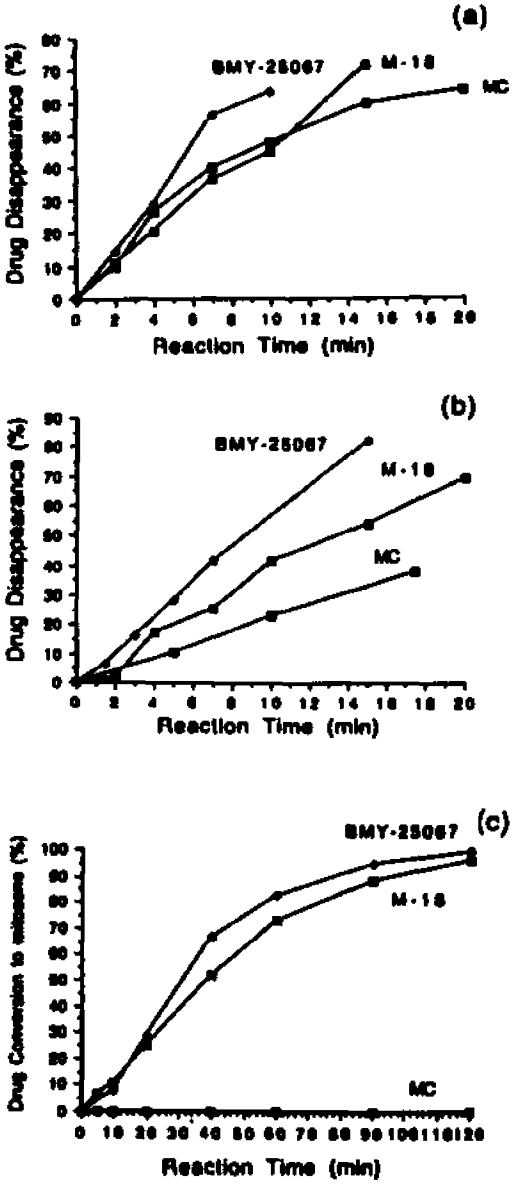

Figure 27. Comparison of the enzymatic activation kinetics of MC, BMY-25067 and M-18 (All drug concentration was 100 nmol/ml) with the GSH activation kinetics of MC, BMY-25067 and M-18. (a) Plot of the drug disappearance (%) by the cytochrome c reductase/NADPH activation as the function of incubation time (minutes). (b) Plot of the drug disappearance (%) by the xanthine oxidase/NADH activation as the function of incubation time (minutes). (c) Plot of the drug conversion to their mitosenes (%) by the GSH activation as the function of incubation time (min).

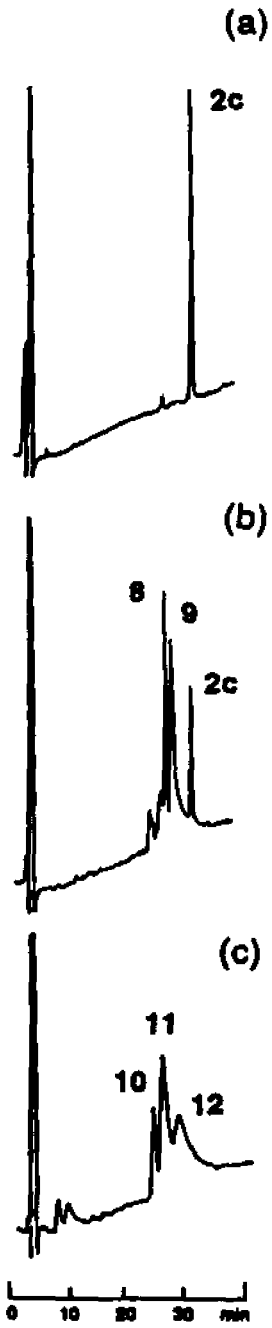

Figure 28. HPLC analysis of M-18 metabolites formed in the acid-catalytic hydrolysis of M-18 in 0.001 N HCl at 37 °C. (a) Standard M-18 (2c). (b) The reaction mixture incubated in 10 min. (c) The reaction mixture incubated in 2 h.

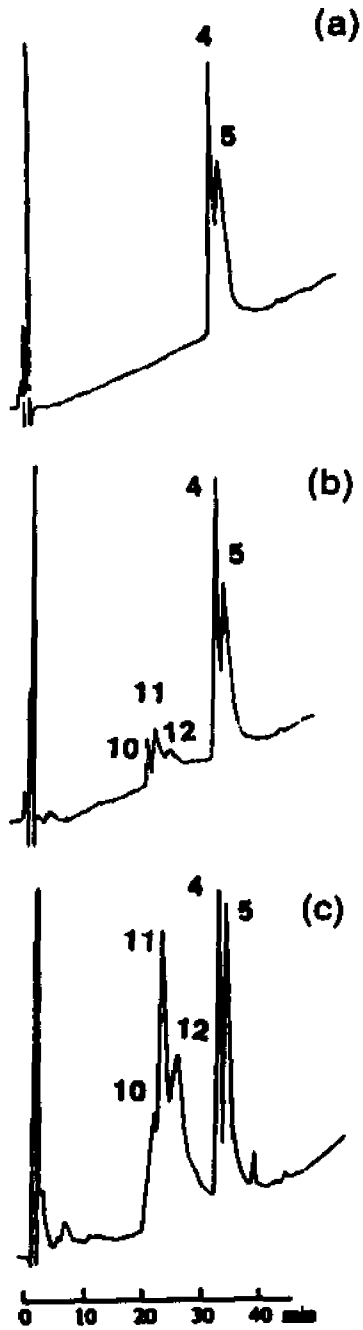

Figure 29. HPLC analysis for the identification of M-18 metabolites 10, 11 and 12. (a) The standard 4 and 5 mixture (4/5 1:1). (b) The formation of 10, 11 and 12 from 4 and 5 by the treatment of 4 and 5 with DTT. (c) The coinjection of the reaction mixture of (b) in this figure with that of (c) in figure 28.

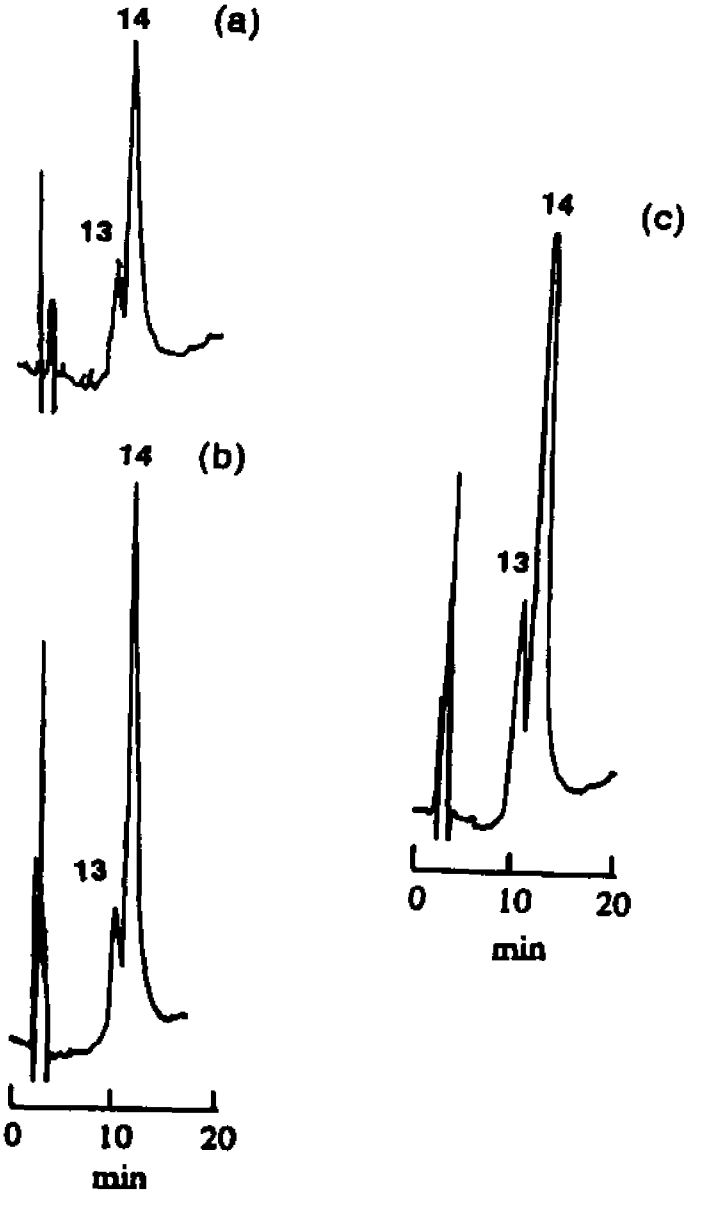

Figure 30. HPLC analysis of M-18 metabolites formed in the acid-catalytic hydrolysis of M-18 in 0.05 N HCl. (a) The reaction mixture incubated in 60 min. (b) Standard 13 (7-OH-M1) and 14 (7-OH-M2) (c) The coinjection of (a) with (b).

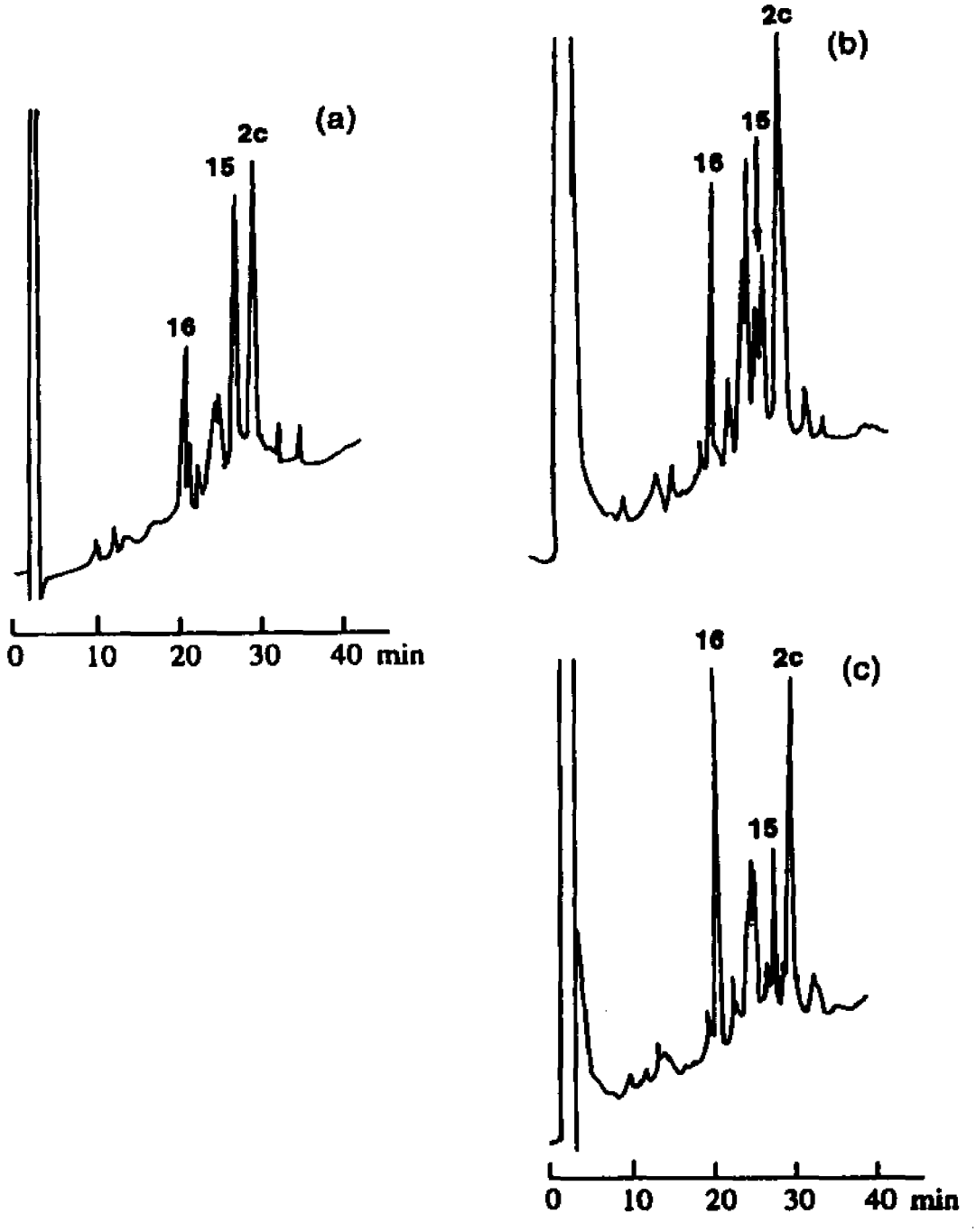

Figure 31. HPLC analysis of M-18 metabolites formed in the chemically and enzymatically reductive activation of M-18. (a) Catalytic hydrogenation (H_2/PtO_2). (b) Xanthine oxidase/NADH activation. (c) NADPH-cytochrome c reductase/NADPH activation.

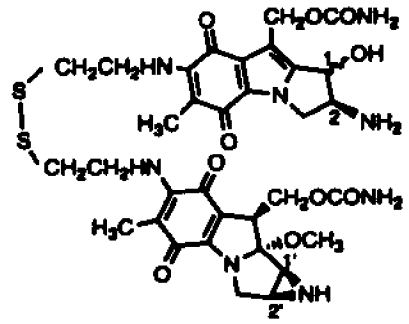

8: 1- α

9: 1- β

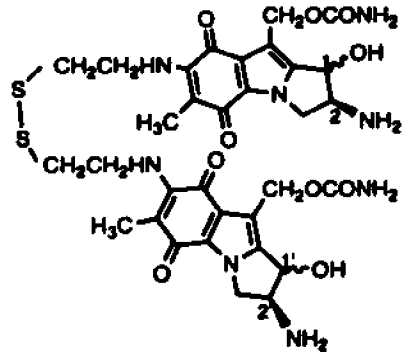

10: 1, 1'-α

11: 1-α, 1'-β

12: 1-β, 1'-β

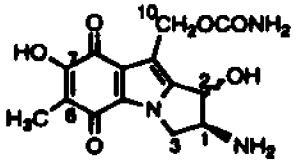

13: 1-α

14: 1-β

15: unknown

16: unknown

Figure 32. Structures of M-18 metabolites.

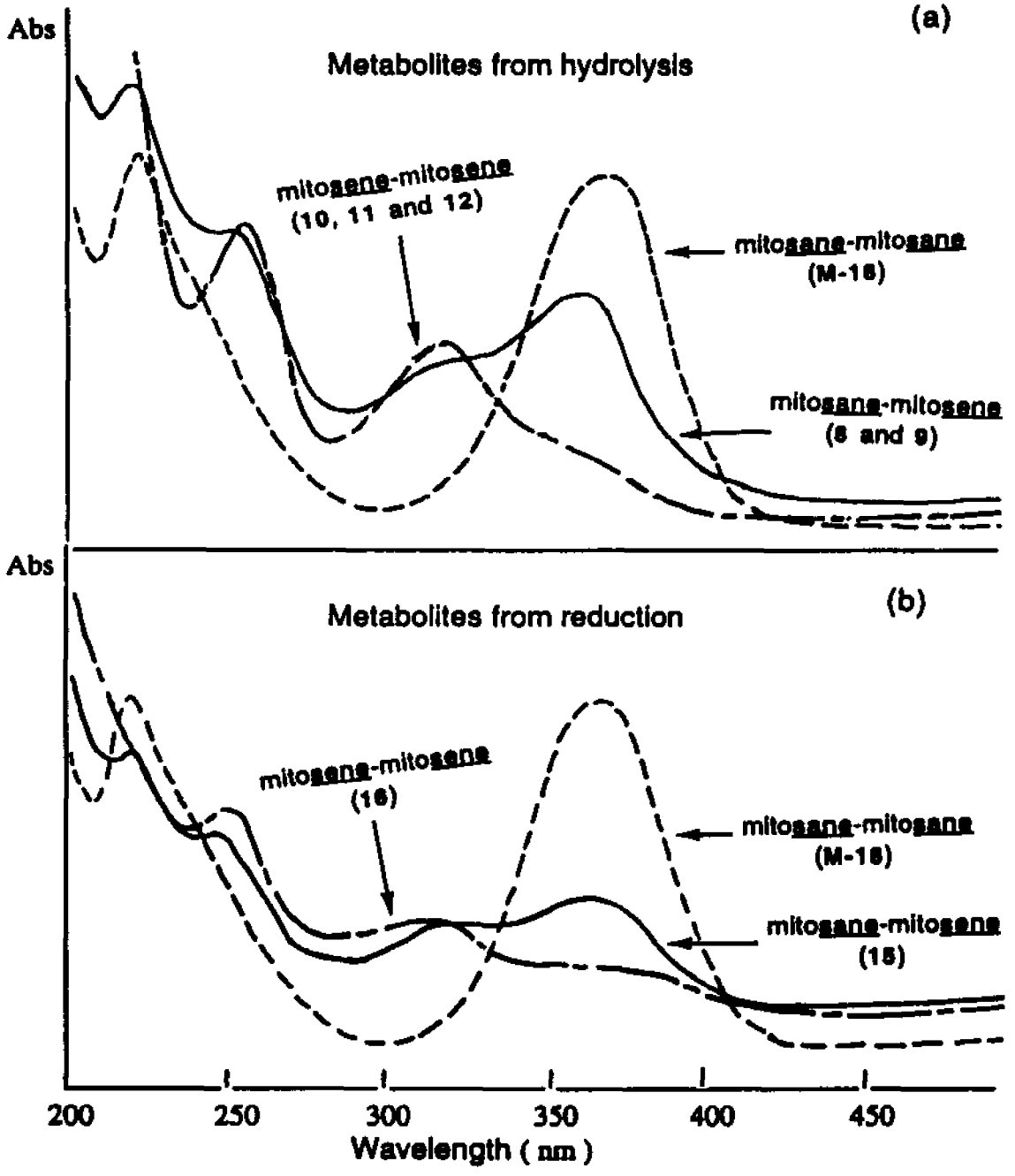

Figure 33. Ultraviolet spectra of M-18 and its metabolites in CH_3OH.

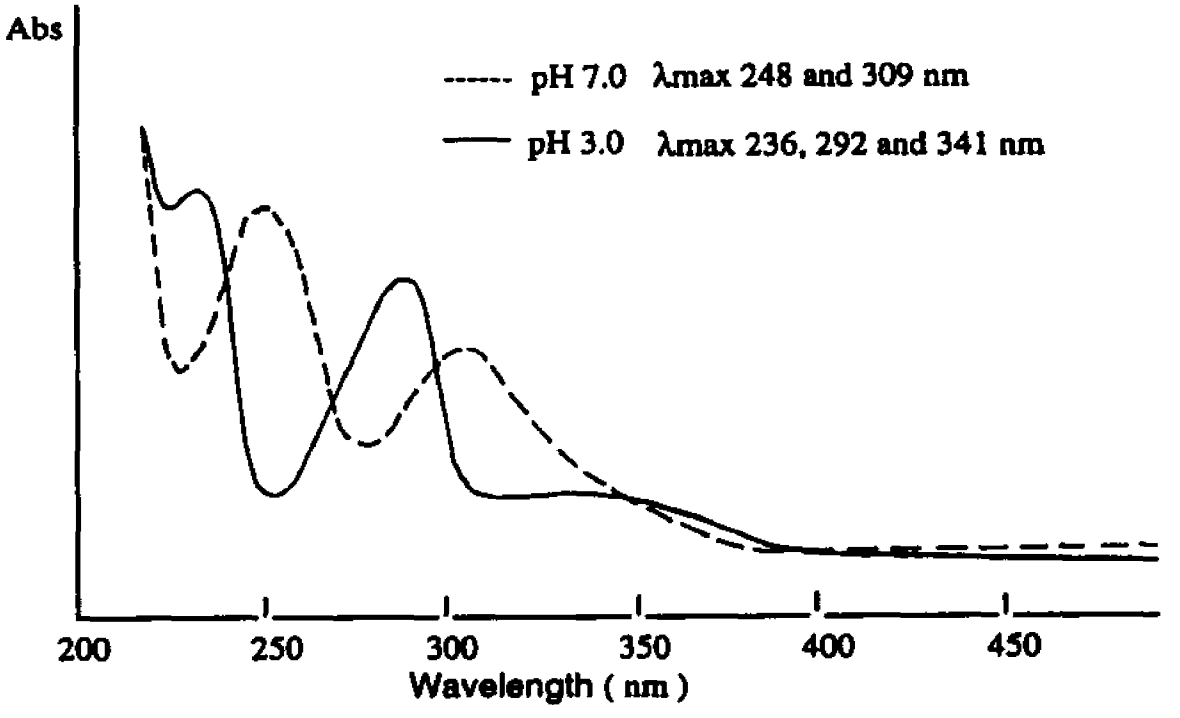

Figure 34. Ultraviolet spectra of 13 and 14 at pH 3 and 7.

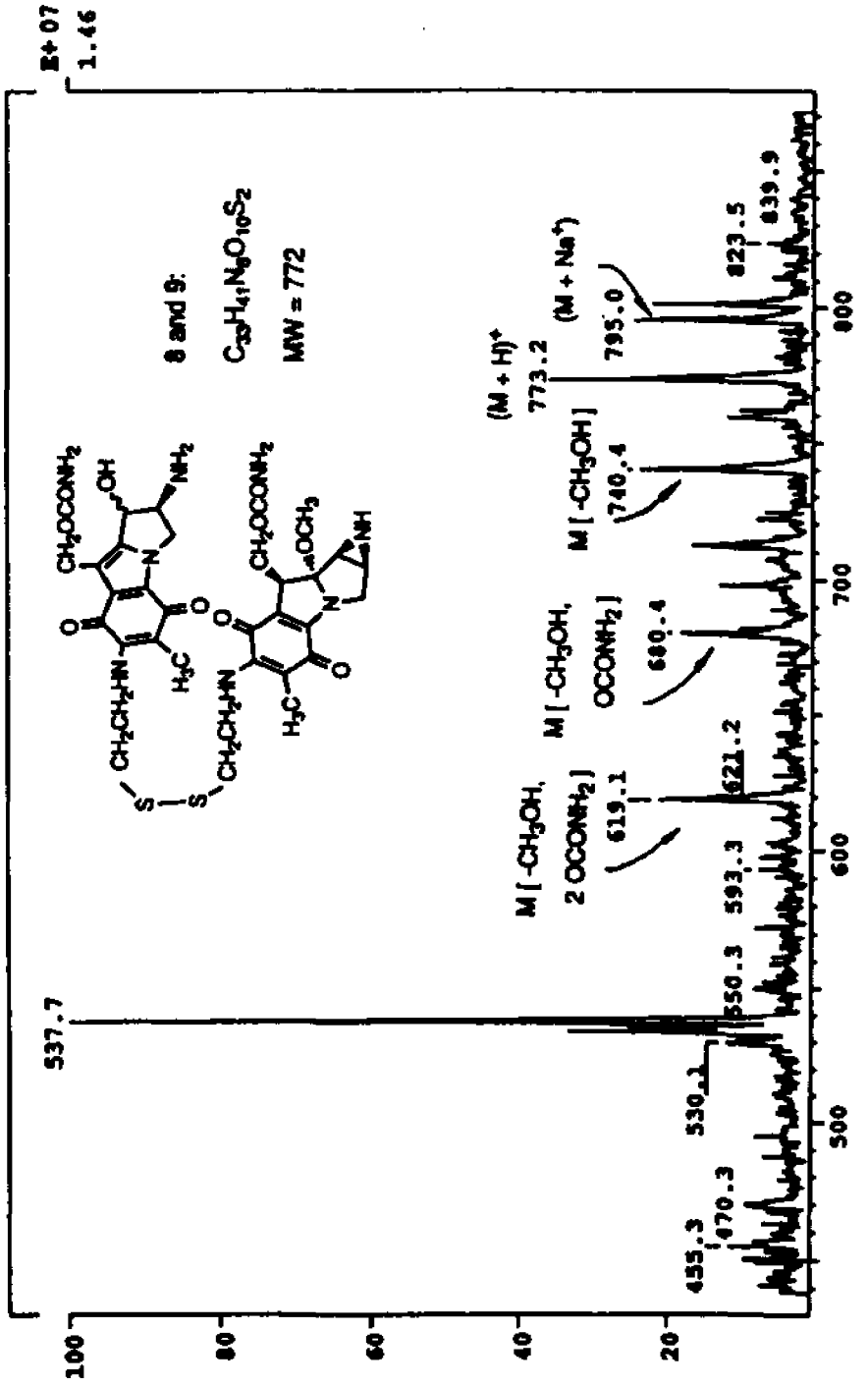

Figure 35. Mass spectra of 8 and 9 (8/9 1:1.6) in an electrospray.

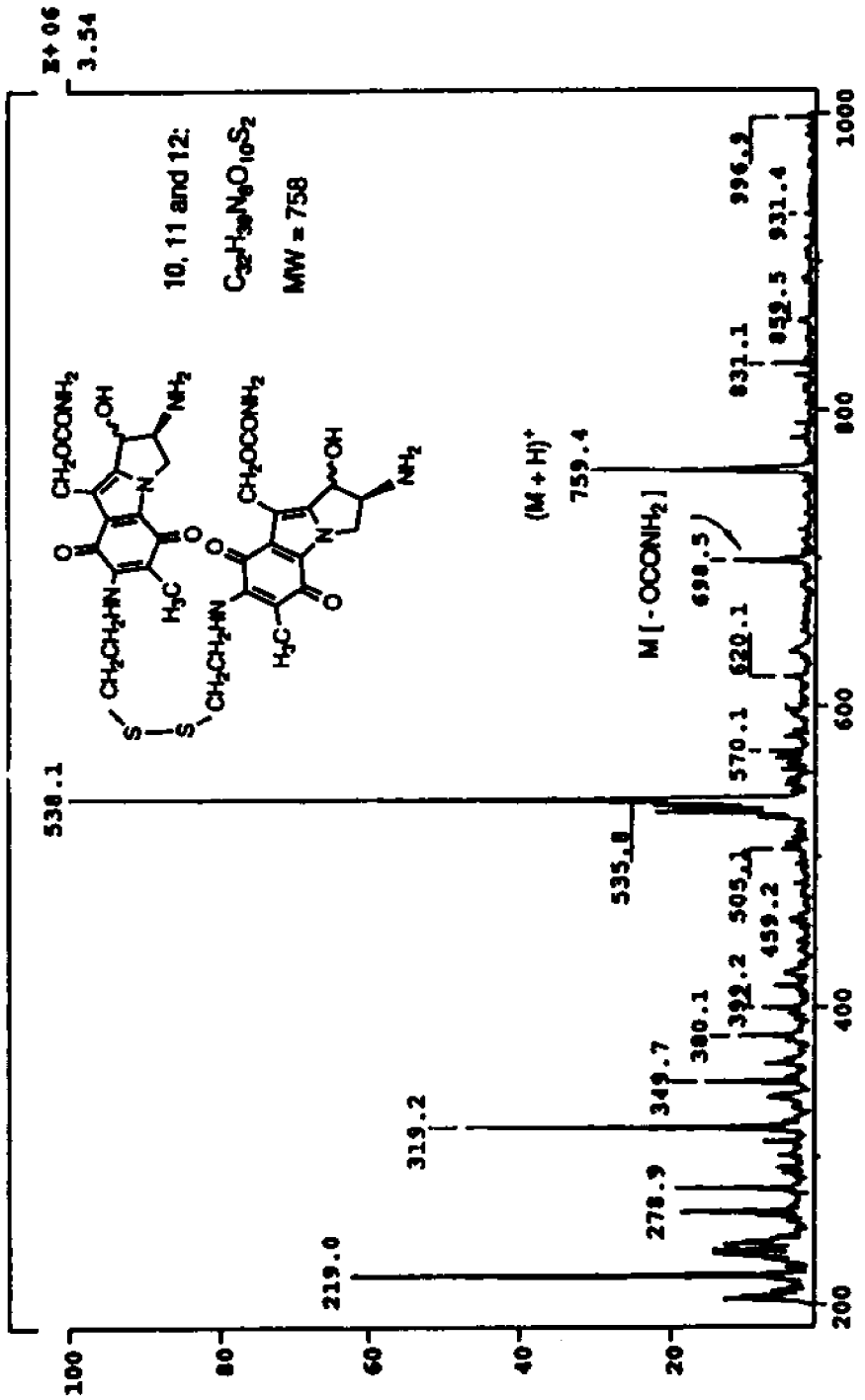

Figure 36. Mass spectra of 10, 11 and 12 (10/11/12 1:2.5:1.6) in an electrospray.

Chapter II. DNA-cross-linking by novel antitumor analogs of mitomycin C

INTRODUCTION

Many drugs used in the treatment of cancer are bifunctional alkylating agents and thus are able to cross-link biological macromolecules (48-50). The most important cellular target is generally believed to be DNA and in many cases the formation of interstrand cross-links may be the most relevant cytotoxic lesion. Such lesions are formed by an initial covalent reaction of the drug with nucleophilic site on DNA to form a monoadduct, which can cross-link the complementary strand of DNA by a further reaction. Not all monoadducts are converted to cross-links, and the "second-arm" reaction is generally assumed to be slow compared to the initial monoadduct formation.

Mitomycin C (MC; **1**, Figure 1)[1] is an antitumor antibiotic used clinically against cancer, and it acts as a DNA alkylating agent (1, 15). DNA-adducts are formed with MC at C-1 or both at C-1 and C-10 covalently linked to N-2 of guanine residues in the minor groove of DNA (Scheme II of Chapter I and Scheme I of Chapter II). Both DNA interstrand and intrastrand cross-links are formed, as the consequence of bisadduct formation between MC and two guanines in opposite strands, and with two adjacent guanines in the same strand, respectively (51). The reactions with DNA are dependent on reductive activation of MC; hence, MC is regarded as the prototype

bioreductive alkylating agent (50). The DNA-damaging activities of MC represent the primary basis of its cytotoxicity.

Intensive research has been undertaken to develop a more selective mitomycin C analog that avoids MC's toxic side effects while maintaining or improving its activity against tumors (3-6). Design of these "second-generation" mitomycins has been based on the mechanistic studies of mitomycin C (18, 21, 26, 30-33). Recently, two disulfide analogs of MC, BMY-25067 (**2**) and KW-2149 (**3**) (Figure 1) have been developed. A disulfide type mitomycin dimer (M-18; **4**, Figure 1) has been synthesized (13). These new analogs of MC all show higher antitumor activity but lower toxicity (especially myelosuppression) than MC (7-13). Mitosene analogs[2] have also been developed that attempt to substitute more effective leaving groups at the drug's known alkylation sites, the 1- and 10- position. A mitosene analog, WV-15 (**6**) (Figure 1), has shown better activity than MC (52). We conducted an investigation of these new antitumor agents (**2, 3, 4, 6**) for their cross-linking properties with DNA under various reductive activation conditions, as compared with MC. Two other mitomycins, mitomycin A (MA; **5**)[1] and the unnatural enantiomer of MC (MC-En)[1] were also included in this SAR[1] type study. MA has been found to be more toxic than MC. It was thought to be a result of the higher redox potential (53) of MA. The enantiomer of MC (MC-En; **7**) has been synthesized recently by Fukuyama's laboratory at Rice University (Houston). This unnatural mitomycin shows 50% lower cytotoxicity than the natural mitomycin C. The comparison of DNA-cross-linking by MC-En with that by MC will be useful to understand the stereochemistry of mitomycin-DNA binding.

The binding ratio of the MC/DNA adducts (mole of MC bound per mole of DNA mononucleotide unit) is determined by a simple UV method

(54). This method shows roughly how much drug has been bound to DNA. However, it is difficult to compare accurately the extent of DNA alkylation by these drugs by this method due to low drug-DNA binding. Furthermore, although the overall DNA binding ratio can be obtained, the individual DNA cross-linking component can not be distinguished by this method. An assay for MC-DNA adduct determination using the enzymatic digestion of the drug-DNA complex and analyzing the adducts in the digest by HPLC has been developed in the Tomasz Lab (30). However, the water insolubility of BMY-25067 and M-18 and the complexity of structure identifications of drug-DNA adducts limit the use of the method. In the present work, we use agarose gel electrophoresis to specifically detect DNA interstrand cross-links. This is based on the method developed by Hartley and co-workers (55): the denaturation of cross-linked DNA is spontaneously reversible and this renatured DNA can be separated from the denatured, non-cross-linked DNA molecules by agarose gel electrophoresis. By using ^{32}P-labeling pBR322 DNA, the agarose gel can be directly autoradiographed and then the amount of interstrand cross-links can be calculated from the density of autoradiograph bands. This method is simple and highly sensitive. In this way, the DNA cross-linking efficiency of antitumor agents **1-6** was determined after activation by $Na_2S_2O_4$, NADPH-cytochrome c reductase/NADPH and thiols (such as DTT and GSH)[1]. The pH dependence of DNA cross-linking by these drugs was investigated. The cross-linking properties of the enantiomer of MC (MC-En) was compared with that of MC. The cross-linking of methylated ^{32}P-pBR322 DNA by MC was determined. The effects of glutathione on cross-linking of DNA by MC was also studied. It is expected that these studies will give some information on what factors effect the formation of drug-DNA cross-links, and consequently,

the cytotoxicities. This will be useful to design more efficient and less toxic anticancer drugs.

MATERIALS

MC and BMY-25067 were generously supplied by Bristol-Myers Squibb Co, Wallingford, CT. KW-2149 and M-16 were supplied by Pharmaceutical Research Laboratories, Kyowa Hakko Kogyo Co, Ltd, Tokyo, Japan. The enantiomer mitomycin C (MC-En) was a generous gift from Dr. Fukuyama, Rice University (Houston). WV-15 (52) was supplied by Marc Maliepaard, Utrecht University, Utrecht, The Netherlands. M-18 and MA were prepared as described in the first chapter. Dimers **8** and **9** were synthesized by a published procedure (13) by Dr. Helena Maruenda in the Tomasz group.

M. luteus DNA was obtained from ICN Biomedicals, Costa Mesa, CA, and calf thymus DNA (type I) was purchased from Sigma Chemical Co, St. Louis, MO. Both DNAs were sonicated before use. The oligonucleotide d(ATATACGTATAT) (oligo 1) was synthesized on an automated DNA synthesizer, Model 380B, Applied Biosystems, Inc., using the phosphoramidite method. All reagents for the synthesis were purchased from Applied Biosystems, Inc., Foster City, CA. The crude products (1 μmol scale, "trityl-off"), after deprotection by concentrated NH_4OH overnight at 55 ^oC, were purified by passage through a Sephadex G-25 (fine) column (2.5 x 56 cm; 0.02 M NH_4HCO_3 eluant). The void volume fractions, containing the oligonucleotide, were lyophilized. HPLC on an analytical C-3 (reverse-phase) column indicated > 95% purity of the oligonucleotides. Enzymes used for DNA digestions and their sources were as follows: DNAse I (code D), snake

venom diesterase (*Crotalus adamanteus* phosphodiesterase I), and *E. coli* alkaline phosphatase (type III-R), Worthington, Freehold, NJ.

Reagents for the assay of cross-linked DNA and their sources were the following: pBR322 DNA, Klenow fragment of DNA polymerase I, and restriction endonuclease *Eco*RI were purchased from GIBCO Bethesda Research Laboratories, Frederick, MD, and [α-^{32}P]dATP was obtained from DuPont Biotechnology Division, Wilmington, DE. Reagents for agarose gel electrophoresis were obtained from Sigma.

SssI methylase and S-adenosyl-methionine were purchased from New England BioLabs, Beverly, MA.

METHODS

Formation of drug-DNA complex under various conditions (i) H_2/PtO_2 as activator: A mixture containing drug (0.5 mM), *M. luteus* DNA (0.5 mM) , 5% DMSO and solid PtO_2 (100 μg/μmol drug) in 0.015 M Tris-HCl (pH 7.5) buffer at room temperature was deaerated by purging it with helium for 10 min. H_2 gas was bubbled through the solution for 5 min, followed by purging again with helium (5 min). The mixture was exposed to air and filtered and the filtrate was chromatographed over a Sephadex G-100 column (2.5 x 56 cm), using 0.02 M NH_4HCO_3 as eluant. The drug-DNA complex (in the void volume) was isolated and lyophilized. (ii) $Na_2S_2O_4$ as activator: A mixture of drug (0.5 mM), *M. luteus* DNA (0.5 mM) and 5% DMSO in 0.015 M Tris-HCl, pH 7.5 buffer was purged with helium for 10 min at room temperature. Aqueous $Na_2S_2O_4$ solution in 1.5 molar excess of drug, made freshly in anaerobic water and kept under continuous purging with helium, was added in 5 equal portions at 10 min intervals from a syringe to the reaction mixture.

The mixture was then exposed to air, the complex was isolated as in (i). (iii) Xanthine oxidase/NADH as activator: A mixture of drug (0.5 mM), *M. luteus* DNA (0.5 mM), NADH (0.5 mM) and 5% DMSO in 0.015 M Tris-HCl pH 7.5 buffer at 37 °C was deaerated as above. In a separate flask xanthine oxidase in a small volume of the above buffer was similarly deaerated at 0 °C, then added to the reaction mixture (0.4 unit/μmol MC). The solution was incubated at 37 °C for 20 minutes, then exposed to air and the complex was isolated as above.

Determination of Binding Ratio: To remove the non-covalent bound drugs, the drug-DNA complex was extensively dialyzed against 200-fold volume of 1.0 M NaCl-0.01 M Na-phosphate (pH 7.5) three times. Each dialysis took at least 3 h at 4 °C. The binding ratio of the drug-DNA complex (mol drug bound /mol DNA mononucleotide) was determined by using a UV spectrophotometric method. The following formula was used for the calculation (54):

$$BR = \text{mol of drug / mol of mononucleotide}$$

$$= \frac{A_{310}-0.005 \times (A_{260} - 1.34 \times A_{310})}{A_{260} - 1.34 \times A_{310}}$$

Drug-duplex oligonucleotide complexes were prepared analogously to drug-DNA complexes , unless otherwise stated.

Preparation of linearized 3'-end-labeled pBR322 DNA (56): pBR322 DNA was treated with *Eco*RI restriction endonuclease as follows: In 625 μl 50 mM Tris-HCl (pH 8.0)-10 mM $MgCl_2$-100 mM NaCl buffer 125 μg DNA was incubated with 250 units of *Eco*RI restriction endonuclease at 37 °C for 2 h. After

addition of 310 µl 7.5 M NH_4OAc the DNA was precipitated by adding 2 volumes of ethanol. After standing at -20 °C for a few hours the sample was centrifuged for 10 min, the pellet was washed with 70% ethanol at -20 °C, and after centrifuging it was lyophilized. 3'-end-labeling: Linearized DNA (5 µg) was incubated with [α-^{32}P] dATP (30 µCi) and 5 units of Klenow fragment of DNA polymerase I for 20 minutes at room temperature in 57 µl 50 mM Tris-HCl (pH 8.0)-10 mM $MgCl_2$-100 mM NaCl buffer, followed by precipitation by ethanol as above.

Cross-linking of ^{32}P-pBR322 DNA with mitomycins: (i) Activation by $Na_2S_2O_4$: A mixture containing approximately 10 ng ^{32}P-pBR322 DNA, 1000 ng calf thymus DNA and varying amounts of drugs in 21 µl 5 mM Tris-HCl (pH 7.4)-0.8 mM EDTA was deaerated by gentle bubbling with argon 2 min. 4 µl of a freshly made, deaerated $Na_2S_2O_4$ solution (7.5 mM) in 0.1 M Tris-HCl (pH 7.4)-2 mM EDTA buffer was added to give final concentrations 118 µM DNA, 0-80 µM drugs and 1.2 mM $Na_2S_2O_4$ in a total volume of 25 µl 20 mM Tris-HCl (pH 7.4)-1 mM EDTA buffer. The reaction mixture was capped tightly and left at room temperature for 1 h. (ii) Activation by NADPH-cytochrome c reductase: A mixture containing approximately 10 ng ^{32}P-pBR322 DNA, 1000 ng calf thymus DNA, 2 nmol drug and 0.1 µmol NADPH in 21 µl 20 mM Tris-HCl (pH 7.4)-1 mM EDTA was deaerated by gentle bubbling with argon for 2 min. 4 µl of a freshly made, deaerated cytochrome c reductase (0.005 unit/µl) in the same buffer was added to give final concentration 118 µM DNA, 80 µM drug, 4 mM NADPH and 0.8 unit/ml cytochrome c reductase in a total volume of 25 µl 20 mM Tris-HCl (pH 7.4)-1 mM EDTA buffer. The reaction mixture was incubated for 20 min at 37 °C. (iii) Activation by DTT: 10 ng ^{32}P-pBR322 DNA and 1000 ng calf thymus DNA was mixed with varying

amounts of drugs in 21 µl of 5 mM Tris-HCl (pH 7.4)-16 mM EDTA. 4 µl of 0.5 mM DTT in 0.1 M Tris-HCl (pH 7.4)-2 mM EDTA was added to the solution to give final concentration 118 µM DNA, 0-80 µM drug, 80 µM DTT in a total volume of 25 µl 20 mM Tris-HCl (pH 7.4)-14 mM EDTA buffer. The mixture was incubated for 1 h at room temperature under aerobic condition. (iv) Activation by GSH: The activation by GSH was obtained analogously to the activation by DTT, as described in (iii), except that 4 mM GSH was used for the reaction instead of 80 µM DTT.

Comparison of cross-linking efficiency of antitumor agents 1-6 at pH 7.4 versus pH 5.8 (activated by $Na_2S_2O_4$): 10 ng ^{32}P-pBR322 DNA and 1000 ng calf thymus DNA were treated with drug at 15.6 µM for MC, 57.2 µM for BMY-25067, 11.5 µM for KW-2149, 19.6 µM for M-18, 4.7 µM for MA and 80 µM for WV-15 by the activation of 1.2 mM $Na_2S_2O_4$ under anaerobic condition as described above. The reaction mixture was incubated for 1 h at room temperature in 20 mM Tris-HCl (pH 7.4)-1 mM EDTA or 20 mM Bis-Tris-HCl (pH 5.8)-1 mM EDTA.

Methylation of pBR322 DNA: Methylation of linearized pBR322 DNA was carried out by using SssI methylase as follows (57): In 750 µl 10 mM Tris-HCl (pH 7.9)-10 mM $MgCl_2$-50 mM NaCl-1 mM DTT buffer 30 µg linearized pBR322 DNA was incubated with 90 units of SssI methylase in the presence of 160 µM S-adenosyl-methionine at 37 ^{o}C for 45 min. The CpG methylase (SssI methylase) methylates cytosine residues within the dinucleotide recognition sequence 5'-CG-3'. To remove proteins, the reaction mixture was extracted twice with an equal volume of phenol [equilibrated with 0.1 M Tris-HCl (pH 8.0) and mixed with an equal volume of $CHCl_3$:isoamyl alcohol (24:1)(v/v)]

and then once with an equal volume of $CHCl_3$:isoamyl alcohol (24:1)(v/v). Each extraction was accomplished by shaking and then centrifuging for 5 min. The DNA solution (the top liquid) was collected. DNA was precipitated by 70% ethanol in the presence of 0.3 M NaAc, as described above. For the determination of the methylation efficiency, 25 μg of methylated pBR322 DNA was digested by enzymes DNAse I, snake venom diesterase (SVD) and alkaline phosphatase, as described previously (30). The digested sample was analyzed by HPLC (reverse-phase C18 column, 4.6 mm x 25 cm), using a mobile phase 0-6% CH_3CN in 0.03 M NH_4Ac (pH 7.0) in 25 minutes. The result showed that 71.5% deoxycytidine in CpG sequence was methylated, calculated from the relative areas of the HPLC peaks of dC and m^5dC and the known CpG frequency of pBR322 DNA (58).

The 3'-end-labeling for methylated pBR322 DNA was the same as that for pBR322 DNA described above.

Cross-linking reactions of methylated ^{32}P-pBR322 DNA with MC: Approximately 10 ng methylated ^{32}P-pBR322 DNA, mixed with 1000 ng calf thymus DNA was treated with varying amounts of MC (0-1 nmol) and 15 nmol of $Na_2S_2O_4$ in a total volume of 25 μl 20 mM Tris-HCl (pH 7.4)-1 mM EDTA buffer at room temperature for 1 h under anaerobic conditions, as described above. The cross-linking reactions of non-methylated ^{32}P-pBR322 DNA with MC was conducted as above for comparison.

Cross-linking of ^{32}P-pBR322 DNA with MC in the presence of GSH under reductive activating conditions. (i) Reactions employing varying concentrations of GSH: A mixture containing approximately 10 ng ^{32}P-pBR322 DNA, 1000 ng calf thymus DNA, 2 nmol MC and varying amounts of

GSH in 21 µl 5 mM Tris-HCl (pH 7.4)-16 mM EDTA was deaerated with argon. 4 µl of a freshly made, deaerated $Na_2S_2O_4$ solution (7.5 mM) in 0.1 M Tris-HCl (pH 7.4)-2 mM EDTA buffer was added to give final concentrations 118 µM DNA, 80 µM MC, 0-40 mM GSH and 1.2 mM $Na_2S_2O_4$ in a total volume of 25 µl 20 mM Tris-HCl (pH 7.4)-14 mM EDTA buffer. The sample was capped tightly and left at room temperature for 1 h. (ii) Reactions in the presence or absence of 20 mM GSH, using varying concentrations of MC: A mixture containing 10 ng ^{32}P-pBR322 DNA, 1000 ng calf thymus DNA, 0.5 µmol GSH and varying amounts (0-2 nmol) MC in 21 µl buffer was deaerated and treated with 4 µl 7.5 mM $Na_2S_2O_4$ as in (i), resulting in final concentration 118 µM DNA, 0-80 µM MC, 20 mM GSH and 1.2 mM $Na_2S_2O_4$ in 25 µl total reaction volume. Further procedures were the same as in (i). Each reaction was repeated without any GSH added to the reaction mixture.

Reaction termination and DNA precipitation: All above reactions of ^{32}P-pBR322 DNA with drugs were terminated by the addition of an equal volume of "stop solution" (0.6 M sodium acetate-1 mM EDTA, 300 µg/ml tRNA) and three volumes of cold ethanol (-20 °C). After standing at -20 °C for a few hours the sample was centrifuged for 10 min, the pellet was washed with 70% ethanol at -20 °C, and after centrifuging it was lyophilized.

Assay of cross-linked ^{32}P-pBR322 DNA by neutral agarose gel electrophoresis (55): The lyophilized sample from the above experiments was dissolved in 2 µl of H_2O, then 20 µl strand separation buffer (30% DMSO-1 mM EDTA-0.02% bromophenol blue-0.02% xylene cyanol) was added. The DNA was denatured by heating the solution at 90 °C for 3 min, then chilling in ice water. Samples were loaded onto a 1.0% agarose gel (20 cm long) and electrophoresed for 16 h

at 40 V. The running buffer was 40 mM Tris-HCl (pH 8.1)-20 mM acetic acid-2 mM EDTA. Gels were dried at 80 ^{o}C onto 3-mm filter paper using a Bio-Rad model 583 gel drier under vacuum. Autoradiography was accomplished using X-OMAT AR film (Kodak) with intensifying screen overnight at -70 ^{o}C. The autoradiogram was scanned by a soft laser scanning densitometer (Biomed Instruments, Inc., model SL-DNA). The % cross-linked (double-stranded) DNA was calculated from the densities of the bands corresponding to denatured (fast-moving) and renatured (slow-moving) ^{32}P-pBR322 DNA in the sample by using the following formula:

$$\% \text{ cross-linked} = [\ (XL_S - XL_C) / (1 - XL_C)\ ] \times 100$$

$$XL_S = \frac{\text{Band density of renatured DNA}_{\text{sample lane}}}{(\text{Band density of renatured DNA} + \text{Band density of denatured DNA})_{\text{sample lane}}}$$

XL_C was calculated from the above formula, except that the density data was from the control denatured DNA lane.

Molecular modeling of the cross-linked d(CGCGCGCGCG)$_2$-M-18 adduct: All-atom minimizations were performed on a VAX station 3100 using the program MacroModel V3.0 (59). The AMBER force field and charges were used in the absence of solvent and counterions, with dielectric R_{ij} and with cutoffs of 8 Å (van der waals) and 13 Å (electrostatic) in the united atom mode. Minimizations were conducted by using a block-diagonal Newton Raphson (BDNR) routine followed by a Polak-Ribiere conjugate gradient (PRCG) to a root-mean-square gradient of 0.01 kJ mol^{-1}Å^{-2} for all structures. In the absence of a crystallographic structure for the mitosene unit, we energy-

minimized 2β-7-diamino-1α-hydroxymitosene by MacroModel. After the 1-OH bond of the mitosene was severed, two such mitosenes were placed visually in the central minor groove region of the computer-generated B-DNA decamer d(CGCGCGCGCG)· d(CGCGCGCGCG) using the Evans and Sutherland 390 graphic system. Covalent bonds were introduced that linked one mitosene C-1 to N^2 of G(4) and the other to N^2 of G(14) in the oligonucleotide:

1 2 3 4 5 6 7 8 9 10
5'-CGCGCGCGCG-3
3'-GCGCGCGCGC-5'
20 19 18 17 16 15 14 13 12 11

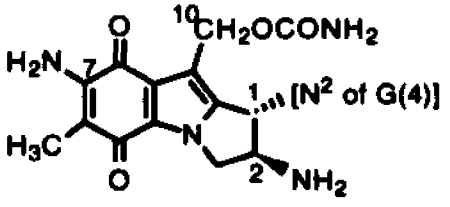

mitosene 1

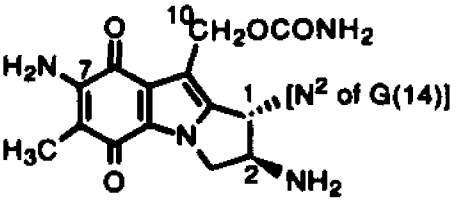

mitosene 2

The 7-positions of the two mitosenes were then covalently connected by the linkage -NH-CH_2-CH_2-S-S-CH_2-CH_2-NH-. The structure was finally refined with the procedure described above. For comparison, the parent decamer duplex was also generated by the MacroModel (GROW mode) and was energy-minimized by the described procedure.

Quantitative analysis of oligonucleotides by UV spectrophotometry was described in detail elsewhere (60). For the analysis of *M. luteus* DNA and calf thymus DNA, ε_{260} = 6960 and 6800 were used, respectively.

RESULTS AND DISUSSION

I. Comparison of the covalent DNA binding affinity of MC versus BMY-25067, using *M. luteus* DNA and a synthetic oligonucleotide as substrates.

The covalent binding affinity of BMY-25067 to DNA was studied by measuring the binding ratio of drug-DNA complexes formed between the drug and DNA upon reductive activation. Chemical reducing agents (H_2/PtO_2, $Na_2S_2O_4$) and enzymatic reduction (xanthine oxidase/NADH) were used. The data in Table I show that the binding ratio of BMY-25067 is similar (same order of magnitude) as that of MC under either chemical ($Na_2S_2O_4$ and H_2/PtO_2) or enzymatic reductions (such as xanthine oxidase/NADH). This indicated qualitatively that both drugs alkylated DNA at a similar frequency. The accuracy of these data were not determined.

In contrast to these positive results, attempts to detect covalent binding of BMY-25067 and M-18 to a prototype self-complementary oligonucleotide d(ATATACGTATAT) (oligo 1) more directly, were unsuccessful. In such efforts, we tried to detect cross-linking of the oligonucleotide by separating the cross-linked from non-cross-linked oligo by HPLC or Sephadex G-50 column chromatography, as done previously in the case of MC (60, 61). We also tried to detect monoalkylation products of the oligonucleotide by HPLC (reverse-phase C_4 column, 10 x 250 mm) with a non-linear gradient 9.6% - 21% CH_3CN in 0.03 M NH_4Ac in 40 min (9.6 - 10.5% CH_3CN in 0.03 M NH_4Ac in 10 min; 10.5 - 12% CH_3CN in 0.03 M NH_4Ac in 10 min; then 12 - 15% CH_3CN in 0.03 M NH_4Ac in 10 min; and 15 - 21% CH_3CN in 0.03 M NH_4Ac in 10 min). As seen in Table II, none of these approaches gave positive results in

the case of BMY-25067 and M-18, in contrast to the good yield obtained with MC.

A new method of activation, i.e. reduction by GSH, was also used in these attempts: A mixture containing 0.25 mM oligo **1**, 1 mM drug (MC, BMY-25067, KW-2149 or MA), 5% DMSO and 50 mM GSH was incubated for 1 h at 0 ^{o}C in 0.1 M Tris-10 mM EDTA (pH 7.4). No cross-links were detected by any of the drugs using a Sephadex G-50 column (2.5 x56 cm) for detection. The same negative result was obtained by using 5 mM GSH instead of 50 mM for KW-2149.

II. Cross-linking efficiency of antitumor agents (1-6) under several different reductive activations, determined by a new sensitive assay, using ^{32}P-labeled DNA.

^{32}P-end-labeled linear pBR322 DNA was used as substrate for the cross-linking reaction. The assay (55) is based on spontaneously reversible denaturation of cross-linked DNA. The renatured DNA can be separated from the denatured, non-cross-linked DNA molecules by agarose gel electrophoresis. The assay in our hands was highly reproducible. All the following results were the average of two duplicate experiments. Two duplicate experiment data points gave a variation in the percentage cross-linked DNA of < 5%.

(i) Activation by $Na_2S_2O_4$

A typical gel autoradiograph of a cross-linking assay is shown in figure 2a, illustrating the drug concentration dependence of cross-linking for mitomycin C (MC). Cross-linking increased with increasing concentration of MC in a roughly linear relationship up to 20 μM MC, as seen in the

densitometry plot of the autoradiograph (Figure 2b). Figure 2b also shows a comparison of cross-linking efficiency among the six antitumor agents (**1-6**). All antitumor agents cross-linked DNA under this activation condition. The drug concentration at 50% cross-linking ($ISCC_{50}$)[1] did not show substantial difference among these antitumor agents. This indicated that these antitumor agents had a similar cross-linking efficiency under $Na_2S_2O_4$ activation.

(ii) Activation by NADPH-cytochrome c reductase/NADPH

The reduction potentials of mitomycins (Table III) are affected by the substituent at the 7-position. MA has the highest reduction potential (-0.19 V) among these mitomycins (62). WV-15 is one of the mitosene[2], which has a higher potential than MC (WV-15, -0.30 V and MC, -0.40 V) (52). The disulfide analogs of MC have also slightly higher potential than MC (43). Therefore, it was expected that these analogs of MC might cross-link DNA under milder reductive activating conditions than that used for MC. M-18 is a dimer of MC. If both mitosane units of M-18 are activated and can alkylate DNA monofunctionally, then cross-links of M-18 with DNA will be formed. To test this hypothesis, these drugs were activated by NADPH-cytochrome c reductase/NADPH in the presence of ^{32}P-pBR322 DNA. The cross-links were detected by gel electrophoresis. It was known that this reductase activated MC only monofunctionally in cell-free systems (32, 44). The results showed that only MA could cross-link DNA under this activation (Figure 3). It is probably due to the relatively high reduction potential of MA. Contrary to expectation, the dimeric mitomycin M-18 did not form any cross-links by this activation. This was even more surprising in light of the fact that our computer simulation results indicated that the dimer M-18 can cross-link B-DNA $d(CGCGCGCGCG)_2$ at two guanines in the opposite strands, four basepairs

apart, by the usual covalent drug-DNA linkages, without any large distortion of B-DNA structures, as shown in figure 4.

Recently, a dimeric molecule containing two of the DNA-alkylating cyclopropa[c]pyrrolo[3,2-e]indol-4-(5H)-one (CPI) subunits of CC-1065 has been synthesized by incorporating a rigid linker into the CPI dimer. This dimer can cross-link DNA with an alkylation-site size as long as six base pairs (63). The biological implications of the increased size of the DNA recognition element are not known, but the increase in size may confer a greater absolute sequence selectivity upon the dimer. It was disappointing that M-18 did not cross-link DNA. The reason for this failure is not clear.

(iii) Activation by DTT

The above results showed that the cross-linking efficiency of the disulfide analogs of MC was not much different from MC under the chemical activation ($Na_2S_2O_4$) and the enzymatic reductive activation (cytochrome c reductase/NADPH). However, the metabolism studies (Chapter I of this thesis) indicated that the disulfide analogs but not MC were activated by thiols such as DTT and GSH. Therefore, it seemed very significant to determine whether these mitomycins formed DNA cross-links when activated by DTT or GSH.

^{32}P-pBR322 DNA was treated with antitumor agents **1-6** under the DTT activating condition. The gel autoradiogram showed that BMY-25067, KW-2149, M-18 and MA all cross-linked DNA, but MC and WV-15 did not do so. Figure 5a and 5b are cross-linking gel autoradiograms of MC and BMY-25067 respectively, and the plot of the percent cross-linked DNA versus drug concentration is shown in figure 5c.

(iv) Activation by GSH

^{32}P-pBR322 DNA was also treated with these drugs **1-6** using GSH for activation under aerobic conditions. As shown in figure 6, qualitatively similar results were obtained to those from the activation with DTT. MA and the disulfide analogs of MC (BMY-25067, KW-2149 and M-18) but not MC and WV-15 were found to cross-link DNA. The extent of cross-linking by MA was 2-3-fold less than that by the disulfide analogs **2-4**.

As described in Chapter I, when MC, BMY-25067, KW-2149, M-18 and MA were treated with GSH in the absence of DNA, all drugs except MC were activated by GSH. The drug conversion to mitosene from disulfide analogs was almost 100% whereas only 50% MA was converted to mitosene[2] (Figure 25, Chapter I). Thus, the cross-linking results for these drugs were consistent with the results obtained from the above metabolism studies.

It was reported (Table III) that the reduction potential of DTT was -0.33 V (64), lower than that of MA, close to that of WV-15 but higher than that of MC and its disulfide analogs (BMY-25067, KW-2149 and M-18). Therefore, it was understandable that DTT reduced MA because of the big difference between their reduction potential -0.14 V. It seemed reasonable that DTT did not activate MC and WV-15, because the reduction potential of DTT was comparable with that of WV-15 and even higher than that of MC. But why does DTT activate the three disulfide analogs of MC, which have similar potentials to that of MC (Table III)? As a result, these disulfide analogs of MC must have a new activation mechanism by thiols.

The DNA cross-linking analysis of the disulfide analogs by both DTT and GSH activations demonstrated that the disulfide analogs were activated to bifunctional alkylating agents by thiols. This represents an extension of the original observation that they were converted by thiols to mitosenes (Chapter

I). Together these two sets of experiments indicate that thiols act as specific activating agents of the disulfide analog group. The proposed mechanism is shown both in Scheme VI of Chapter I and in Scheme II of this Chapter. Thiols cleave the disulfide bond of the disulfide analogs of MC to form a free thiol in the molecules. Then the quinone is reduced to semiquinone by this intramolecular thiol, followed by elimination of a methoxy group as methanol and aziridine ring opening, to lead to an intermediate quinone methide, as established in the case of mitomycin C. The quinone methide could be attacked by the 2-NH_2 group of guanine in DNA to result in alkylation at the C-1 position of mitomycins. Cross-linking occurs through the C-10 position of the molecule following loss of carbamate and production of an electrophilic imine moiety, which is then attacked by a second 2-NH_2 group of guanine in DNA, in analogy to the well-established mechanism in the case of reduction of mitomycin C (26, 30).

To further prove this mechanism, the DNA-cross-linking efficiency of a series of disulfide analogs of MC (BMY-25067, KW-2149, dimers M-18, **8**, **9** and the methyl sulfide form of mitomycins (M-16, **10**) (Figure 1)) has been compared under the activation by GSH. There are two, four and six carbons between the disulfide bond and C-7-N in the dimers M-18, **8** and **9**, respectively. It was hypothesized that the internal redox reaction should be favorable in the case of M-18 but not of the dimers **8** and **9**, because the sulfhydryl group formed after thiol activation in **8** and **9** is too far removed to reduce the quinone intramolecularly (8- and 10-membered ring intermediates are required). Therefore, **8** and **9** could not cross-link to DNA under this activation. The methyl sulfide bond of M-16 is stable under the thiol activation, as a result, M-16 could not cross-link to DNA either by thiol activation. A mixture of 10 ng ^{32}P-pBR322 DNA, 1000 ng calf thymus DNA,

40 μM drug and 4 mM GSH in 20 mM Tris-HCl (pH 7.4) - 14 mM EDTA was incubated for 1 h as described above. The cross-linked DNA was separated by electrophoresis. The results showed that BMY-25067, KW-2149 and M-18 cross-linked to DNA with 20% yield, but dimers **8**, **9** and M-16 could not cross-link to DNA as expected (Figure 7). It is very interesting that both the cytotoxicity and the antitumor activity of the dimer M-18 is much higher than that of dimers **8** and **9** in rodent systems, as reported recently (13). Our finding of the relative cross-linking efficiency of these dimeric mitomycins is consistent with these results.

III. pH dependence of ^{32}P-pBR322 DNA cross-links induced by antitumor agents 1-6 under activation by $Na_2S_2O_4$.

^{32}P-pBR322 DNA was treated with drugs **1-6** under the activation by $Na_2S_2O_4$ at pH 7.4 and 5.8 respectively. It was found that the amount of cross-linking increased with decreasing pH for all six drugs, although the quantitative effect of pH varied with drug. The difference between the amount of cross-linking at pH 5.8 and pH 7.4 was quite remarkable in the case of WV-15 (Figure 8). DNA cross-linking after chemical reductions (such as $Na_2S_2O_4$ and $NaBH_4$) and enzymatic reduction (DT-diaphorase) of mitomycin C was previously reported to depend on pH with lower pH favoring increased cross-linking (65, 66). Our data is in agreement with previous studies. Early work has also shown that mitomycin C exhibits greater toxicity to EMT6 cells (67) and to HeLa cells (68) at acidic pH values. This presumably reflects proton-assisted loss of the methoxy group and aziridine ring opening in the mitomycins which facilitates the generation of the reactive intermediate quinone methide. In the case of the analog WV-15,

the replacement of C-1 and C-10 leaving groups (-$OCOCH_3$) by the amino group of guanines in DNA is catalyzed by protons, therefore, which explains why the extent of DNA cross-linking by WV-15 is also greater at the acidic pH than at the neutral pH.

IV. Cross-linking of ^{32}P-pBR322 DNA by the unnatural enantiomer of MC (MC-En) under activation by $Na_2S_2O_4$.

MC-En has been synthesized and shows lower cytotoxicity than MC. Therefore, it was of interest to determine the DNA cross-linking efficiency of MC-En. A mixture of 10 ng ^{32}P-pBR322 DNA, 1000 ng calf thymus DNA and varying amount of MC-En (0-2 nmol) was treated with 30 nmol of $Na_2S_2O_4$ in 25 µl 20 mM Tris-HCl (pH 7.4)-1 mM EDTA buffer as described above. Cross-linked DNA was separated by electrophoresis on agarose gel. The extent of cross-linking was increased with increasing MC-En concentration, as in the case of MC (Figure 9). The cross-linking efficiency of MC-En was compared with that of MC. It was found that MC cross-linked DNA in 1.3-6 fold higher than MC-En in the drug concentration range from 0 to 80 µM. In the lower % cross-link range (0-40%) in which this assay is most accurate, approx. 3-fold lower activity of MC-En was noted. For example, the $ISCC_{30}$ value of MC is 7 µM and that of MC-En is 22 µM. These results are consistent with the finding that the cytotoxicity of MC-En is approximately 50% lower than that of MC in certain tumor cell lines (Kyowa Hakko Kogyo Co., unpublished data).

V. Cross-linking of methylated ^{32}P-pBR322 DNA with MC under activation by $Na_2S_2O_4$.

It has been known that MC alkylates guanines of DNA with a CpG sequence selectivity (61, 66, 69 and 70). The recognition of 5-meCpG (the cytosine in CpG sequence is 5-methylated) by MC is enhanced 2-fold relative to the non-methylated CpG, with oligonucleotides as substrates (W. Johnson in the Tomasz' laboratory, unpublished). This preferred alkylating and cross-linking target of MC, i.e. 5-meCpG, occurs most frequently in transcriptional regulatory regions of mammalian DNA. We wanted to find out whether this sequence selectivity, observed with oligonucleotides is also observable with high molecular weight DNA. Therefore, we first methylated pBR322 DNA with SssI methylase, which is specific to C in CpG sequences. 71.5% CpG in pBR322 DNA was methylated. This methylated ^{32}P-pBR322 DNA was treated with MC under activation by $Na_2S_2O_4$ and compared with the non-methylated ^{32}P-pBR322 DNA. Methylated ^{32}P-pBR322 DNA had 2- to 2.5-fold higher cross-linking efficiency than the corresponding non-methylated DNA in the 0-40% cross-link range (Figure 10), in remarkable agreement with the results obtained with the oligonucleotide system in which a completely different methodology was used for assay.

VI. Inhibition of MC-induced interstrand cross-linking of DNA by GSH under activation by $Na_2S_2O_4$.

It has been observed using cell-free enzymatic systems that GSH was involved in the overall metabolism of MC to non-toxic metabolites, and the binding ratio of MC to *M. luteus* DNA was lowered by 40-75% in the presence

of GSH, as described in Sharma 's dissertation (71). The resistance of certain tumor cell lines to MC has been correlated with elevated cellular GSH level in several recent studies (72, 73). We wanted to see whether the cross-linking of DNA by MC is directly affected by GSH in some way. Therefore, ^{32}P-pBR322 DNA was treated with MC under $Na_2S_2O_4$ activating conditions in the presence and absence of GSH. The extent of cross-linking of DNA by MC under anaerobic $Na_2S_2O_4$ activation decreased markedly with increasing concentration of GSH (Figure 11a, b). 20 mM GSH induced a 50-60% decrease of cross-linking over a wide range of MC concentration (Figure 11c). The observed inhibition is likely to be due to competition of GSH with DNA for reaction with the activated MC, since previous results showed that in the absence of DNA, activated MC reacts avidly with GSH forming inactive mono- and bis-GSH-conjugates (71). This inhibitory effect of GSH on MC-DNA cross-link formation could in principle protect DNA from MC-induced damage in the cell and thus contribute to the modulation of MC cytotoxicity by GSH levels, observed in certain tumor cells (72, 73).

SUMMARY AND SIGNIFICANCE

The influence of the 7-substituent on the DNA-cross-linking activity of the mitomycins was studied in detail. This activity is believed to be the fundamental cause of tumor cell death, induced by these drugs. One member of this group, MC is widely used in cancer chemotherapy. Several hundred analogs, all variants in the 7-substituent have been prepared and tested in the past 25 years. Only two of these have been selected, recently, to undergo clinical trials, based on their superior pharmacological properties as compared to MC. Although these two new analogs, BMY-25067 and KW-2149 were the

main focus, we included a number of other pertinent 7-substituent analogs and a mitosene-type analog in our structure-activity relationship study, in order to gain a clear understanding of the factors which modulate DNA-cross-linking. The results are summarized in Table III. It has been known that the 7-substituent is a determinant of quinone redox potential (6): other factors being equal, 7-O-substituents result in higher $E^{o'}$ than 7-N-substituents and consequently in faster reductive activation rates (43, 53). It is clear from the present results that reductive activation is the key to DNA-cross-linking: MA cross-links DNA under $Na_2S_2O_4$, NADPH-cytochrome c reductase and thiol reductive conditions, but WV-15 and MC do so only under the strongest, $Na_2S_2O_4$ conditions. The corresponding $E^{o'}$s (MA > MC = WV-15) correlate with the fact that MA is activated by the two "weaker" activating agents, NADPH-cytochrome c reductase and thiols, as discussed in detail above. This is the first time that MA is shown to cross-link DNA under thiol activation. All this is also correlated with cytotoxicity. It is known that MA and other 7-O-substituted mitomycins are more cytotoxic than MC and other low-redox potential (7-N) analogs (43).

The most significant finding is that the analogs containing a disulfide linkage in the 7-substituent (BMY-25067, KW-2149 and M-18) cross-link DNA under activation by thiols, despite the fact that they are low-redox-potential, 7-N-substituted analogs, like MC. It is shown that a new type of activation mechanism is responsible for this property, namely reduction of the disulfide group by DTT or GSH, which then triggers intramolecular reduction of the quinone by the sidechain sulfhydryl group. This unique property may be responsible of the higher bioactivity of these analogs compared to mitomycin C.

Table 1. Binding ratio[a] of BMY-25067 and MC to *M. luteus* DNA.

Reducing agents	MC	BMY-25067
H_2 / PtO_2	0.136	0.127
$Na_2S_2O_4$	0.06	0.012
xanthine oxidase /NADH	0.107	0.186

[a] Mol bound drug / mol DNA mononucleotide unit

Table II. % yield of drug-oligonucleotide adduct under various reductive conditions.

Reducing Agent (Drug-Oligo Adduct)	MC	BMY-25067	KW-2149	Analytical methods	Reaction Conditions
$Na_2S_2O_4$ (Cross-links)	33.0%	4%	8%	Sephadex G-50 Column (2.5 x 56 cm)	2 mM MC 0.5 mM oligo 1 3 mM $Na_2S_2O_4$ at 0 °C for 1 h
H_2/PtO_2 (Mono-adducts)	35.5%	0	0	HPLC	2 mM MC,0.96 mg PtO_2 0.5 mM oligo 1 at 0 °C, hydrogenated for 2 h
H_2/PtO_2 (Cross-links)	56.5%	0	0	"	Same as above, except hydrogenated overnight
NADPH cytochrome c reductase (CCR) /NADPH (Mono-adducts)	29.6%	0	0	"	2 mM MC 0.5 mM oligo 1 4 mM NADPH,3 unit/ml CCR at 0 °C for 1 h

Table III. DNA-cross-linking activity of various motomycins: Summary.

Mitomycin Analogs	Substituent atom in 7-position	Disulfide in 7-substituent	E^o, V[a]	DNA-cross-linking activity under activation by		
				$Na_2S_2O_4$	NADPH-cytochrome c reductase	thiols
MC	N	–	-0.40	+	–	–
MA	O	–	-0.19	+	+	+
WV-15 (a mitosene)	O	–	-0.30	+	–	–
BMY-25067	N	+	-0.40 to -0.45	+	–	+
KW-2149	N	+		+	–	+
M-18	N	+		+	–	+
MC-En	N	–		+		

[a]Reference: Standard H_2-electrode (E^o = 0.0 V).

Scheme I. Formation of adducts of mitomycin C with DNA upon reductive activation.

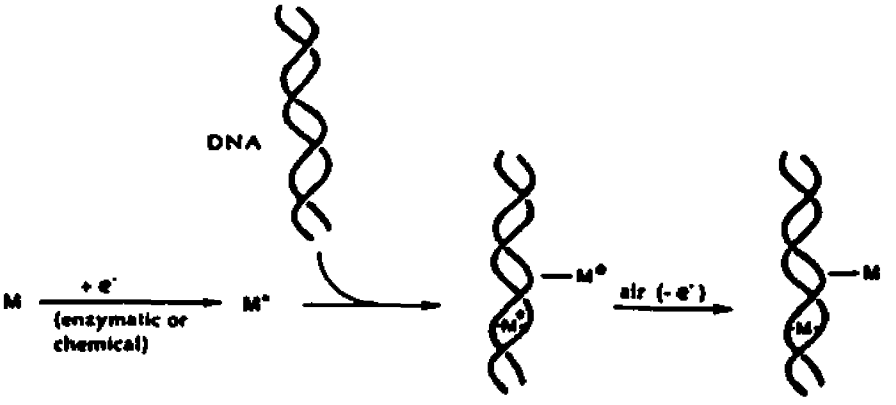

Scheme II. BMY-25067 (KW-2149 and M-18) DNA-alkylation pathway under thiol activation.

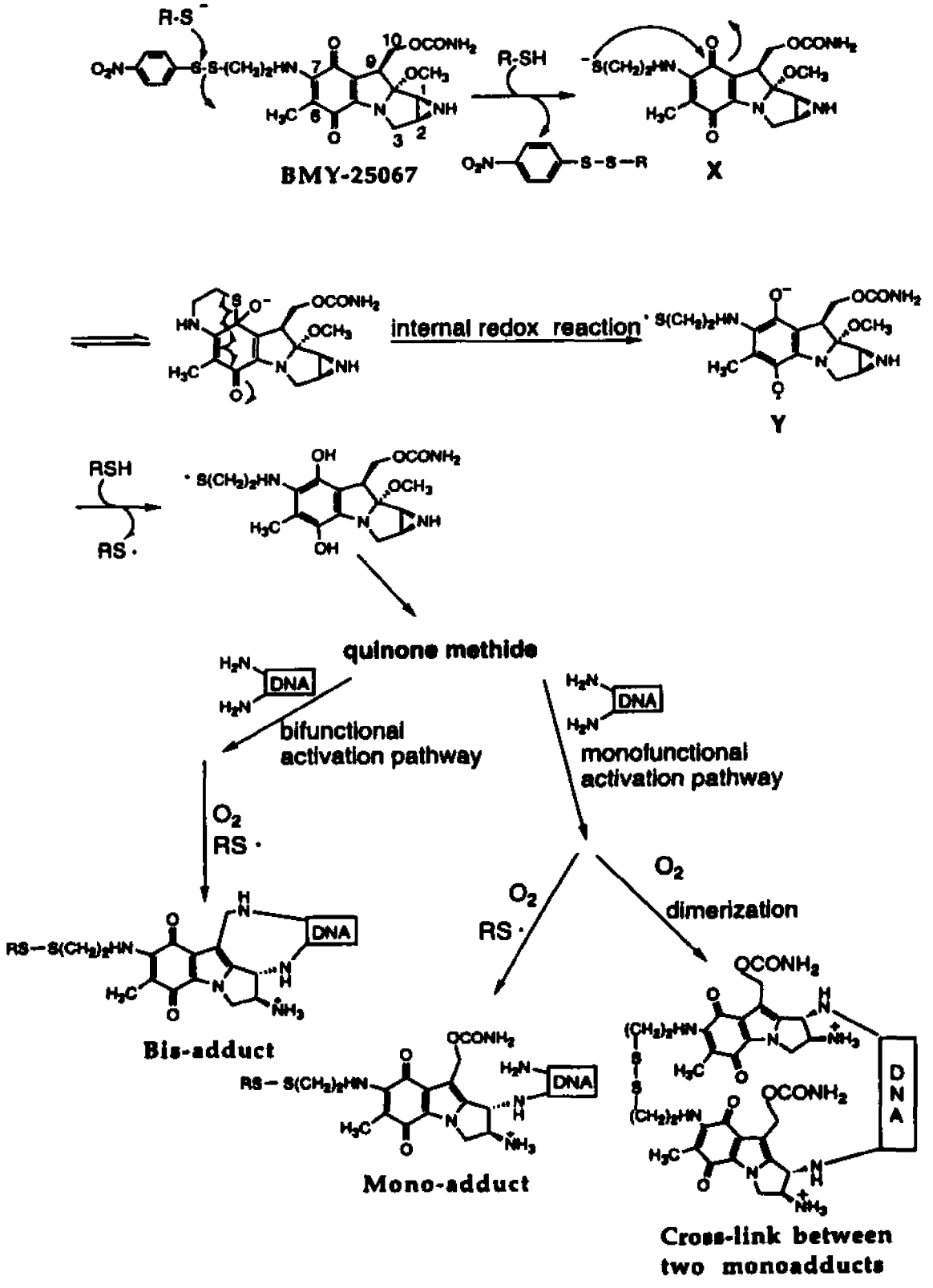

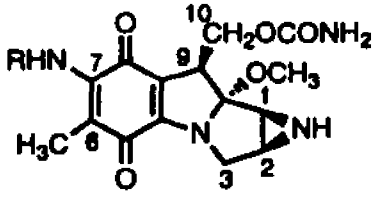

Mitomycin C (MC; 1): R = H

BMY-25067 (2): R = $(CH_2)_2$-S-S- 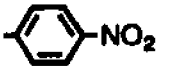 -NO_2

KW-2149 (3): R = $(CH_2)_2$-S-S-$(CH_2)_2$NH-γ-L-Glu

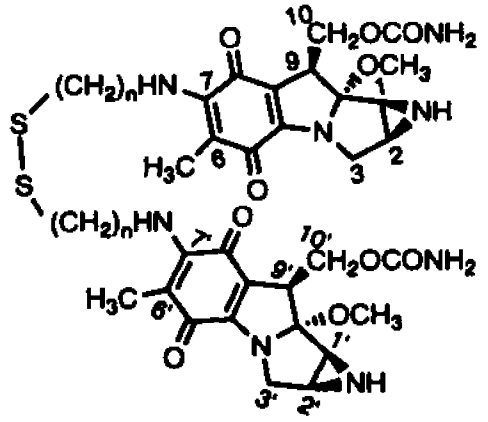

M-18 (4): n = 2

8: n = 4

9: n = 6

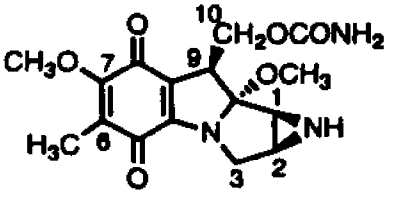

Mitomycin A (MA; 5)

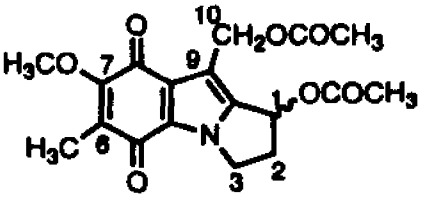

WV-15 (6)

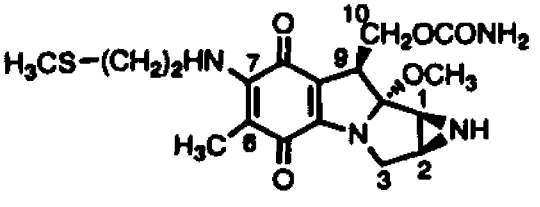

M-16 (10)

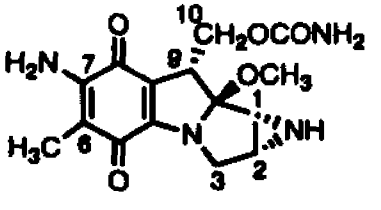

MC Enantiomer (MC-En; 7)

Figure 1. Structure of mitomycin C and its analogs.

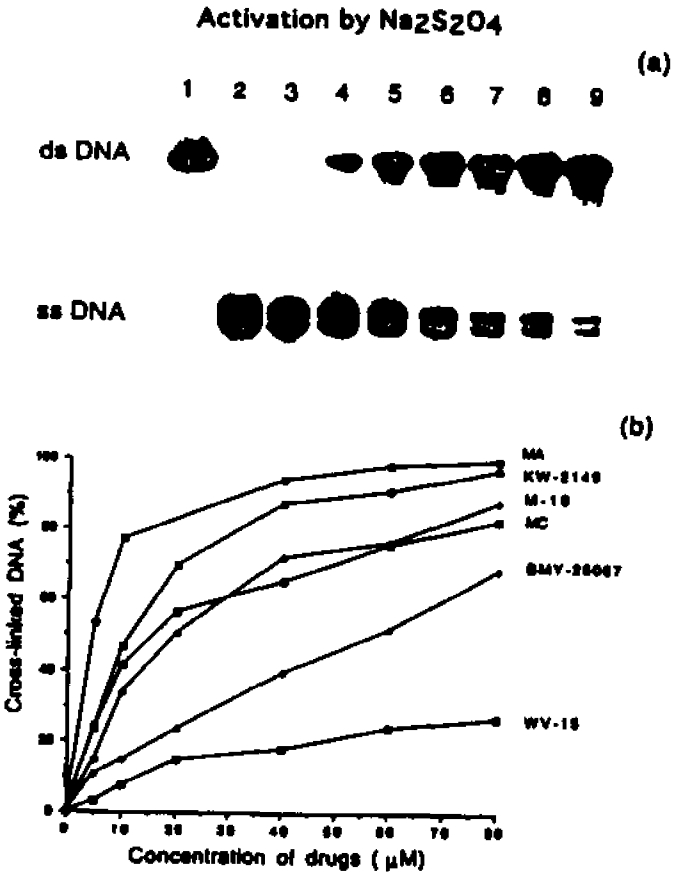

Drugs	MC	BMY-25067	KW-2409	M-18	MA
$ISCC_{50}$ (μM)	15.6	57.2	11.5	19.6	4.7

Figure 2. Cross-linking efficiency of antitumor agents 1-6 under the activation by $Na_2S_2O_4$. (a) Autoradiogram of an agarose gel showing the dependence of ^{32}P-pBR322 DNA cross-linking by MC on the concentration of MC. Complete system: 118 μM DNA was treated with the varying amount of MC and 1.2 mM $Na_2S_2O_4$ under anaerobic condition followed by heat-denaturation as described in the Method. Lanes # 1-9 contained the following: 1: control linear ^{32}P-pBR322 DNA; 2: control linear ^{32}P-pBR322 DNA, heat-denatured; 3-9: complete system; MC concentration are 0, 5, 10, 20, 40, 60 and 80 μM, respectively. (b) Plot of % cross-linking as function of drug concentration, measured by densitometry of the autoradiogram of the gel for drugs 1-6. The drug concentration at 50% interstrand cross-links ($ISCC_{50}$) was list in the inserted Table.

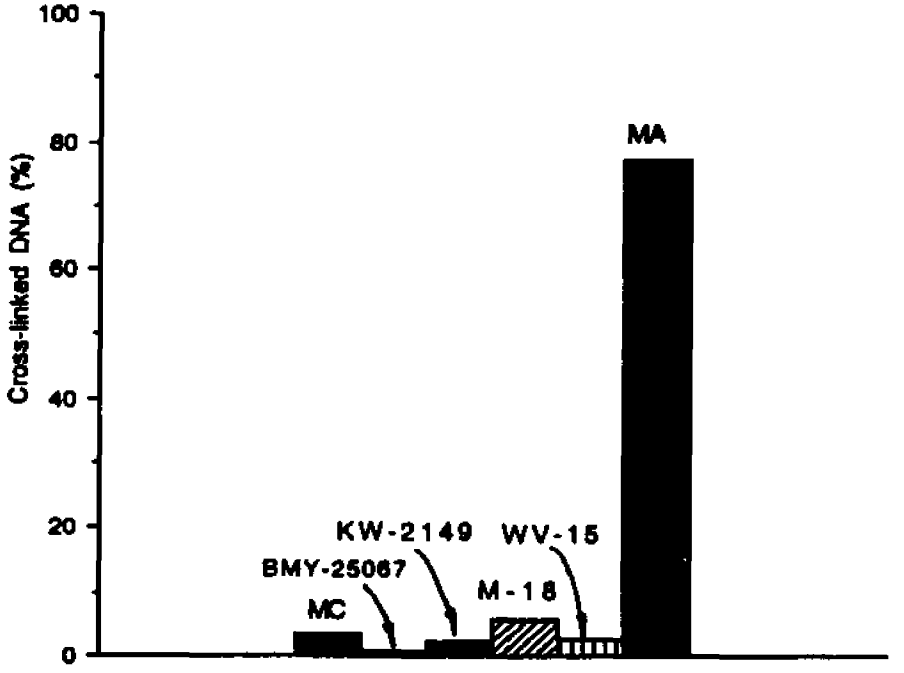

Figure 3. Comparison of the cross-linking efficiency of antitumor agents 1-6 under enzymatic activation (NADPH-cytochrom c reductase/NADPH). A mixture containing 118 μM DNA, 80 μM drug, 4 mM NADPH and 0.8 unit/ml cytochrome c reductase was incubated at 37 °C for 20 min under anaerobic condition in 25 μl 20 mM Tris-HCl (pH 7.4)-1 mM EDTA buffer.

5'-CGCGCGCGCG-3
\M-M\
3'-GCGCGCGCGC-5'

Where M-M is the dimer M-18.

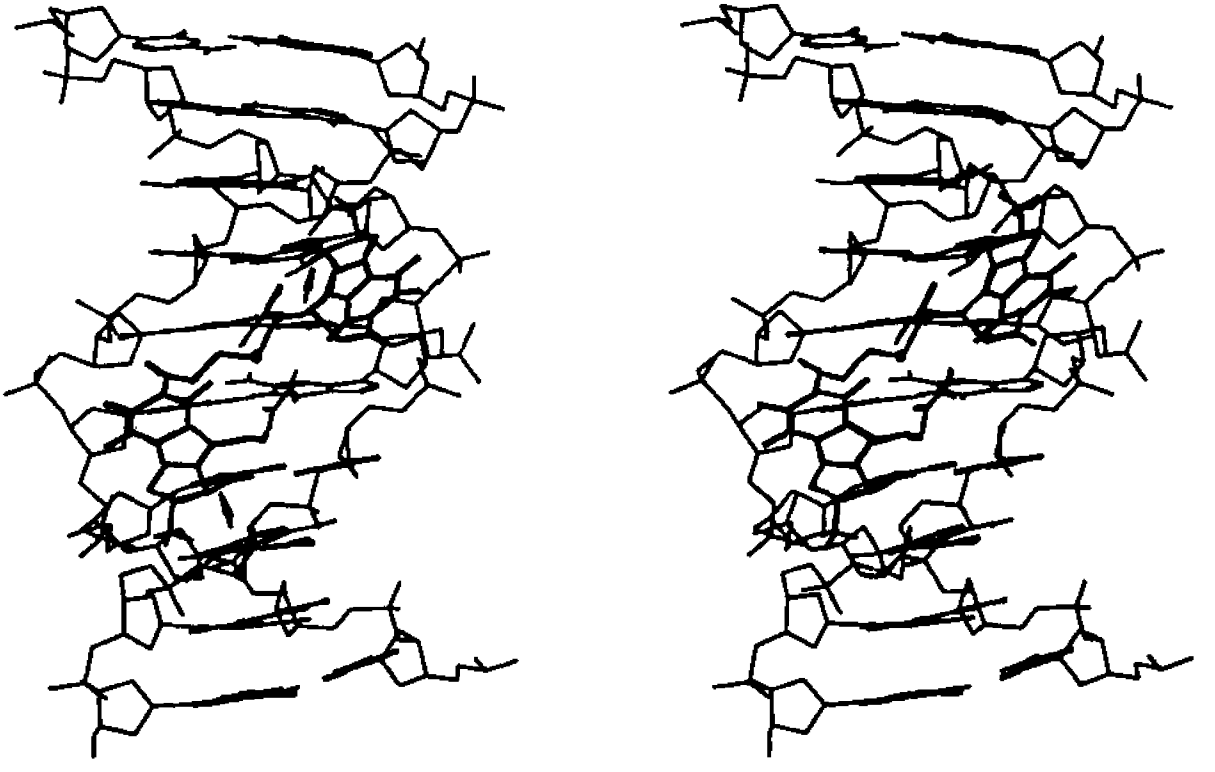

Figure 4. Stereoview of the cross-linked d(CGCGCGCGCG)$_2$-M-18 adduct. M-18 was located in the minor groove of the computer-generated B-DNA, which was then refined with MacroModel minimization routines BDNR and PRCG respectively. The arrows show the two covalent drug-DNA linkages.

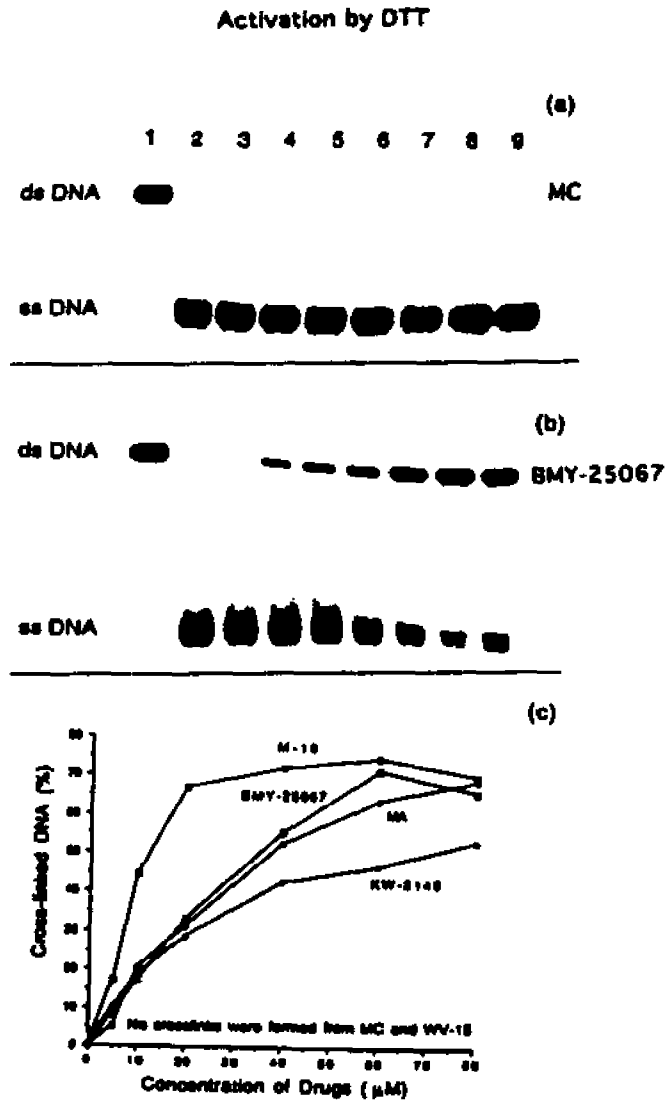

Figure 5. DNA cross-linking by BMY-25067 under the activation by DTT. (a) Autoradiogram of an agarose gel which shows no DNA-cross-linking by MC. Complete system: 118 μM DNA was treated with varying amount of MC and 80 μM DTT at room temperature for 1 h, followed by heat-denaturation as described in Methods. Lanes # 1-9 contained the following: 1: control linear ^{32}P-pBR322 DNA; 2: control linear ^{32}P-pBR322 DNA, heat-denatured; 3-9: complete system; MC concentrations are 0, 5, 10, 20, 40, 60 and 80 μM, respectively. (b) Autoradiogram of an agarose gel assay of ^{32}P-pBR322 DNA cross-linking by BMY-25067. Complete system was the same as (a), except that the drug was BMY-25067 instead of MC. (c) Plot of % cross-linking by MC analogs as function of drug concentration, measured by densitometry of the corresponding gel autoradiograms of drugs 1-6.

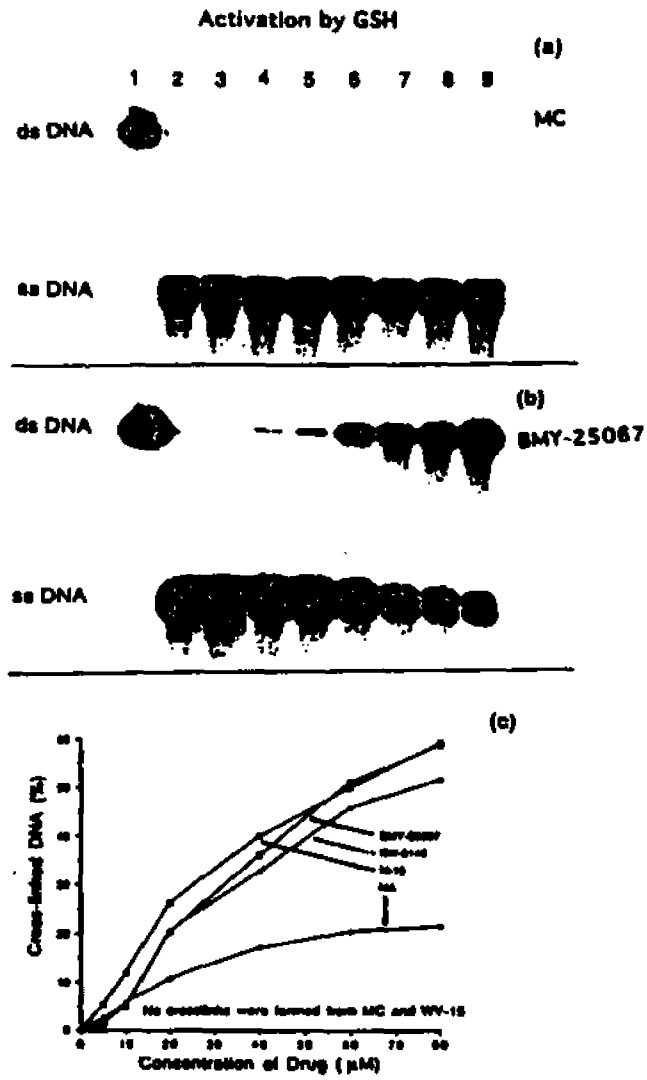

Figure 6. DNA cross-linking by BMY-25067 under the activation by GSH. (a) Autoradiograph of an agarose gel which shows no DNA-cross-linking by MC. Complete system: 118 μM DNA was treated with the varying amount of MC and 4 mM GSH at room temperature for 1 h, followed by heat-denaturation as described in the Method. Lanes # 1-9 contained the following: 1: control linear ^{32}P-pBR322 DNA; 2: control linear ^{32}P-pBR322 DNA, heat-denatured; 3-9: complete system; MC concentration are 0, 5, 10, 20, 40, 60 and 80 μM, respectively. (b) Autoradiograph of an agarose gel showing the dependence of ^{32}P-pBR322 DNA cross-linking by BMY-25067 on the concentration of BMY-25067. Complete system was the same as (a), but the drug was BMY-25067 instead of MC. (c) Plot of % cross-linking by MC analogs as function of drug concentration, measured by densitometry of the autoradiogram of the gel for drugs 1-6.

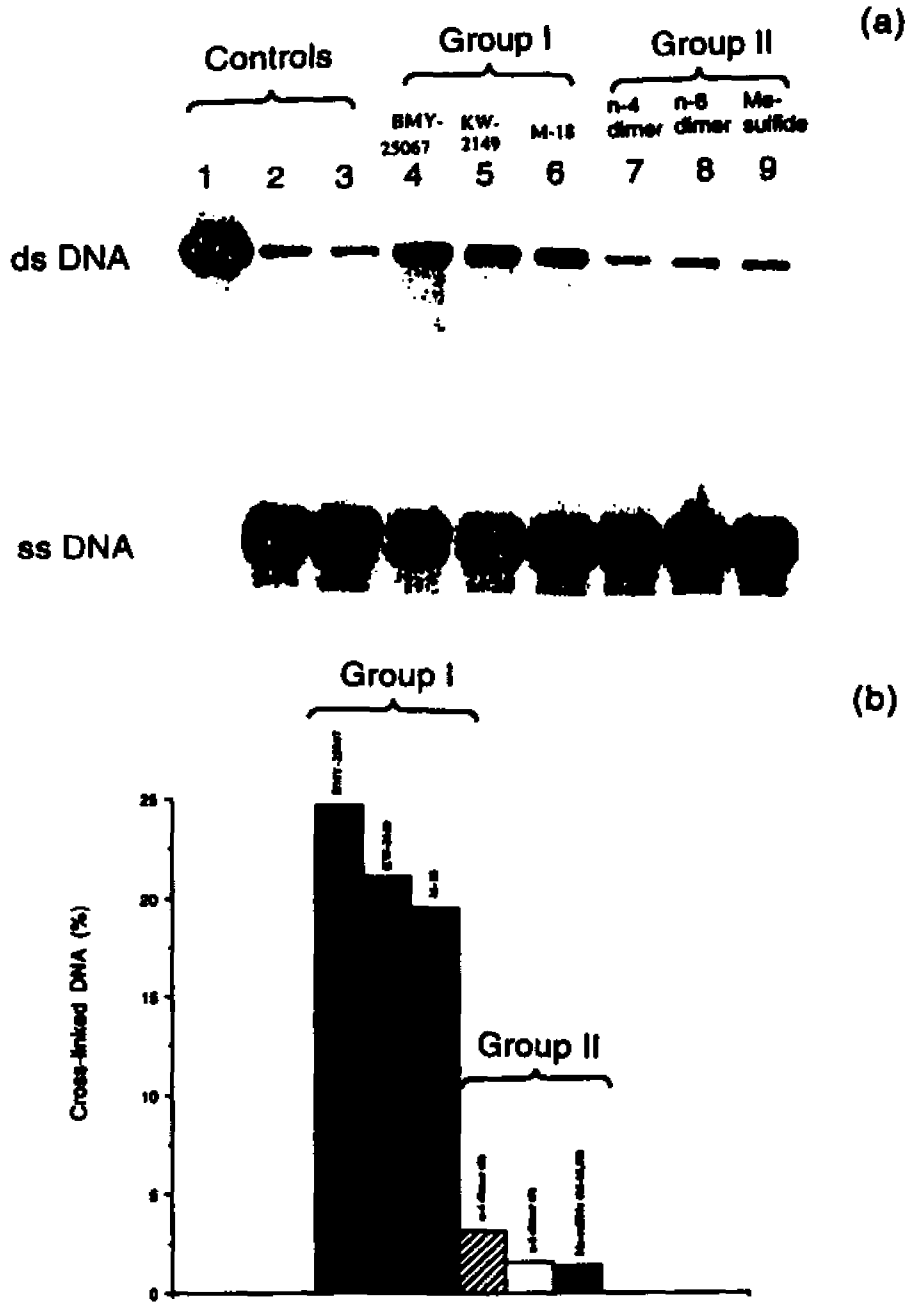

Figure 7. Cross-linking of disulfide analogs of MC under the activation by GSH. (a) Autoradiograph of an agarose gel. Complete system: 118 μM DNA was treated with 40 μM of drug and 4 mM GSH at room temperature for 1 h, followed by heat-denaturation as described in the Method. Lanes # 1-9 contained the following: 1: control linear ^{32}P-pBR322 DNA; 2: control linear ^{32}P-pBR322 DNA, heat-denatured; 3-9: complete system; 3, no drug; 4, BMY-25067 (2); 5, KW-2149 (3); 6, M-18 (4); 7, dimer 8; 8, dimer 9; and 9, M-16. (b) Comparison of the cross-linking efficiency of the disulfide analogs of MC.

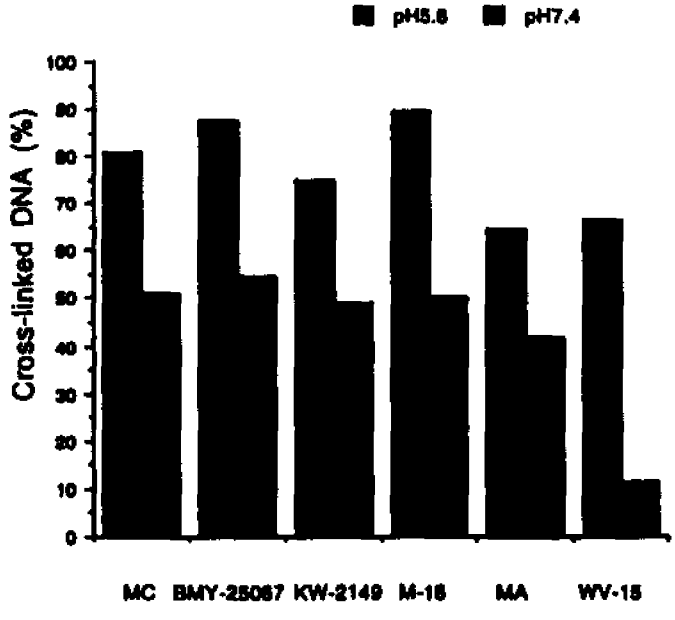

Figure 8. pH-dependent DNA-cross-linking by various antitumor agents (1-6) under the activation by $Na_2S_2O_4$. 10 ng ^{32}P-pBR322 DNA, 1000 ng calf thymus DNA were treated with drug at 15.6 μM for MC, 57.2 μM for BMY-25067, 11.5 μM for KW-2149, 19.6 μM for M-18, 4.7 μM for MA and 80 μM for WV-15 by the activation of 1.2 mM $Na_2S_2O_4$ under anaerobic condition. The reaction took one hour at room temperature in 20 mM Tris-HCl (pH 7.4)-1 mM EDTA or 20 mM Bis-Tris-HCl (pH 5.8)-1 mM EDTA, following by heat-denaturation as described in the Method.

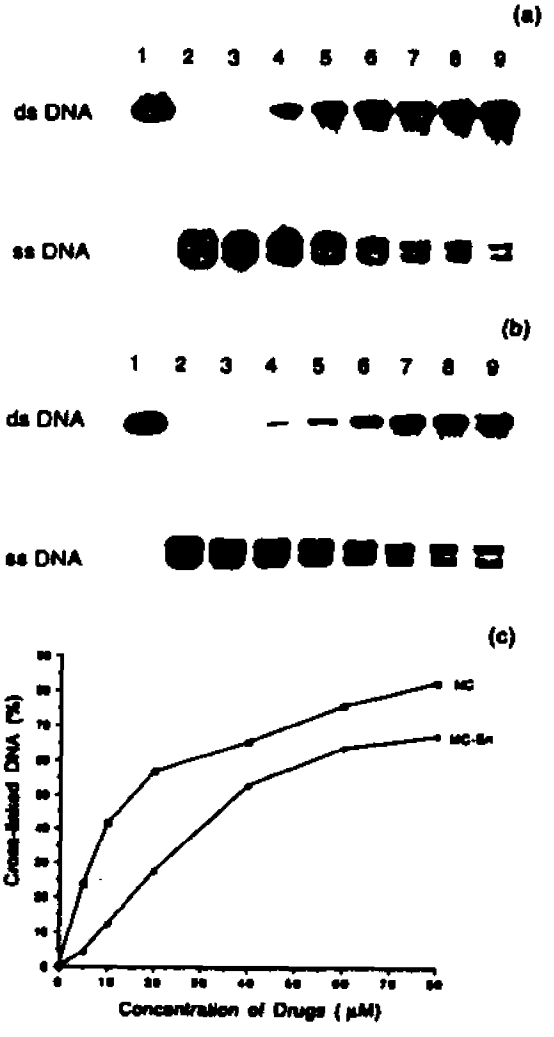

Figure 9. Comparison of cross-linking efficiency of MC-En with MC under the activation by $Na_2S_2O_4$. (a) Autoradiograph of an agarose gel which was showing the DNA-cross-linking by MC. Complete system: 118 μM DNA was treated with the varying amount of MC and 1.2 mM $Na_2S_2O_4$ at room temperature for 1 h under anaerobic condition, followed by heat-denaturation as described in the Method. Lanes # 1-9 contained the following: 1: control linear ^{32}P-pBR322 DNA; 2: control linear ^{32}P-pBR322 DNA, heat-denatured; 3-9: complete system; MC concentration are 0, 5, 10, 20, 40, 60 and 80 μM, respectively. (b) Autoradiograph of an agarose gel showing the dependence of ^{32}P-pBR322 DNA cross-linking by MC-En on the concentration of MC-En. Complete system was the same as (a), but the drug was MC-En instead of MC. (c) Plot of % cross-linking as function of drug concentration, measured by densitometry of the autoradiogram of the gel for MC and MC-En.

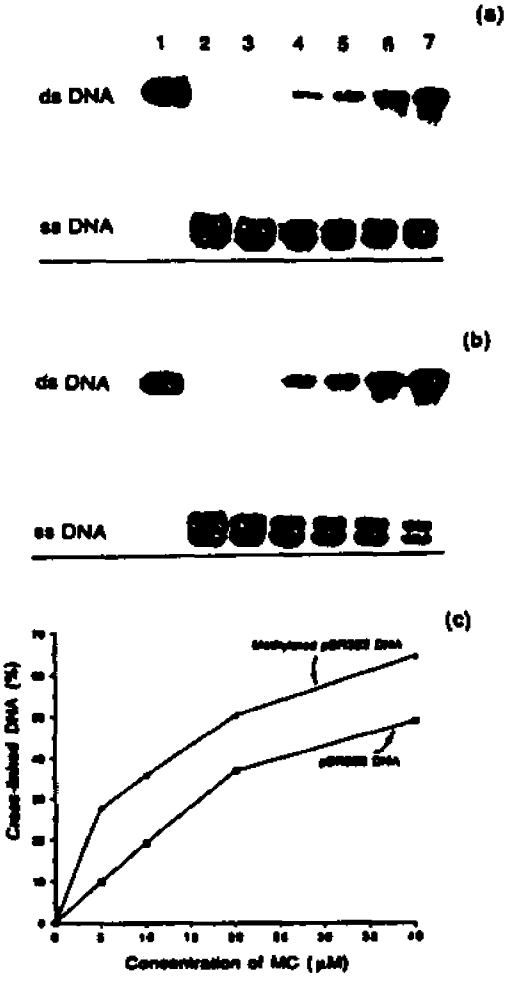

Figure 10. Methylated DNA-cross-linking efficiency by MC under the activation by $Na_2S_2O_4$, as compared with the non-methylated DNA. (a) Autoradiograph of an agarose gel which was showing the non-methylated DNA-cross-linking by MC. Complete system: 118 μM DNA was treated with the varying amount of MC and 0.6 mM $Na_2S_2O_4$ at room temperature for 1 h under anaerobic condition, followed by heat-denaturation as described in the Method. Lanes # 1-7 contained the following: 1: control linear ^{32}P-pBR322 DNA; 2: control linear ^{32}P-pBR322 DNA, heat-denatured; 3-7: complete system; MC concentration are 0, 5, 10, 20 and 40 μM, respectively. (b) Autoradiograph of an agarose gel showing the methylated ^{32}P-pBR322 DNA cross-linking by MC. Complete system was the same as (a), but the methylated DNA (71.5% cytosine residues in the sequence 5'-CG-3') was used instead of the non-methylated DNA. (c) Plot of % cross-linking as function of drug concentration, measured by densitometry of the autoradiogram of the gel for the both DNA.

Figure 11. Inhibition of MC-induced cross-linking of linear ^{32}P-pBR322 DNA by GSH. (a) 1% agarose gel electrophoresis of linear ^{32}P-pBR322 DNA cross-linked by MC in the presence of GSH, followed by heat-denaturation. Complete system: DNA was treated with MC, GSH and $Na_2S_2O_4$, followed by heat-denaturation as described in the Method Section. Lanes # 1-9 contained the following: 1: control linear ^{32}P-pBR322 DNA; 2: control linear ^{32}P-pBR322 DNA, heat-denatured; 3: Complete system containing 40 mM GSH and 1.2 mM $Na_2S_2O_4$, but no MC was added; 4-9: complete system; GSH concentration are 0, 5, 10, 20, 30 and 40 mM, respectively. (b) Plot of % cross-linking as function of GSH concentration, measured by densitometry of the autoradiogram of the gel in (a). (c) % Cross-linked DNA as function of MC concentration, in the absence or presence of 20 mM GSH, measured by densitometry of the autoradiogram of a gel run of reactions similar to those in (a), except that the MC concentrations varied (see Method Section).

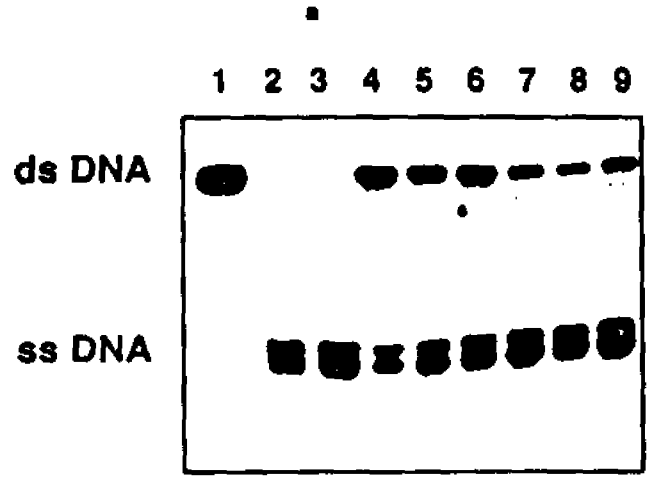
a
1 2 3 4 5 6 7 8 9
ds DNA
ss DNA

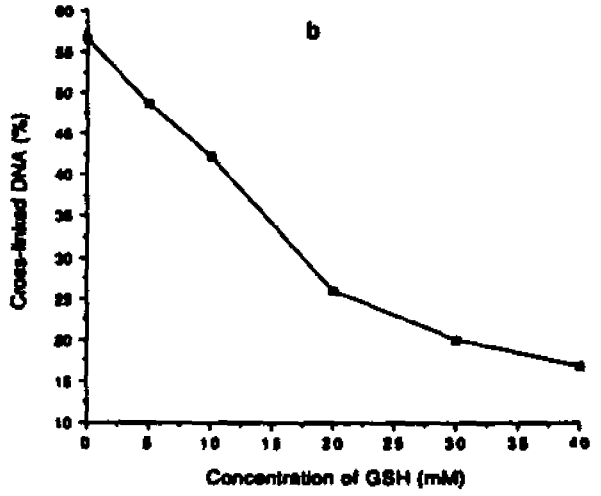
b
Cross-linked DNA (%)
Concentration of GSH (mM)

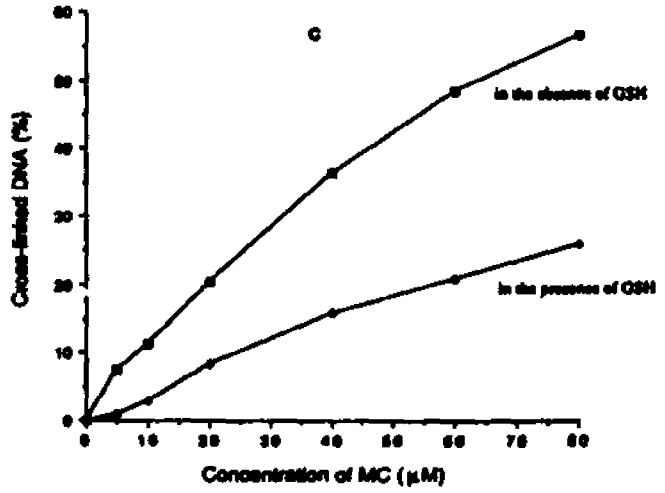
c
Cross-linked DNA (%)
Concentration of MC (μM)

Chapter III. Non-covalent binding of mitomycins to DNA

INTRODUCTION

There has been considerable interest in elucidating those factors that determine affinity and selectivity in binding of small molecules to DNA (74-78). A quantitative understanding of such factors that determine recognition of DNA sites would be valuable in the rational design of sequence-specific DNA binding molecules for application in chemotherapy and in the development of tools for biotechnology. Much work has focused on the elucidation of non-covalent interactions with DNA by small natural products and their synthetic derivatives. These small molecules are stabilized in binding to DNA through a series of weak interactions, such as the π-stacking interactions associated with intercalation of aromatic heterocyclic groups between the base pairs, electrostatic forces, hydrogen-bonding and van der Waals interactions of functionalities bound along the groove of the DNA helix. It would be valuable to understand quantitatively the contributions from these different modes to stabilization of the bound complex at a DNA site.

We have examined the non-covalent interactions of mitomycins with DNA. The mitomycins are a group of potent antibiotics. Mitomycin C (MC, Figure 1) is widely used in clinical anticancer chemotherapy against a broad spectrum of solid tumors. The covalent interaction mechanism of MC with

DNA has been well-known. The activation of MC is required by enzymatic or chemical reduction or mild acidic treatment, converting MC to an alkylating agent capable of monofunctional and/or bifunctional covalent interaction with DNA. MC bonds bifunctionally to DNA with a CG·CG sequence specificity (61, 66). In fact, there is 5'-CG-3' sequence pre-selection in the formation of the monoadduct of MC with DNA (69, 70). It is possible that MC is attracted to DNA before and after activation. The study for mitomycin binding to DNA has been carried out in order to examine the existence of non-covalent binding of MC and its derivatives, mitomycin A (MA) and two semi-synthesized mitomycins, BMY-25282 and BMY-25067 (Figure 1). It is of greater interest, however, to obtain information about the DNA-binding affinity of the active form of mitomycin C, since this is the actual DNA-alkylating molecule. Although the structure of this form is relatively well-established as the quinone methide (Figure 1), it is too short-lived to study its binding to DNA directly (79). We tested DNA binding by using the stable "activated form analogs" of mitomycin C, such as M2 and M3 (Figure 1). These mitosene quinones, especially M3, resemble the active form quinone methide. In this report we explore the non-covalent interactions of "activated form analogs" of MC with DNA using classical equilibrium dialysis (78) and spectroscopic titration methods (80). The study of "activated form analogs" non-covalently binding to DNA offers the opportunity to research systematically how such factors as electrostatic force and hydrogen bond stabilize the small molecules on DNA. We used DNAs with different base composition and sequence to examine whether the binding has a specific selection for the base composition and sequence of DNA. The non-covalent binding parameters, such as the intrinsic binding constant K_b, and the

binding site size n, of "activated form analogs" to DNA were determined from these studies.

MATERIALS

Materials and their sources were as follows: Calf thymus DNA (Type I) was from Sigma, St. Louis, MO. *M . luteus* DNA was from ICN Biomedicals, Costa Mesa, CA. Both DNAs were sonicated and dialyzed before use. Poly (dG-dC)·poly (dG-dC), Poly (dA-dT)·poly (dA-dT), d(CG)5 and d(AT)5 were from Pharmacia Biotech, Piscataway, NJ, and they were also dialyzed before use. Dialysis tubings and dialysis membranes were from Spectrum Medical Industries, Inc, Los Angeles, CA. Mitomycin C, porfiromycin, [1a-^{3}H] porfiromycin (19.7 mCi /mmol), BMY-25067 and BMY-25282 were generously supplied by Bristol-Myers Squibb Co. Other reagents were obtained from Aldrich Chemical Co. Mitosenes M2 and M2-P were obtained upon the acidic hydrolysis of MC followed by purification of this hydrolysis mixture with a Sephadex G-25 column as described (34). DM2 and PM2 were prepared from 10-decarbamoyl mitomycin C and porfiromycin by a similar procedure, respectively. M3 and DM3 were synthesized by the hydrogenation of mitomycin C and 10-decarbamoyl mitomycin C by H_2/PtO_2 at pH 5.0 followed by purification of this reaction mixture with a Sephadex G-25 column according to the published procedure (18). MA was synthesized by hydrolysis of MC to an unstable intermediate, 7-hydroxyl mitomycin, followed by methylation (39, 40).

METHODS

Binding of mitomycins and the "activated form analog" M2 to DNA. The non-covalent binding of mitomycins were determined by the classical equilibrium dialysis method. 4 ml of 3.5 mM calf thymus DNA in 10 mM tris buffer, pH 7.5, were sealed inside a 5/8 " dialysis tubing (MWCO 3500). A magnetic stirrer and the dialysis tubing were placed in a test tube containing 7 ml mitomycin solution (80 μM or 250 μM) in the same buffer. The dialysis was performed at room temperature for 24 hours under stirring. At the end of this period, NaCl was added to the solution inside the tubing as well as to that outside the tubing to a final concentration 0.5 M, and the absorbance of both solutions were recorded at λ_{max} of the drug (Table I). The following formulae were used for the calculation of K_b.

$$M + DNA \rightleftharpoons M\text{-}DNA$$

$$K_b = [M\text{-}DNA]/\{[M]\,[DNA]\}$$

$$= \frac{[A_{in} - A_{out} - A_{DNA}]/\varepsilon\lambda max}{(A_{out}/\varepsilon\lambda max) \times [(A_{260\ DNA}/\varepsilon_{260}) - (\text{numerator})]}$$

A_{in}: absorbance of the solution inside the tubing at λ_{max} of the drug.

A_{out}: absorbance of the solution outside the tubing at λ_{max} of the drug.

A_{DNA}: absorbance of DNA at λ_{max} of the drug.

$A_{260\ DNA}$: absorbance of DNA at 260 nm.

$\varepsilon\lambda max$: molar extinction coefficient of the drug (Table I).

ε_{260}: molar extinction coefficient of DNA (Table I).

A DNA and A 260 DNA were measured before the dialysis.

Determination of the non-covalent binding parameters of "activated form analog" PM2 to DNA by Scatchard plot. Intrinsic binding constant (K_b) and binding site size (n). The binding of tritium-labeled PM2 (Figure 1) to calf thymus DNA was conducted by equilibrium dialysis, which was performed in 10 mM phosphate buffer, pH 6.0 for 24 hours at room temperature by using a dialysis cell [1-ml size (cell-half), 5-cavity, Equilibrium Type, Bel-Art Products, Inc, NJ]. Dialysis membrane with 6000 molecular weight cut-off was used. The dialysis membrane was cut to size, washed in 10 mM EDTA and then in boiling water for 20 min, and finally secured in the dialysis apparatus. In each cell, on one side of the membrane, was placed 0.5 ml of DNA solution (0.294 mM, measured in mononucleotide). On the other side of the membrane was placed 0.5 ml of a solution containing varying amounts of drug (0 - 8 mM in the same buffer, specific radioactivity 7865.5 cpm/Aλ_{max}). The samples were agitated on a shaker for 24 h at room temperature, then 0.2 ml of the solution from each side of each cell was added to 4 ml of scintillation liquid, and was analyzed by counting with a Beckman LS 6800 Liquid Scintillation Counter with a tritium window. This analysis provided information on the drug concentration on each side of the membrane, enabling calculation of the amount of PM2 bound to the DNA and the concentration of free PM2. From this, values of r and C_f (free drug concentration) were tabulated.

$$r = \frac{\text{cpm of DNA side - cpm of drug side}}{\text{sp. activity} \times 11.1 \times 10^3 \times [\text{DNA}]}$$

where r is the molar ratio of bound drug to DNA (mononucleotide).

11.1×10^3 l . mol^{-1} . cm^{-1} is the extinction coefficient of PM2.

A plot of r/C_f to r was analyzed by the site exclusion model of McGhee and von Hippel (81), with a least-square non-linear regression analysis procedure in Statistical Analysis System (SAS). As a result, K_b and n were obtained.

$$r/C_f = K_b(1-nr)\{(1-nr)/[1-(n-1)r]\}^{n-1}$$

K_b: the intrinsic binding constant (M^{-1})

n: binding site size averaged over all possible sequences of the DNA

Absorption Titration Method (80). K_b can be determined from the data obtained by the absorption titration method as well in 10 mM phosphate, pH 6.0 buffer, using the following formula:

$$[DNA]/(\varepsilon-\varepsilon_o) = [DNA] / (\varepsilon_B - \varepsilon_o) + 1 / [K_b \times (\varepsilon_B - \varepsilon_o)]$$

ε, ε_o and ε_B correspond to A/[drug], the extinction coefficient for the free drug, and the extinction coefficient for the drug in the fully bound form, respectively. A is the observed absorbance of drug in the solution. This formula can be modified as follows.

$$[DNA]/(A-A_o) = [DNA] / (A_B - A_o) + 1 / [K_b \times (A_B - A_o)]$$

$$(\text{or } [DNA] / (A - A_o) = [DNA][M]/(\varepsilon_B - \varepsilon_o) + [M]/[K_b(\varepsilon_B - \varepsilon_o)])$$

[M] is the drug concentration. A, A_O and A_B correspond to the observed absorbance of drug in the solution, the absorbance for the free drug, and the absorbance for the drug in the fully bound form,

For this titration, 0 to 2.6 ml of DNA solution (2.94 mM) were added to aliquots of 0.4 ml of drug solution (0.57 mM), then diluted to 3 ml to 76 μM final drug concentration, and 0 - 2.55 mM DNA concentration in 10 mM phosphate, pH 6.0. After the drug-DNA solution was mixed and incubated for 10 minutes, the absorbance of the mixture was determined at the λ_{max} of drugs (Table I). The plot of [DNA]/(A-A_O) to [DNA] was obtained, and gave a linear curve. Therefore, K_b was calculated from the slope and intercept by a linear analysis.

$$K_b = \text{slope/intercept } (M^{-1})$$

Determination of pKa. The pk_a of PM2 and M2 was measured as follows: 15 ml of 50 μM of PM2 in 0.01 M tris - 0.1 M NaCl pH 10.95 buffer were titrated with 1 N HCl. The pH and absorbance (at 258 nm) of the mixture were determined after each addition of 3 μl of 1 N HCl. The measurement was repeated until the pH reached 2. A titration curve of absorbance *versus* pH was plotted and the pK_a of PM2 was shown to be 7.33. In the same way the pKa of M2 was obtained as 7.10 (Figure 7c).

Non-covalent binding of drugs to oligonucleotides d(CG)5 and d(AT)5 was determined by the equilibrium dialysis method. The dialysis took 3 days at 4 ^oC by using 1000 MWCO membrane.

UV spectra were recorded on a Varian Cary 3 spectrophotometer. A Gilford 250 spectrophotometer was used for absorbance determination. The extinction coefficients and λmax of DNA and drugs are listed in Table I.

RESULTS AND DISCUSSION

I. Non-covalent binding of mitomycins to DNA.

The binding constant (K_b) of mitomycins to calf thymus DNA was determined by equilibrium dialysis in 10 mM tris pH 7.5. As shown in figure 2, MC, MA as well as the two semi-synthetic analogs, BMY-25282 and BMY-25067 all exhibited no binding to DNA. However, the "activated form analog" M2 of mitomycin C demonstrated binding to DNA. These results indicated that the mitomycins themselves do not bind to DNA in the non-covalent binding step before activation.

II. Determination of binding parameters.

The binding of [^{3}H]-PM2 to DNA was conducted by equilibrium dialysis, which was performed in 10 mM phosphate buffer, pH 6.0 for 24 h at room temperature. The results showed that the binding of PM2 to DNA fitted the McGhee and von Hippel model (Figure 3). The calculated intrinsic binding constant K_b is 3164 M^{-1} and the binding site is 4.5 base pairs.

III. Use of the absorption titration method to further characterize the binding.

The binding of "activated form analogs" of mitomycin C to DNA was accompanied by hypochromism and red shift of the UV spectral maximum in the 300-400 nm range (Figure 4). Therefore absorption titration could be used as alternative method to equilibrium dialysis. For example, a mixture of 42 μM M2 and varying amounts of calf thymus DNA (0, 62, 185, 372 and 433 μM) was prepared and the UV spectra for these mixtures were recorded, as shown in figure 4. A well-behaved titration of M2 with calf thymus DNA was displayed. The spectra showed clearly that addition of DNA yielded hypochromism and a small red shift. In order to find out what factors affect the binding to DNA, equilibrium binding constants K_b of "activated-form analogs" of MC to DNA were determined under various conditions, by using the absorption titration method. "Activated form" M2, DM2, M3, DM3, PM2 and M2-P (Figure 1) were used for this study.

(i) Effect of ionic strength

The binding constant K_b was measured in the presence of different amounts of NaCl (0-49 mM) as follows. A series of mixtures of 76.6 μM M2 and varying amounts of DNA (0-2.94 mM) in 3 ml of 1 mM phosphate buffer pH 6.0 were prepared. The absorbance of each mixture was determined at 310 nm. It was shown that the absorbance was decreased with increasing concentration of DNA. Then a titration curve of A_o/A versus [M]/[DNA] was obtained. The K_b was calculated, as described in Methods. 3 μl of 1 M NaCl was added to each mixture prepared as above to yield a final concentration of 1 mM NaCl. In the same way a titration curve and K_b were obtained. The measurement was repeated by addition of 8, 30, 75, and 150 μl of 1 M NaCl to give final NaCl concentrations 2.7, 10, 24.4 and 49 mM, respectively. The

results showed that the absorbance change was dependent on the concentration of NaCl, resulting in six titration curves (Figure 5a). The absorbance change was decreased with increasing the NaCl concentration. This indicated that there was an apparent decreasing binding affinity as the salt concentration increased (Figure 5b). The linear least squares best fit line (the solid line in Figure 5c) is log K_b = 1.87 - 0.64 log [Na^+] (R^2 = 0.96). This remarkable salt dependence of the binding affinity demonstrated that there was electrostatic attraction between DNA and the protonated 2-NH_3^+ group of the drug. This was confirmed by determining the pH-dependence of the binding. First, the pKa of PM2 and M2 were determinated by spectrophotometric titration (Figure 6c), giving pKa 7.3 and 7.1, respectively. The basic function is the 2-amino group in these substances (82). The K_b of PM2 and M2 were determined at pH 6.0 and it was found that PM2 showed a slightly higher binding than M2 (Figure 6a, b). This might be due to the slightly higher pKa of PM2. A marked decrease of the DNA-binding constants of M2 and M3 with increasing pH in the range of pH 5.0 - 9.0 was determined previously in this laboratory (83). Thus, binding to DNA by the mitosenes M2, PM2 (and others) is dependent on the positively charged 2-aminogroup. Consistent with this, the mitomycins did not bind to DNA, as described above. The lack of DNA binding by the parent mitosane drugs[2] is apparently due to the lack of basicity of their aziridine (pKa approx. 2 to 3). The neutral molecules have no affinity to DNA. Activation, however, generates the basic 2-amino group in mitosenes[2] which accounts for the electrostatic attraction of M2, DM2, M3, DM3 and PM2 to DNA (Figure 2, 6 and 7). Electrostatic binding of mitosenes to polyvinyl sulfate and polyphosphate is also known (84).

To further confirm the factor of electrostatic attractions, the binding affinity of "activated form" M2-P was determined by the equilibrium dialysis

method. As shown in figure 1, M2-P has a phosphate group at C-1 position, which contains a negative charge. This negative charge neutralizes the positive charge on the amino group at C-2 position. Thus there are no electrostatic attractions between M2-P and DNA. Our results show that M2-P does not bind to DNA at all in either 20 mM MES - 1 mM EDTA, pH 5.5, or 10 mM tris, pH 7.5 buffer, in contrast to M2 (Figure 8). This result strongly supports the proposal that the electrostatic attraction between DNA and the protonated 2-NH_3^+ group of the drug is the dominant factor for the binding of these drugs to DNA.

As reported in the previous chapter of this thesis and in previous studies (65, 66), the cross-linking efficiency of MC and several mitomycin derivatives under the activation by $Na_2S_2O_4$, $NaBH_4$ and DT-diaphorase is increased with decreasing pH. This may be a result of the higher electrostatic attraction between the activated form of the drugs and DNA at lower pH.

(ii) Hydrogen bond between drugs and DNA.

In order to find out whether the 10-carbamate group contributes to the non-covalent binding, the binding constants of M2, M3, 10-Decarbamoyl M2 (DM2) and 10-decarbamoyl M3 (DM3) (Figure 1) to DNA in 10 mM phosphate, pH 6.0 buffer were measured by the titration method. It is probable that stronger hydrogen bonds can be formed between the 10-carbamate and DNA than between the 10-CH_2OH group and DNA. The results showed that the binding of 10-decarbamoyl mitosenes DM2 and DM3 was slightly lower than that of M2 and M3 respectively (Figure 7), suggesting that non-specific H-bonds contribute weakly to the stability of the electrostatic complex.

(iii) Base composition and sequence of DNA

The binding constant (K_b) of M3 to DNAs with different base composition and sequence was measured by the equilibrium dialysis method.

We selected three pairs of DNA: calf thymus DNA and *M. luteus* DNA (the G·C content is 72% in *M. luteus* DNA and only 42% in calf thymus DNA); poly(dG-dC)·poly(dG-dC) and poly(dA-dT)·poly(dA-dT); d(CG)5 and d(AT)5. The dialysis was performed in 10 mM tris-0.1 mM EDTA, pH 7.5, at least in duplicate by using a dialysis cell, as described in Methods. In each cell, on one side of the membrane was placed 0.5 ml of DNA solution at 200 μM, 500 μM and 1000 μM concentrations, respectively. On the other side of the membrane was placed 0.5 ml of M3 solution (130 μM). The binding constants of M3 to DNA did not show consistent and substantial changes with the varying base composition and sequence of these three pairs of DNA, as shown in figure 9. Thus the binding appears to be non-specific with respect to the base composition and sequence of DNA. In accordance with this conclusion, Crothers and coworkers (66) detected indirectly the binding of the reduced mitomycin species to synthetic oligonucleotides using an elegant experimental design. Cross-linking of C·G-containing oligonucleotides by the activated mitomycin was shown to be competitively inhibited by oligonucleotides containing only A·T basepairs, i.e. no cross-link sites. Kinetic data of the inhibition fitted a simple model in which the active mitomycin binds non-specifically to the oligonucleotides, regardless of base composition or base sequence. This indicated that the transient active species has only a non-specific DNA binding affinity.

It is concluded that mitomycins do not bind to DNA non-covalently, but their "activated form" can do so. The electrostatic attraction between drug and DNA predominately affects the drug's binding to DNA. The hydrogen bonds between 10-carbamate group and DNA may contribute moderately to the stability of the complex. It is not determined by these experiments whether the drug intercalates between basepairs, binds in the minor or major

groove or on the periphery of DNA. The drug-DNA non-covalent binding is non-specific with respect to DNA composition and sequence. Therefore, the preferential reaction of mitomycin with guanine of DNA cannot be explained on the basis of selectivity at the non-covalent binding step.

The most important significance of the non-covalent binding of activated mitomycin to DNA is that such binding concentrates this reactive intermediate at its covalent target, facilitating the DNA alkylation step kinetically. This effect is likely to prevent inactivating reactions with low molecular weight nucleophiles, especially with water, known to occur rapidly in the absence of DNA (18). These findings have important implications for the design of mitomycin analogs intended to act similarly to mitomycin C in the tumor tissue.

Table I. Extinction coefficient (ε) at the λ_{max} of DNA and drugs.

DNA	ε ($l \cdot mol^{-1} \cdot cm^{-1}$)	λ_{max} (nm)
Calf thymus DNA	6,800	260
M luteus DNA	6,960	260
Poly (dG·dC)	8,400	254
Poly (dA·dT)	6,600	262
d $(CG)_5$	9,850	256
d$(AT)_5$	10,250	260
Drugs	ε ($l \cdot mol^{-1} \cdot cm^{-1}$)	λ_{max} (nm)
MC	21,800	367
MA	8,910	320
BMY-25282	11,200	396
BMY-25067	16,800	373
M2 (DM2, PM2 & M2-P)	11,100	310
M3 (DM3)	11,100	314

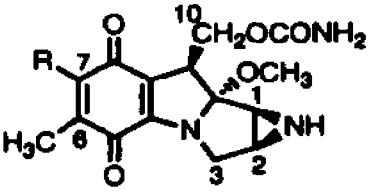

Mitomycin C (MC): R = NH_2

Mitomycin A (MA): R = OCH_3

BMY-25282: R = $N{=}CHN(CH_3)_2$

BMY-25067: R = $NHCH_2CH_2{-}S{-}S{-}C_6H_4{-}NO_2$

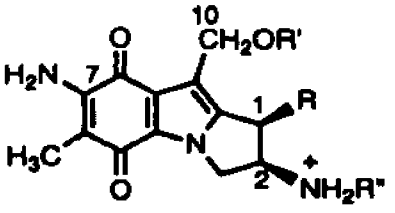

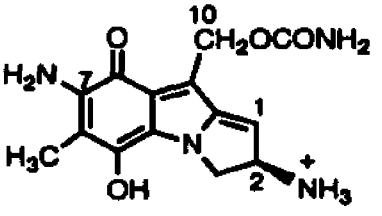

Quinone Methide

Drugs	R	R'	R"
M2:	OH	$CONH_2$	H
DM2:	OH	H	H
M3	H	$CONH_2$	H
DM3	H	H	H
PM2	OH	$CONH_2$	CH_3
M2-P	OPO_3^-	$CONH_2$	H

Figure 1. Structures of mitomycin C, its derivatives and "activated form analogs".

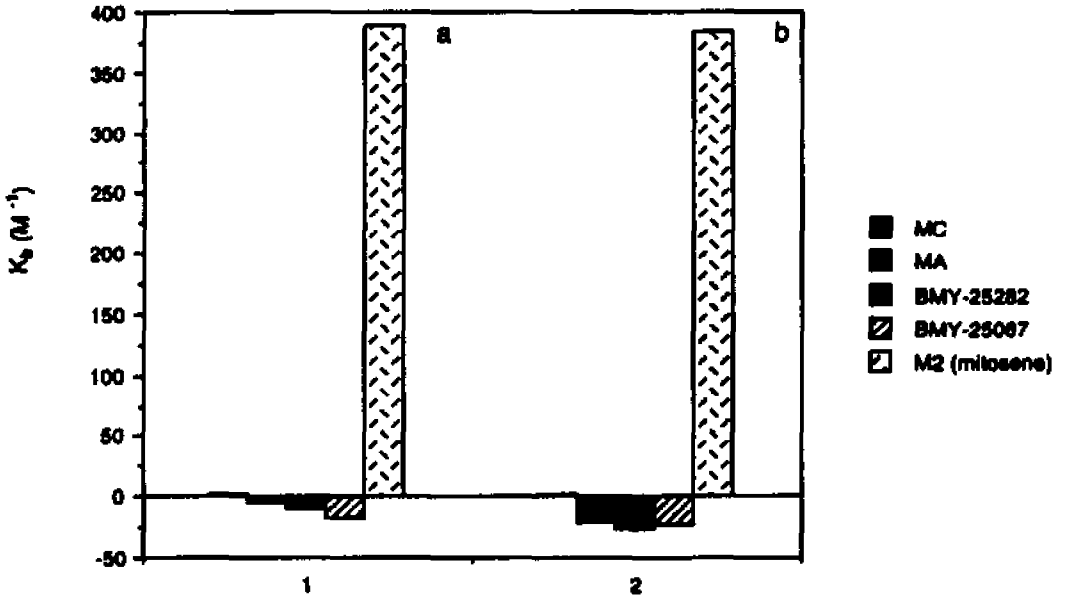

Figure 2. Binding constants for binding of mitomycins and "activated form analog M2" to calf thymus DNA (3.5 mM), determined by the equilibrium dialysis method. Drug concentration (a) 250 μM and (b) 80 μM.

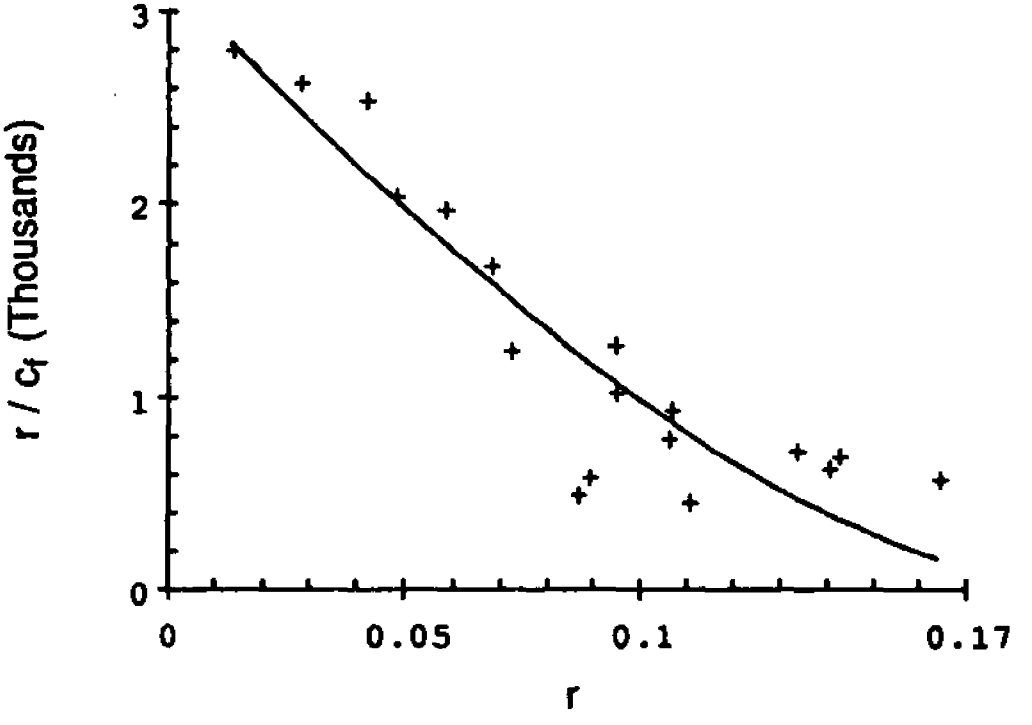

Figure 3. Scatchard plot of binding of an "activated form analog" of MC (M2) to calf thymus DNA in 10 mM phosphate buffer, pH 6.0 at room temperature, where r is the molar ratio of bound M2 to DNA (mononucleotide) and C_f is the concentration of free M2. The solid line is the best fit to the McGhee and von Hippel equation governing noncooperative binding to the helix.

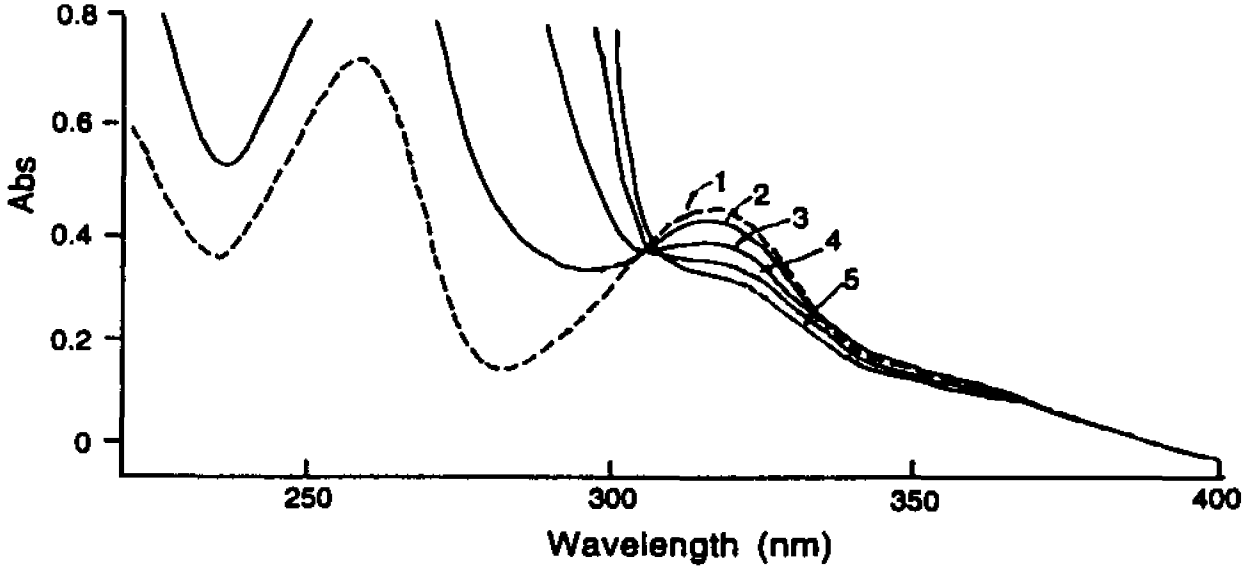

Figure 4. UV absorption spectra of M2 in the absence (curve 1, --) and presence (_) of varying amount of DNA (curve 2: 62 μM; 3: 185 μM; 4: 372 μM and 5: 433 μM).

(a)

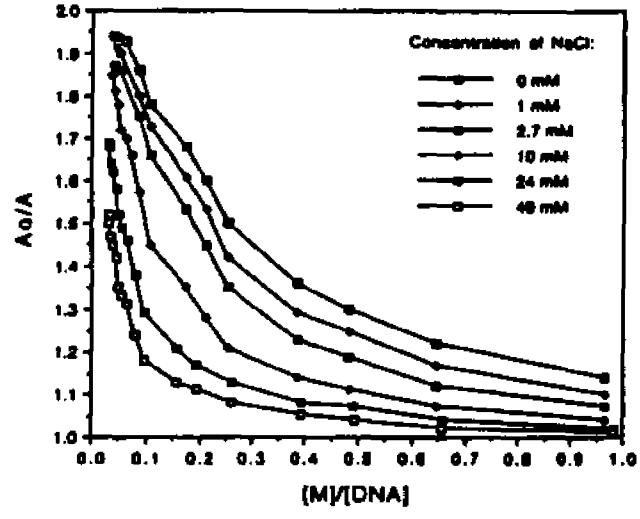

(b)

Concentration of NaCl (mM)	0	1	2.7	10	24.4	49
K_b (M^{-1})	2811	2601	2361	1657	801	472

(c)

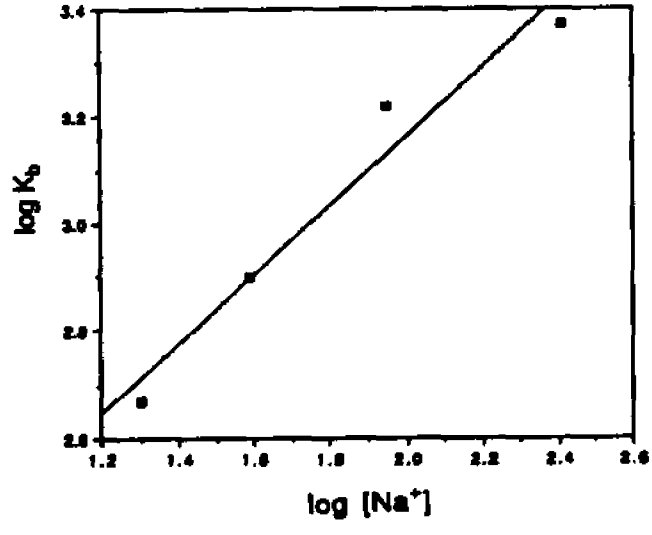

Figure 5. (a) Titration curves of A_O/A versus [M]/[DNA] in the absence and presence of NaCl. A_O/A represents the ratio of absorbance of free drug M2 (in the absence of DNA) to the absorbance as a function of increasing concentrations of added DNA. (b) Binding constants K_b at a varying amount of NaCl. (c) Dependence of M2 binding to calf thymus DNA on sodium ion concentration. Experimental data (▪). Linear least squares best fit line to experimental data (–).

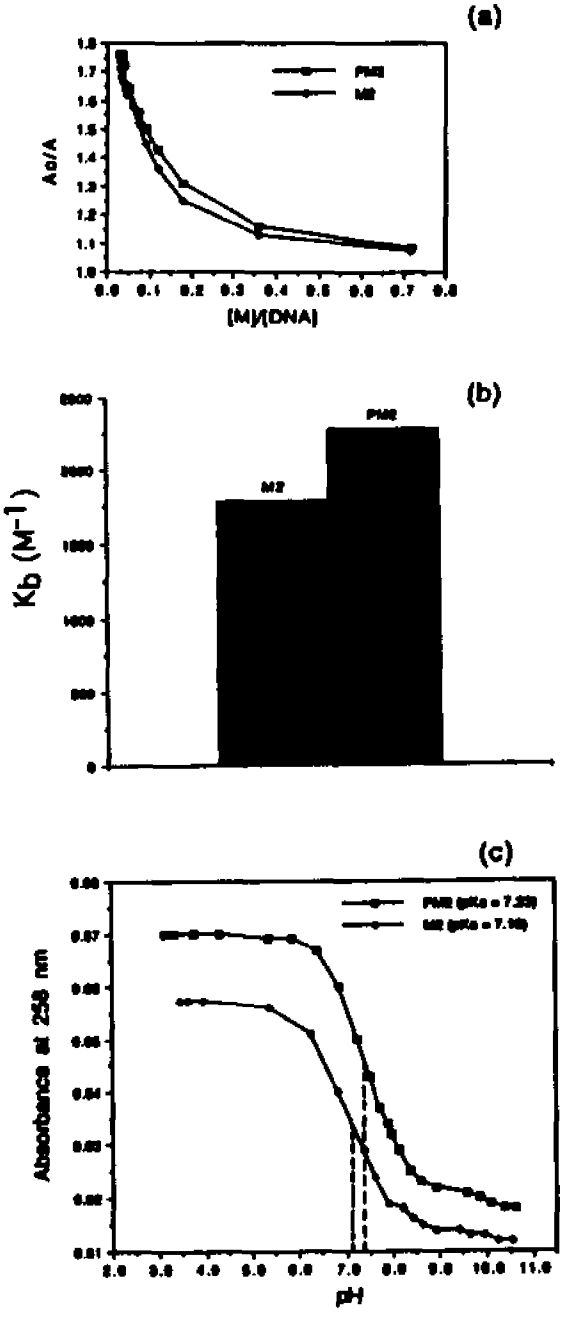

Figure 6. Effect of the drug basicity on the binding to DNA. (a)titration curves of A_O/A versus [M]/[DNA] for M2 and PM2. A_O/A represents the ratio of absorbance of the free drug (in the absence of DNA) to the absorbance as a function of increasing concentrations of added DNA. (b) Binding constants K_b of M2 and PM2. (c) Titration curve of absorbance versus pH of the drug solution for obtaining the pK_a.

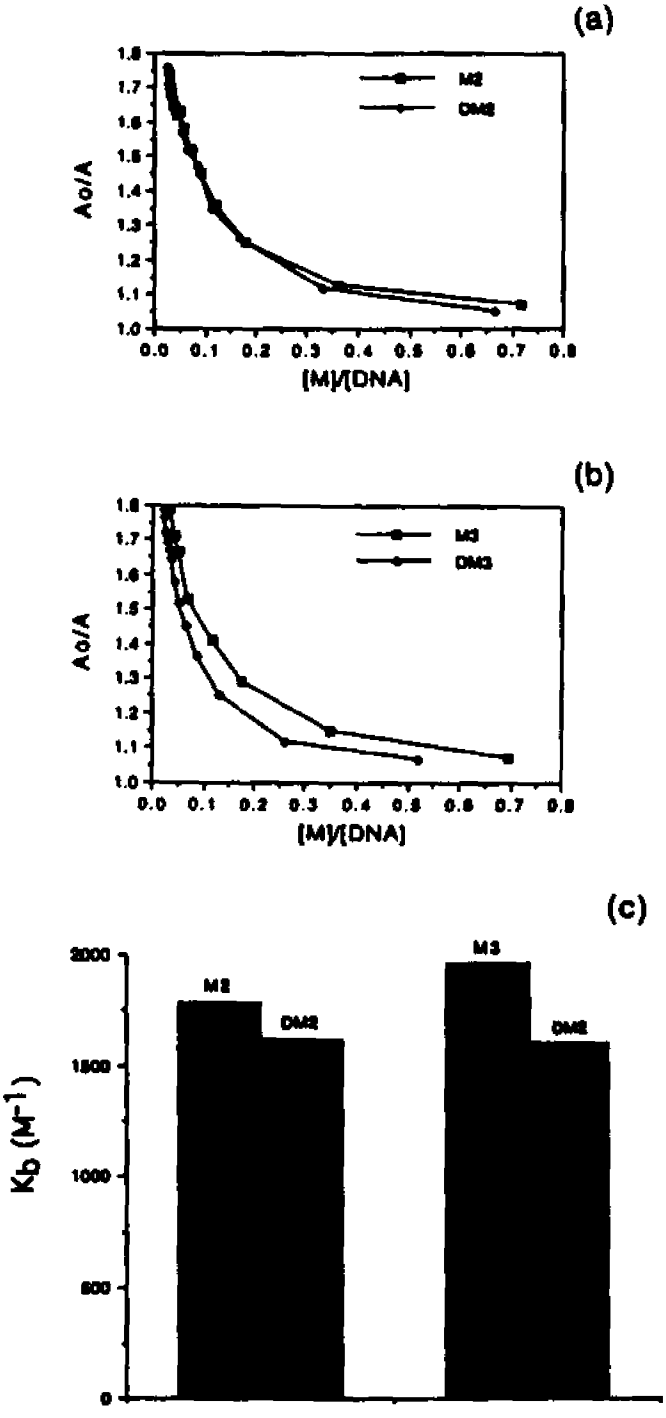

Figure 7. Effect of H-bonding on the binding of drugs to DNA. (a) and (b) are titration curves of A_O/A versus [M]/[DNA]. A_O/A represents the ratio of absorbance of the free drug (in the absence of DNA) to the absorbance as a function of increasing concentrations of added DNA. (a) For M2 and DM2 and (b) for M3 and DM3. (c) Comparison of the binding constant K_b of M2 with DM2 and M3 with DM3.

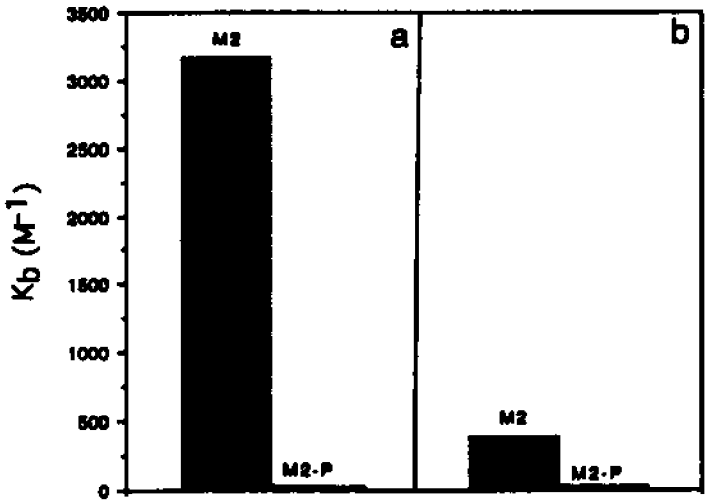

Figure 8. Effect of the drug charge on the binding to DNA. Binding constants Kb of M2 and M2-P (a) in 20 mM MES - 1 mM EDTA buffer pH 5.5. (b) in 10 mM tris buffer pH 7.5.

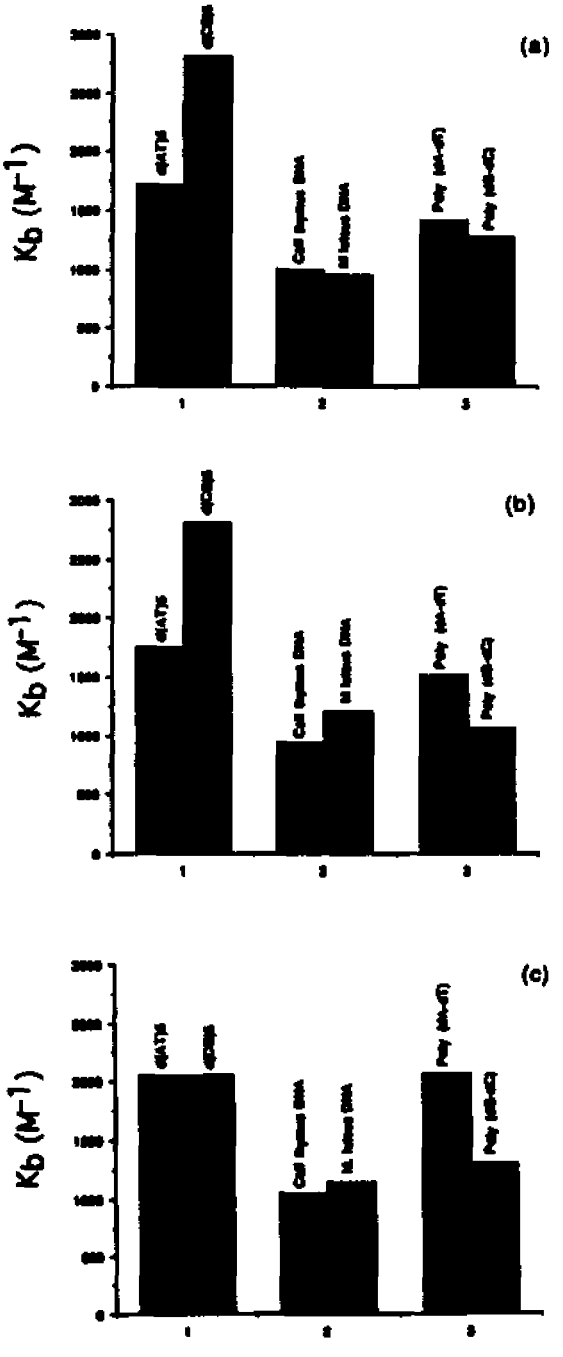

Figure 9. Binding of M3 to DNA with different composition and sequence. DNA concentration (in mononucleotide) (a) 200 μM, (b) 500 μM and (c) 1000 μM

FOOTNOTE 1

ATP	adenosine triphosphate
DMAP	dimethyl amino pyridine
DNA	deoxyribonucleic acid
DTT	dithiothreitol
EDTA	ethylene diamine N, N, N', N'-tetraacetate
ES-MS	electrospray mass spectroscopy
GSH	glutathione
HPLC	high performance liquid chromatography
$ISCC_{50}$	the drug concentration at 50% cross-linking
MA	mitomycin A (Figure 1, Chapter I)
MC	mitomycin C (Figure 1, Chapter I)
MC-En	enantiomer mitomycin C (Figure 1, Chapter II)
NADH	nicotinamide adenine dinucleotide (reduced form)
NADPH	nicotinamide adenine dinucleotide phosphate (reduced form)
NMR	nuclear magnetic resonance
SAR	structure-activity relationship
UV	Ultraviolet

FOOTNOTE 2

The term "mitosane" refers to the dihydro-indoloquinone structure and "mitosene" refers to the indoloquinone form, as defined by Webb et al (J. Am. Chem. Soc. 84 (1962), 3185-3187) and shown at the bottom of Scheme I (Chapter I).

REFERENCES

1. Carter, S. K. (1979) Reflections and Prospects. In Mitomycin C: Current Status and New Developments (Carter, S. K. & Cooke, S. T., Eds.) 251-254, Academic Press, New York.

2. Whittington, R. M. & Close, H. P. (1970) Cancer Chemother Rep (Part I) 54, 195-198.

3. Iyengar, B. S., Lin, H.-J., Cheng, L., Remers, W. A., & Bradner, W. T. (1981) J. Med. Chem. 24, 975-981.

4. Iyengar, B. S., Sami, S. M., Remers, W. A., Bradner, W. T. & Schurig, J. E. (1983) J. Med. Chem. 26, 16-20.

5. Iyengar, B. S., Sami, S. M., Tarnow, S. E., Remers, W. A., Bradner, W. T. & Schurig, J. E. (1983) J. Med. Chem. 26, 1453-1457.

6. Iyengar, B. S., Remers, W. A. and Bradner, W. T. (1986) J. Med. Chem. 29, 1864-1868.

7. Bradner, W. T., Rose, W. C., Schurig, J. E. & Florczyk, A. P. (1990) Investigational New Drugs 8, S1-S7.

8. Bradner, W. T., Rose, W. C., Schurig, J. E., Huftalen, J. B. & Vyas, D. (1985) In Recent Advances in Chemotherapy. Anticancer Section 1 (ISHIGAMI, J., Ed.) 517-518, University of Tokyo Press, Tokyo.

9. Kono, M., Saitoh, Y., Kasai, M., Sata, A., Shirahata, K., Morimoto, M. & Ashizawa, T (1989) Chem. Pharm. Bull. 37, 1128-1139.

10. Ashizawa, T., Okabe, M., Gomi, K. & Tadashi, H. (1993) Anti-Cancer Drugs 4, 181-188.

11. Kobayashi, E., Okaba, M., Kono, M., Arai, H., Kasai, M., Gomi, K., Lee, J.-H., Inaba, M. & Tsuruo, T. (1993) Cancer Chemother. Pharmacol. 32, 20-24.

12. Morimoto, M., Ashizawa, T., et al. (1991) Cancer Res. 51, 110-115.

13. Kono, M., Saitoh, Y., Kasai, M., Shirahata, K., Morimoto, M. & Ashizawa, T. (1993) J. Antibiotics 46, 1428-1438.

14. Szybalski, W. & Iyer, V. N. (1963) Proc. Natl. Acad. Sci USA 50, 355-362.

15. Iyer, V. N. & Szybalski, W. (1964) Science (Washington, D. C.) 145, 55-58.

16. Kennedy, K., Rockwell, S. & Sartorelli, A. C. (1980) Cancer Res. 40, 2356-2360.

17. Moore, H. (1977) Science (Washington, D. C.) 197, 527-532.

18. Tomasz, M. & Lipman, R. (1981) Biochemistry 20, 5056-5061.

19. Kohn, H., & Zein, N. (1983) J. Am. Chem. Soc. 105, 4105-4106.

20. Pan. S.-S., Andrews, P. A., Glover, C. J. & Bachur, N. R. (1984) J. Biol. Chem. 259, 959-966.

21. Peterson, D. M. & Fisher, J. (1986) Biochemistry 25, 4077-4084.

22. Danishefsky, S. J. & Egbertson, M. (1986) J. Am. Chem. Soc. 108, 4648-4649.

23. Egbertson, M. & Danishefsky, S. J. (1987) J. Am. Chem. Soc. 109, 2204-2205.

24. Hornemann, U., Iguchi, K., Keller, P. J., Vu, H. M., Kozlowski, J. F. & Kohn, H. (1983) J. Org. Chem. 48, 5026-5033.

25. Rao, G. M., Begleiter, A., Lown, J. W. and Plambeck, J. A. (1977) J. Electrochem. Soc. 124, 199-202.

26. Tomasz, M., Lipman, R., Chowdary, C., Pawlak, J., Verdine, G. L. & Nakanishi, K. (1987) Science 235,1204 -1208.

27. Cummings, J., Chirrey, L., Willmott, N., Halbert, G. W. and Smyth, J. F (1993) J. Chromatography, 612, 105-113.

28. Pan, S.-S. & Iracki, T. (1988) Mol. Pharmacol. 29, 622-628.

29. Tomasz, M., Lipman, R., Snyder, J. K. & Nakanishi, K. (1983) J. Am. Chem. Soc. 105, 2059-2063.

30. Tomasz, M., Chowdary, C., Lipman, R., Shimotakahara, S., Veiro, D., Walker, V. & Verdine, G. L. (1987) Proc. Natl. Acad. Sci. USA 83, 6702-6706.

31. Tomasz, M., Lipman, R., McGuinness B. and Nakanishi, K. (1988) J. Am. Chem. Soc. 110, 5892-5896.

32. Tomasz, M., Chawla, A. K. and Lipman, R. (1988) Biochemistry 27, 3182-3187.

33. Bizanek, R., McGuinness, B. F., Nakanishi, K. and Tomasz, M. (1992) Biochemistry 31, 3084-3091.

34. Tomasz, M. and Lipman, R. (1979) J. Am. Chem. Soc. 101, 6063-6067.

35. Tomasz, M., Lipman, R., Verdine, G. L. and Nakanishi, K. (1985) J. Am. Chem. Soc. 107, 6120-6121.

36. Keyes, S. R., Fracasso, P. M., Heimbrook, D. C., Rockwell, S., Sligar, S. G., and Sartorelli, A. C. (1984) Cancer Res., 44, 5638-5643.

37. Vyas, D. M., Chiang, Y., Benigni, D., Rose, W. C., Bradner, W. T. (1985) In Recent Advances in Chemotherapy. Anticancer Section I. (Ishigami, J., Ed.) 485-486, University of Tokyo Press, Tokyo.

38. Senter, P., Langley, D., Manger, W. E. And Vyas, D. M. (1988) J. Antibiotics XLI, 199-201.

39. Matsui, M., Yamada, Y., Uzu, K. & Hirata, T. (1968) J. Antibiotics XXI, 189-198.

40. Vyas, D. M., Benigni, D., Partyka, R. A. and Doyle, T. W. (1986) J. Org. Chem. 51, 4307-4309.

41. Carmichael, J., DeGraff, W. G., Gazdar, A. F., Minna, J. D. & Mitchell, J. B. (1987) Cancer Res. 47, 936-942.

42. Tomasz, M., Jung, M., Verdine, G. & Nakanish, K. (1984) J. Am. Chem. Soc. 106, 7367-7370.

43. Pan, S.-S. and Gonzalez, H. (1990) Mol. Pharmacol. 37, 966-970.

44. Franck, R. W. & Tomasz, M. (1990) in Chemistry of Antitumour Agents, (Wilman, D. E. V., Ed.) 379-394, Blackie & Son Ltd. Glasgow.

45. Kobayashi, S., Ushiki, K., Takai, Okumura, S., et al. (1993) Cancer Chemother. Pharmacol. 32, 143-150.

46. Komiyama, T., Kikuchi, T. and Sugigar, Y. (1982) Biochem. Pharmacol. 31, 3651-3656.

47. Ohno, A. and Oae, S. (1977) Organic Chemistry of Sulfur, 121-159.

48. Kohn, K. W. (1981) in Molecular Actions and Targets for Cancer Chemotherapeutic Agents (Sartorelli, A. C., Lazo, J. S., and Bertino, J. R., Eds.), 3-16, Academic Press, New York.

49. Hemminki, K. and Ludlum, D. B. (1984) J. Natl. Cancer Inst. 73, 1021-1028.

50. Lin, A. J., Cosby, L. A. and Sartorelli, A. C. (1976) Cancer Chemotherapy (Sartorelli, A. C., Ed.), 71-86, Academic Press, Washington, D. C..

51. Tomasz, M. (1993) Molecular Aspects of Anticancer Drug-DNA Interactions: Part 2 (Neidle, S. and Waring, M. J., Eds.) 312-349, The MacMillan Press Ltd., Basingstoke, U.K.

52. Maliepaard, M., de Mol, N. J., Janssen, L. H. M., van der Neut, W., Verboom, W. & Reinhoudt, D. N. (1992) Anti-Cancer Drug Design 7, 415-425.

53. McGuinness, B., Lipman, R., Goldstein, J., Nakanishi, K. & Tomasz, M. (1991) Biochemistry 30, 6444-6453.

54. Tomasz, M., Mercado, C. M., Olson, J. & Chatterjie, N. (1974) Biochemistry 13, 4878-4887.

55. Hartley, J., Berardini, M. D. & Souhami, R. L. (1991) Analytical Biochemistry 193, 131-134.

56. Sambrook, J., Fritsch, E. F. & Maniatis, T. (1989) Molecular Cloning: Book 2, 2nd ed., 1051-1053, Cold Spring Harbor, New York.

57. Stefan, K., Renz, D. & Doerfler, W. (1993) Nuclei Acids Research 21, 2339-2342.

58. Sutcliffe, J. G. (1979) Cold Spring Harb Symp Quant Biol (United States) 43 (Pt 1), 77-90.

59. Mohamadi, F., Richards, N. G. J., Guida, G. C., Liskamp, R., Lipton, M., Canfield, C., Chang, G., Hendrickson, Th., Still, W. C. (1990) J. Comput. Chem. 11, 440-467.

60. Borowy-Borowski, H., Lipman, R., Chowdary, D. & Tomasz, M (1990) Biochemistry 29, 2992-2999.

61. Borowy-Borowski, H., Lipman, R., & Tomasz, M (1990) Biochemistry 29, 2999-3006.

62. Kinoshita, S., Uzu, K., Nakano, K., Shimizu, M., Takahashi, T. & Matsui, M. (1971) J. Med. Chem. 14, 103-109.

63. Mitchell, M., Kelly, R. C. Wicnienski, N. A., et al. (1991) J. Am. Chem. Soc. 113, 8994-8995.

64. Cleland, W. W. (1964) Biochemistry 3, 480-482.

65. Siegel, D., Beall, H., Senekowitsch, C., Kasai, M., Aral, H., Gibson, N. W. & Ross, D. (1992) Biochemistry 31, 7879-7885.

66. Teng, S. P., Woodson, S. A., & Crothers, D. M. (1989) Biochemistry 28, 3 901-3907.

67. Kennedy, K. A., McGurl, J. D., Leondaridis, L. & Alabaster, O. (1985) Cancer Res. 45, 3541-3547.

68. Kohnoe, S., Emi, Y., Takahashi, I., Yoshida, M., Maehara, Y. & Sugimachi, K. (1991) Anticancer Res. 11, 1401-1405.

69. Kumar, S., Lipman, R. & Tomasz, M. (1992) Biochemistry 31, 1399-1407.

70. Li, V. & Kohn, H. (1991) J. Am. Chem. Soc. 113, 275-283.

71. Sharma, M. (1993) Doctoral Dissertation, The City University of New York (Advisor: Prof. M. Tomasz).

72. Xu, B. H. and Singh, S. (1992) Cancer Res. 52, 6666-6670.

73. Perry, R. R., Greaves, B. R., Rasberry, U. & Barranco, S. C. (1992) Cancer Res. 52, 4608-4612.

74. Pyle, A. M., Rehmann, J. P., Meshoyrer, R., Kumar, C. V., Turro, N. J. & Barton, J. K. (1989) J. Am. Chem. Soc. 111, 3051-3058.

75. Geacintov, N. E., Shahbaz, M., et. al. (1988) Biochemistry 27, 8380-8387.

76. Shahbaz, M., Geacintov, N. & Harvey, R. G. (1986) Biochemistry 25, 3290-3296.

77. Barton, J. K., Goldberg, J. M., et. al., (1986) J. Am. Chem. Soc. 108, 2081-2088.

78. Plum, G. E. & Bloomfield, V. A. (1988) Biopolymers 27, 1045-1051

79. Hoey, B. M., Butler, J. & Swallow, A. J. (1988) Biochemistry 27, 2608-2614.

80. Wolfe, A., Shimer, G. H. & Meehan, T (1987) Biochemistry 26, 6392-6396.

81. McGhee, J. & Hippel, P. H. von (1974) J. Mol. Biol 86, 469-489.

82. Stevens, C. L., Taylor, K. G., et. al., (1964) J. Med. Chem. 8, 1-10.

83. Tomasz, M., Borowy-Borowski, H. & McGuinness, B. F. (1990) Molecular Basis of Specificity in Nucleic Acid-Drug Interactions, (Pullman, B. and Jortner, J., eds.) 551-564, Kluwer Academic Publishers, Dordrecht, The Netherlands.

84. Lipman, R., Weaver, J. & Tomasz, M. (1978) Biochim. Biophys. Acta 521, 779-791.